Substrate Localisation as a Therapeutic Option for Pompe Disease

A thesis submitted to The University of Adelaide for the degree of

DOCTOR OF PHILOSOPHY

by

Christopher Travis Turner, BBtech (Hons)

Lysosomal Diseases Research Unit

Department of Genetic Medicine

Women's & Children's Hospital

North Adelaide, South Australia, 5006

October 2013

Paediatrics

Paediatrics and Reproductive Health

The University of Adelaide

Table of Contents

Abstract

Pompe disease is a progressive form of muscular dystrophy caused by a deficiency in the lysosomal enzyme α-glucosidase (GAA). GAA catabolises glycogen and its deficiency leads to glycogen accumulation in the vesicular network of affected cells. Multiple therapies exist to treat Pompe disease but these are not completely effective (Winkel *et al.,* 2003), necessitating the development of new therapeutic strategies. A number of enzymes that reside outside of the lysosome, either in the cytoplasm (Watanabe *et al.,* 2008) or in circulation (Ugorski *et al.,* 1983), can catabolise glycogen. It was postulated that if vesicular glycogen in Pompe cells was transferred out of these compartments it could then be alternatively degraded. The ability to remove vesicular glycogen from Pompe cells may reduce the onset/progression of the disorder, providing a therapeutic option for patients.

Exocytosis is a ubiquitous cellular mechanism where intracellular vesicles fuse with the cell surface and permit vesicle content to be released from the cell. It was postulated that exocytosis may provide a mechanism to release accumulated glycogen from Pompe cells. Approximately 4% of vesicular glycogen was exocytosed from Pompe skin fibroblasts after 2 hrs in culture. Pompe cells exocytosed 2.7-fold more glycogen than unaffected cells. A cellular mechanism was therefore identified that had the capacity to release glycogen from Pompe cells.

Culture conditions can alter the amount of exocytosis in fibroblasts (Martinez *et al.,* 2000). In this study the effect of cell confluence and components of the culture media on lysosomal exocytosis was examined in Pompe skin fibroblasts. Increasing the

extracellular concentration of Ca^{2+} led to a 1.4-fold increase in glycogen release compared to cells cultured in standard media conditions. Culture confluence had a key influence on glycogen exocytosis, with sub-confluent Pompe cells releasing >80% of glycogen after 2 hrs in culture, 35-fold higher than confluent cells. Exocytic mechanisms therefore exist that allow up-regulation of glycogen exocytosis in Pompe skin fibroblasts.

A number of pharmacological compounds induce exocytosis in cultured cells (Amatore *et al.*, 2006). Pompe skin fibroblasts treated with three compounds; calcimycin, lysophosphatidylcholine and α-L-iduronidase, each demonstrated a ≥ 1.5-fold increase in glycogen exocytosis, when compared to untreated Pompe controls. Calcimycin was the most effective compound for inducing glycogen exocytosis, with 12% released after 2 hrs of treatment, but confluent Pompe cells released less than that observed from sub-confluent Pompe cells. This difference in glycogen release may have resulted from the induction of different exocytic mechanisms. Complete exocytosis, where the vesicle completely fuses with the cell surface and releases all vesicle content, is induced in sub-confluent Pompe cells. In contrast, cavicapture, involving only a partial pore opening and limited vesicle content release, is induced in response to calcimycin treatment. The identification of a compound capable of inducing complete exocytosis may therefore improve glycogen release from Pompe cells. Taken together, natural glycogen exocytosis and the ability to induce glycogen exocytosis with pharmacological compounds provided proof-of-concept for exocytic induction as a strategy to re-locate accumulated glycogen from Pompe cells, potentially providing a new therapeutic option for the disorder.

Declaration of Authenticity

I, Christopher Turner, declare this thesis contains no material which has been accepted for the award of any other degree or diploma in any University and that, to the best of my knowledge and belief, the thesis contains no material previously published or written by another person, except where due reference is made in the text. The author consents to the thesis being made available for photocopying and loan if applicable, if accepted for the award of the degree.

…….

Christopher Turner

Acknowledgments

I wish to thank my supervisors Peter Meikle, Doug Brooks, John Hopwood and Maria Fuller. I would also like to acknowledge the following colleagues; Sophie Lazenkis, Phil van der Ploeg, Tim Nielsen, Glen Borlace, Anthony Fidelli, Debbie Lang, Emma Parkinson-Lawrence, Jana Pacyna, Mark Proedehl and Karissa Phillis. I would like to thank Stephen Duplock, Tomas Rozek and Troy Stomski for their mass spectrometry expertise, David Stapleton for assistance with the isolation and visualization of glycogen, Greg Hodge for flow cytometry training, Lyn Waterhouse and Ruth-Ellen Williams for assistance with the TEM and confocal microscope, Alvis for assistance with preparing the TEM samples, Lou for running a number of lactate dehydrogenase assays, Kathy Nelson for providing cell lines and culturing information and Nancy Briggs for statistical analysis. I would also like to acknowledge the support of Felicity, Marilyn, Stephen, Bella and Paige Turner.

Abbreviations

^{o}C	degrees celcius
%	percentage
<	less than
>	greater than
µg	microgram
µL	microlitre
µmol	micromoles
µM	micromolar
β	beta
β-hex	beta-hexosaminidase
4-MU	4-methylumbelliferyl
AA	arachidonic acid
AMP	adenosine monophosphate
amu	atomic mass units
ANOVA	analysis of variance
BAPTA-AM	1,2-bis(o-aminophenoxy)ethane-N,N,N',N'-
tetraacetic	acid-acetoxymethyl ester
BCA	bicinchoninic acid
BME	Basal modified Eagle's medium
BSA	bovine serum albumin
Ca^{2+}	divalent calcium ion

calcimycin	calcimycin A23187
cAMP	cyclic AMP
CRIM	cross-reactive immunological material
DAPI	4',6-diamidino-2-phenylindole
DIC	differential interference microscopy
DMEM	Dulbecco's modified Eagle's medium
EPA	eicosapentaenoic acid
EPAC	exchange proteins activated directly by cyclic AMP
ERT	enzyme replacement therapy
ESI-MS/MS	electrospray ionization tandem mass spectrometry
FBS	fetal bovine serum
g	gravitational force
GAA	acid α-glucosidase
G1P	glucose-1-phosphate
G6P	glucose-6-phosphate
HCl	hydrochloric acid
H_2O	water
HPLC	high pressure liquid chromatography
Idua	α-L-iduronidase
kDa	kilodalton
KH_2PO_4	monopotassium phosphate
LAMP	lysosomal associated membrane protein

LC/ESI-MS/MS	liquid chromatographic electrospray ionization tandem mass spectrometry
LDH	lactate dehydrogenase
LPC	lysophosphatidylcholine
LSD	lysosomal storage disorder
min	minute
mg	milligram
MLD	metachromatic leukodystrophy
mol	moles
MPR	mannose-6-phosphate receptor
MPS	mucopolysaccharidosis
MRM	multiple reaction monitoring
ms	milliseconds
MS	mass spectrometry
m/z	mass-to-charge ratio
MW	molecular weight
N_2	nitrogen
NaCl	sodium chloride
Na_2HPO_4	disodium phosphate
NaOH	sodium hydroxide
NB-NBJ	N-butyldeoxynorjirimycin
ng	nanograms
nm	nanometers

nmol	nanomoles
NRK	normal rat kidney
OD	optical density
PBS	phosphate buffered saline
PC	phosphatidylcholine
PMA	phorbol 12-myristate 13-acetate
PMP	1-phenyl-3-methyl-5-parazolone
PtdIns3K	phosphatidylinositol 3-kinase
PtdIns3P	phosphatidylinositol 3-phosphate
QC	quality control
SLP	synaptotagmin-like protein
SNAP	soluble N-ethylmaleimide-sensitive factor attachment protein
SNARE	soluble N-ethylmaleimide-sensitive factor attachment protein receptor
S-1-P	sphingosine-1-phosphate
Syt	synaptotagmin
TFEB	bHLH-leucine zipper transcription factor EB
TOR	target of rapamycin
VAMP	vesicle-associated membrane protein
V-ATPases	vacuolar ATPases
v/v	volume per volume
w/v	weight per volume

List of Figures

Supplementary Data

List of Tables

Chapter 1: Introduction

1.1 The endosome-lysosome system

The endosome-lysosome system is an intracellular network of membrane-enclosed acidic compartments (Huotori and Helenius, 2011). These compartments, which include endosomes, lysosomes and autophagosomes, each have distinct morphologies, intracellular locations and biological functions (Luzio *et al*., 2001). The primary functions of the endosome-lysosome network are to internalise extracellular material into the cell, traffic cargo to different intracellular destinations and to degrade macromolecules. The endosome-lysosome system is integral to the functioning of a range of biological processes including cell-cell signaling, cell growth and division, the turnover and recycling of intracellular waste and the defence of the host against pathogens (Mellman, 1996).

1.1.1 The Endosome

There are three main types of endosomes; early endosomes, late endosomes and recycling endosomes. Early endosomes are localised close to the cell surface and are tubulovesicular in appearance. The limiting membrane of the early endosome contains a number of sub-domains (Zerial and McBride, 2001), which are typically associated with tubular extensions (Jovic *et al*., 2010). Late endosomes have a perinuclear localisation, which places them in close proximity to both the Golgi complex and the microtubule organising centre. Morphologically, late endosomes are spherical or oval in shape and contain multiple internal membranes. It is the presence of these intra-lumenal vesicle structures that provides the alternative name for late endosomes; multivesicular bodies.

Similar to early endosomes, recycling endosomes are tubulovesicular in appearance but they are located in the perinuclear region (Li and Difiglia, 2011).

Two models are proposed for the traffic of cargo from early endosomes to late endosomes (Luzio *et al*., 2009; Mullins and Bonafacino, 2001). In the 'kiss-and-run' model the transfer of luminal content and membrane from one compartment to another involves only a transient interaction (Luzio *et al*., 2009) with a partial and reversible fusion of early endosomes with late endosomes, creating a transient aqueous pore (Neher, 1993). The second model involves a process of vesicle maturation whereby the early endosomes mature into late endosomes. Maturation involves a rapid bi-directional exchange of membrane and contents between endosomes and the endoplasmic reticulum/trans-Golgi network, allowing the removal of some early endosome components and the recruitment of both late endosome markers and acid hydrolases (**Figure 1.1**; Huotori and Helenius, 2011). During maturation, endosomes are trafficked via microtubules from the cell periphery to a perinuclear location, assisted by specific motor proteins (Huotori and Helenius, 2011). One study has indicated that both models may operate, with ‘kiss and run’ transfer possibly a precursor to fusion events (Luzio *et al*., 2009).

Vesicle acidification is a key component of endosome maturation, with the decreasing pH in successive compartments contributing to receptor-ligand uncoupling and providing an acidic environment for acid hydrolases to degrade substrate (Saftig and Klumperman, 2009). Vacuolar ATPases (V-ATPases) are membrane-bound protein complexes that function as proton pumps in the endosomal membrane, and are responsible for endosome acidification (Huotari and Helenius, 2011). The differences in

the lumenal pH between early endosomes (pH 6.8 to 6.1) and late endosomes (pH 6 to 4.8) are related to the amount of V-ATPase, including the type of V-ATPase isoform and the amount of hydrophobic membrane sector (V0)/peripheral catalytic sector (V1) complex association in the endosomal membrane (Scott and Gruenberg, 2011).

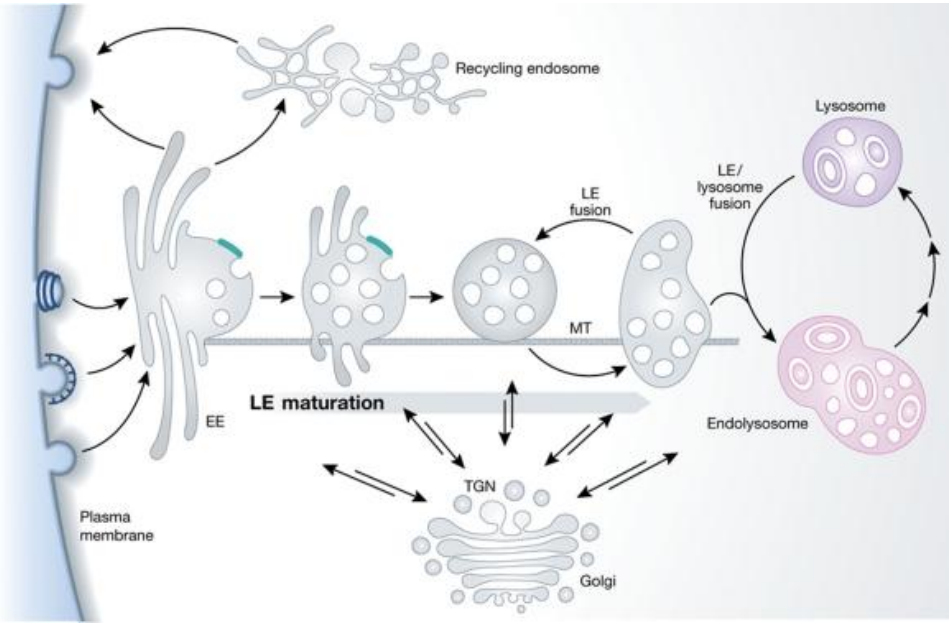

Figure 1.1: The endosome/lysosome system. Early endosomes undergo a maturation process to become lysosomes, with late endosomes produced as an intermediate step. Early endosomes are located near the cell surface but as the vesicle matures they are trafficked along microtubules to the perinuclear region. During maturation, cytoplasmic or extracellular cargo is trafficked to lysosomes from early endosomes. Also, newly synthesised lysosomal hydrolases and membrane components are recruited, with these derived from the trans-Golgi network, recycling endosomes or the cell surface. Abbreviations in figure are early endosome (EE), late endosome (LE) microtubule (MT) and trans-Golgi network (TGN). Image from Huotari and Helenius, 2011.

Endosome maturation changes the complement of acid hydrolases, receptors and membrane proteins associated with different endosomal compartments. Early endosomes are rich in endo-hydrolases, enzymes capable of internal cleavage of substrates to produce smaller fragments (Pillay *et al*., 2002). Acid exo-hydrolases, enzymes that cleave at the non-reducing end of substrates (Ni *et al*., 2006), are progressively recruited during the maturation of early endosomes into late endosomes. These hydrolases are delivered by two pathways with the majority arriving from the trans-Golgi network (Braulke and Bonifacino, 2009) and smaller amounts being trafficked from the cell surface (Seaman, 2008). There is also a progressive accumulation of newly synthesised membrane proteins in late endosomes, including lysosomal-associated membrane protein (LAMP)-1 and -2 (Saftig and Klumperman, 2009). These dynamic changes in endosome composition lead to the gradual remodeling of the early endosome into a later stage endosome and eventually a lysosome.

The small GTPase proteins Rab5 and Rab7 are important for the transition from early- to late endosomes during endosome maturation. Rab5 is associated with the cytosolic surface of early endosomes and binds to a number of effector proteins, including VPS34 (a member of the PI3/PI4-kinase family) early endosome antigen-1 (a tethering molecule involved in homotypic fusion of early endosomes) and Rabenosyn-5 (a key element in clathrin-mediated endocytosis and the initial node for transferrin receptor sorting; Jovic *et al*., 2010; Navaroli *et al*., 2012). During endosomal maturation Rab5 is replaced by Rab7. SAND1/Mon-1 and Ccz1, vacuole targeting pathway proteins, are recruited from the cytosol to the endosomal membrane and this contributes to the switch from Rab5 to Rab7 (Poteryaev *et al*., 2010). Rab7 then recruits its own

complement of effector proteins, including RILP, which connect late endosomes to dynein motors, thereby allowing the translocation of the endosome to the perinuclear region. Components of the HOPS complex are also recruited by Rab7, which provide a tether for fusion of late endosomes with other compartments, including lysosomes (Huotari and Helenius, 2011). The Rab switch therefore contributes to an exchange in the fusion machinery on the endosomal membrane.

The phosphatidylinositides (PtdIns') (3)P and (3,5)P(2) are differentially associated with endosomal membranes, and with PtdIns(3)P enriched in early endosomes (Huotari and Helenius, 2011). The recruitment of the GTPase Rab5 to the membrane of the early endosome is responsible for initiating PtdIns(3)P synthesis (Jovic *et al*., 2010). PtdIns(3)P assists the recruitment of effector proteins, including early endosome antigen-1, Rabenosyn-5 and Hrs, with these contributing to both the sorting of cargo and the regulation of endosome fusion. PtdIns(3,5)P(2) is enriched in late endosomes and interacts with a different set of effector proteins, including the endosomal sorting complexes required for transport machinery, ultimately contributing to the formation of intra-lumenal vesicles and the degradation of cargo (Deretic *et al*., 2007). Through the sequential recruitment of specific effector proteins, PtdIns phosphorylation plays a crucial role in endosome maturation.

Recycling receptors, including the transferrin receptor, can be trafficked from early endosomes to the cell surface. This involves the pinching off of narrow membrane tubules from early endosomes in a process called geometry based sorting (Eggers *et al*., 2009), with these tubules then maturing into recycling endosomes (Grant and Donaldson, 2009). Rab 4 and Rab11 contribute to recycling endosomal trafficking by

interacting with actin filament bundles and recruiting effector proteins to specific membrane domains (Lock and Stow, 2005; Eggers *et al*., 2009). Rab11 vesicles are transported along microtubules to the cell periphery and directly regulate vesicle exocytosis at the plasma membrane, in concert with the exocyst complex, which helps mediate vesicle fusion with the plasma membrane (Takahashi *et al*., 2012). Recycling endosomes play a major role in receptor delivery back to the cell surface.

Endosomes act as the major sorting compartment for the cell, providing a mechanism to traffic proteins and receptors to and from the cell surface, and to deliver acid hydrolases to lysosomes, along with cargo destined for lysosomal degradation. Endosomes also interact with the other degradative compartments in the endosome-lysosome system, including phagosomes and autophagosomes; the latter of which will be discussed in section 1.1.3 because of their critical involvement in glycogen degradation.

1.1.2 The Lysosome

The lysosome is the terminal compartment in the endosome-lysosome pathway, and was first described by Christian de Duve in 1955 (de Duve and Wattiaux, 1966). Using centrifugal fractionation techniques to analyse rat liver extracts, lysosomes were recognized as saclike structures containing a variety of enzymes and surrounded by membrane. The lysosome is now recognised as an acidified degradative compartment that contains multiple acid hydrolases (de Duve, 2005). Lysosomes contribute to a number of cellular/biological processes, including substrate turnover, cholesterol homeostasis, organelle quality control, cell survival, antigen presentation, removal of

pathogens, plasma membrane repair, tissue remodeling, tumor metastasis, autophagic cell death, mammalian target of rapamycin (TOR) activation and autophagosome maturation (Boya, 2012). Lysosomes are heterogeneous in morphology, having either a tubular or spherical appearance (de Duve, 1983). The limiting membrane is a single phospholipid bi-layer and lysosomes often contain electron dense material or membrane whorls. Lysosomes are localised to the perinuclear region of the cell in close proximity to both late endosomes and the microtubule organizing centre. Approximately 5% of the intracellular volume of the cell can be accounted for by lysosomes (Luzio *et al*., 2007).

Lysosomes are thought to be produced by the maturation of late endosomes (**Figure 1.1**; Huotari and Helenius, 2011). During this maturation event, the compartment is acidified and there is further recruitment of acid hydrolases. Protons pumped into the lysosomal lumen by V-ATPases control this acidification, generating a pH of approximately 4.5 to 5.0. Ion transporters, including the sodium-proton exchanger, chloride channels, two-pore channels and transient receptor potential mucolipins, also contribute to lowering the pH during maturation (Scott and Gruenberg, 2011). Moreover, these ion transporters also contribute to maintaining the pH within the lysosome once the compartment is sufficiently acidified. The low pH of the lysosome is critical for acid hydrolase activity (Pillay *et al*., 2002). In addition, a number of acid hydrolases are proteolytically processed to their mature forms under the acidic conditions in the lysosome (Hasilik, 1992). The maintenance of an acidified pH is therefore critical for optimal lysosome function.

Lysosomes contain in excess of 50 acid hydrolases, and these include sulphatases, glycosidases, lipidases, nucleases, phosphatases, proteinases and peptidases (Bainton,

1981). Together, these enzymes are capable of catabolising a wide range of complex substrates, including proteins, lipids, DNA, glycoproteins, glycosaminoglycans and glycogen (Schröder *et al*., 2010). Lysosomal hydrolases also contribute to other degradative processes in the cell, including degradation of extracellular matrix and initiating apoptosis (Saftig and Klumperman, 2009). Lysosomal enzymes therefore facilitate the degradation of complex substrates into their monomeric constituents, which can then be recycled back to the cell. A number of other proteins are also associated with the lysosome, including lysosomal membrane proteins (Pillay *et al*., 2002; Pisoni and Thoene, 1991), more than 25 of which reside in the lysosomal-limiting membrane (Schröder *et al*., 2010). These lysosomal membrane proteins contribute to the acidification of the lysosomal compartment, allow protein import from the cytosol, and are involved in vesicle transport, membrane fusion and the traffic of degraded material to the cytoplasm (Boya, 2012). LAMPs are one of the most abundant lysosomal membrane proteins, also functioning to maintain the structural integrity of the lysosomal membranes (Eskelinen, 2006).

A number of delivery mechanisms have been described for the transfer of cargo from late endosomes to the lysosome, including a vesicular and a hybrid model (Luzio *et al*., 2007). In the vesicular model, vesicles can bud from late endosomes and be trafficked to the lysosome. In the hybrid model, late endosomes and lysosomes permanently fuse to create a hybrid compartment. Maturation and 'kiss and run' models have also been described for cargo transfer from late endosomes to the lysosome. The exact contribution of these models to cargo delivery has yet to be elucidated.

Soluble N-ethylmaleimide-sensitive factor attachment protein receptor (SNARE) proteins, N-ethylmaleimide-sensitive factor and N-ethylmaleimide-sensitive factor-attachment proteins are required for endosome-lysosome fusion (Luzio *et al*., 2010). The specificity of the fusion is provided by the interaction of both GTPase Rab and SNARE proteins with tethering and effector proteins. There are two types of events, homotypic and heterotypic fusion. Q-SNARE proteins, including syntaxin-7, syntaxin-8 and Vti1b, are required for both types of fusion events. However, homotypic fusion events require an R-SNARE; vesicle-associated membrane protein-8 (VAMP-8), whereas heterotypic fusions require the R-SNARE; VAMP-7. The complement of effector proteins associated with the lysosome will therefore dictate the type of fusion event that occur.

1.1.3: Autophagosomes

Autophagy is the process responsible for the delivery of cytosolic cargo to the endosome-lysosome network, and involves the formation of autophagosomes, which are double membrane structures that surround cytosolic contents. Experiments with mouse kidney cells performed during the late 1950s, led to the discovery of autophagy (Clark, 1957; Novikoff, 1959); in those studies, mitochondria were observed inside membrane-bound vesicles that also contained acid hydrolases. The identification of partially degraded mitochondria and endoplasmic reticulum within these compartments (Ashford and Porter, 1962) led to the concept of autophagy as the mechanism by which cytoplasmic constituents are sequestered and degraded.

Autophagy is sub-divided into microautophagy, chaperone-mediated autophagy and macroautophagy (**Figure 1.2**; Yen and Klionsky, 2008). Microautophagy involves a local deformation/rearrangement at the lysosomal membrane, allowing the direct engulfment of portions of cytoplasm into the lysosome (Li *et al*., 2011). Chaperone-mediated autophagy involves the internalisation of proteins from the cytoplasm directly across the lysosomal membrane, and requires specific membrane surface receptors, namely LAMP-2a. Only proteins that contain a consensus peptide sequence are recognized for transfer and the lysosomal chaperone, hsp70, assists in the translocation of these proteins to lysosomes (Majeski and Dice, 2004). Approximately 30% of total cytoplasmic proteins have been reported to be internalised into the endosome-lysosome network by chaperone-mediated autophagy (Dice, 2007). Macroautophagy involves the engulfment of cytosolic constituents into specialised compartments called autophagosomes (Codogno and Meijer, 2005). Macroautophagy is the only mechanism capable of trafficking cytosolic glycogen into the endosome-lysosome network (Kotoulas *et al*., 2004) and, as such, this mechanism will now simply be referred to as autophagy in this thesis.

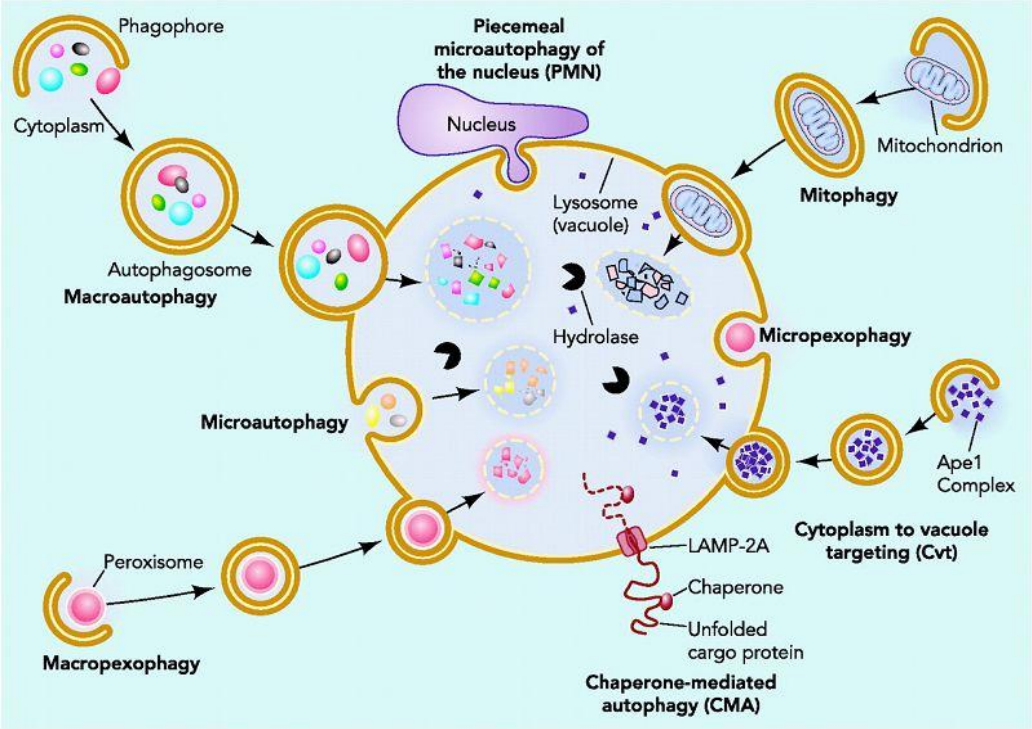

Figure 1.2: Autophagy. The three major types of autophagy are macroautophagy, microautophagy and chaperone-mediated autophagy. Macroautophagy and microautophagy are responsible for the trafficking of cytoplasmic protein and other small molecules into the vesicular network. Microautophagy involves a local deformation at the vesicle membrane, allowing the direct engulfment of portions of cytoplasm into the lysosome. Macroautophagy involves the engulfment of cytosolic constituents into specialised compartments called autophagosomes. Only specifically tagged proteins can undergo chaperone-mediated autophagy, requiring specific membrane surface receptor binding. Mechanisms also exist for the autophagic uptake of mitochondria (mitophagy), peroxisomes (macropexophagy and pexophagy micropexophagy) and nuclear content. Image from Yen and Klionsky, 2008.

In most cell types, autophagy is suppressed to a basal level (Martinet, 2005). The induction of autophagy is typically associated with maintaining cellular homeostasis, with a fine balance between catabolism and anabolism of cytoplasmic constituents, ensuring normal growth and development. Autophagy has been reported to occur in response to cellular stress (Klionsky, 2005), cellular injury (Martinet and De Meyer, 2008), nutrient starvation (Munafo and Colombo 2001), deprivation of insulin and insulin-like growth factors (Kondomerkos *et al*., 2004), hypoxia, the formation of reactive oxygen species (Ryter and Choi, 2013) or micro-organism invasion (He and Klionsky, 2009). Autophagy therefore plays a vital role in many cellular functions.

Mammalian TOR contributes to the regulation of autophagy (Kliosky, 2005), it is a serine/threonine protein kinase that is a sensor for growth factors, energy status and nutrient signals (Yang and Klionsky, 2010b). Mammalian TOR also acts in a signal transduction cascade that controls the phosphorylation of a number of effectors, some of which are linked to autophagy induction (Kliosky, 2005). Phosphtidylinositol 3-kinase (PtdIns3K) is one of the most important proteins downstream of mammalian TOR and has three classes; PtdIns3K -I, PtdIns3K -II, and PtdIns3K -III. PtdIns3K -I and PtdIns3K -III have been reported to specifically act as inhibitors of autophagy, with PtdIns3K -I inhibition associated with membrane binding and subsequent activation of Akt/protein kinase B and pyruvate dehydrogenase lipoamide kinase isozyme-1 (Arico *et al*., 2001), which leads to activation and formation of autophagosomes (Tassa *et al*., 2003). AMP-activated protein kinase and p53 have also been reported to play a role in autophagy induction (Yang and Klionsky, 2010a).

Autophagosomes are spherical/oval compartments with an average diameter of approximately 600 nm, and a heterogeneous intracellular distribution (Eskelinen, 2008). Such compartments are initially formed as a double lipid bi-layer membrane structure. Electron microscopy has identified membrane whorls, ribosomes and organelles within these membranes, as well as electron-dense material, including glycogen (Bellu and Kiel, 2003; Kotoulas *et al*., 2004). Autophagosomes are classified as either early (initial; AVi) or late (degradative; AVd) autophagic vacuoles (Eskelinen, 2008); thus AVi vesicles contain relatively intact cytoplasmic material, when compared to AVd vesicles.

Vesicle nucleation is the first step in the formation of autophagosomes, and initially involves the formation of a phagophore (**Figure 1.3**; Reggiori *et al*., 2005). Two main models have been proposed for phagophore membrane formation (Chen and Klionsky, 2011). In one model, multiple sub-domains derived from the endoplasmic reticulum (omegasomes; Tanida, 2011) bind together to produce the phagophore (Hayashi-Nishino *et al*., 2009). In the other model, the phagophore results from the addition of lipids together in sequence within the cytosol (Kovács *et al*., 2007). In either case, the initiation of phagophore formation requires the recruitment of the Beclin-1/Class III PtdIns3K complex, which is formed in response to interactions with a number of proteins, including Beclin-1, UV irradiation resistance-associated tumor suppressor gene, endophilin and Atg14 (Wong *et al*., 2011). Assembly of the phagophore membrane requires the PtdIns3K complex, Vps15, Atg14, and Atg6/Vps30 (He and Klionsky, 2009). The PtdIns3K complex produces phosphatidylinositol 3-phosphate (PtdIns3P), which leads to the recruitment of a number of Atg proteins, including Atg18, Atg20, Atg21, and Atg24 (Obara *et al*., 2008). The PtdIns3K complex

then recruits the conjugation complexes, Atg12-Atg5-Atg16 and Atg8-phosphatidylethanolamine to the phagophore, which regulates membrane elongation and expansion (Suzuki *et al*., 2007). The lipidation of Atg8 (mammalian homolog is microtubule-associated protein-1 light chain-3) to Atg-phosphatidylethanolamine, which localises to both sides of the phagophore, contributes to the monitoring of phagophore formation (He and Klionsky, 2009).

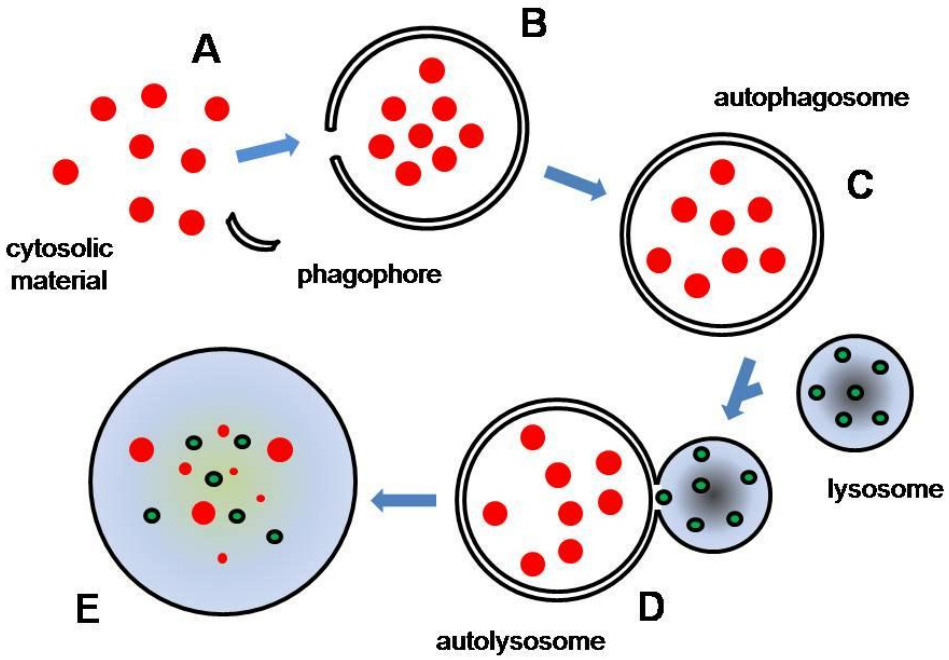

Figure 1.3: Autophagosome formation and substrate degradation. Uptake of cytoplasmic content (red) into the vesicular network (A, B); formation of a double-membrane autophagosome (C); the autophagosome fuses with a lysosome, combining the autophagocytosed cytoplasmic content with lysosomal hydrolases (green; D); the vesicle contents are degraded by lysosomal hydrolases (E). Figure adapted from Xie and Klionsky, 2007.

Autophagosomes are produced by the elongation and eventual closure of the phagophore. Atg7, Atg10, Atg5 and Atg12 are critical in this process as they interact with phosphatidylethanolamine and lead to the recruitment of Atg8, a marker of autophagosomes (Wong *et al*., 2011). The proteins, phosphoinositide 3-phosphatase, 'Jumpy' and WIPI-1 are also localised to the phagophore, although their precise roles are yet to be elucidated (Vergne *et al*., 2009). The process of autophagosome-lysosome fusion in mammalian cells is not completely understood, but the proteins, LAMP-2, Rab7, UVRAG, Rubicon, syntaxin-5 and presenilin-1 have been implicated (Tanida, 2011; Wong *et al*., 2011). The microtubule network is also linked to the fusion process (Bursch *et al*., 2000). In mammalian cells, autophagosomes can also fuse with endosomes, leading to the formation of amphisomes (Yang and Klionsky, 2010b), the first stage in autophagosome maturation. The fusion of autophagosomes and/or amphisomes with lysosomes leads to the formation of autolysosomes. The recruitment of acid hydrolases from lysosomes in conjunction with an increase in the acidity of the autolysosome contributes to the progressive degradation of the autophagocytosed material.

A unique feature associated with the maturation of autophagosomes into autolysosomes is the degradation of the inner but not the outer membrane of the compartment (Klionsky, 2005). The outer membrane appears to be modified so as to protect it from degradation. Proteinases A and B, and cathepsin B, D and L have been reported to contribute to inner vesicle degradation within the autophagosome (He and Klionsky, 2009), but the precise mechanism involved in this process is yet to be elucidated.

The endosome-lysosome network is an integral cellular component that carries out a number of functions, including trafficking of cargo to different intracellular destinations, the internalisation of extracellular material and the degradation of macromolecules. However, impairment in the hydrolytic capacity of the lysosome is the molecular basis for a range of lysosomal storage disorders (LSDs).

1.2: Pompe disease:

Pompe disease belongs to the family of inherited metabolic diseases known as lysosomal storage disorders. Convention describes LSDs as progressively accumulating substrate within the endosome-lysosome network. Over 50 LSDs have been identified with a collective clinical incidence of approximately one in 7,700 live births in Australia (Meikle *et al*., 1999). The majority of LSDs are caused by a dysfunction in the activity of acid hydrolases, but some result from dysfunctioning lysosomal membrane proteins or other proteins associated with the endosome-lysosome system (Poupětová *et al*., 2010).

Pompe disease was one of the first LSDs to be identified and led to much of the initial knowledge on LSD pathogenesis and lysosome biology. Pompe disease, also known as acid maltase deficiency or glycogen storage disorder type II, is an autosomal recessive lysosomal disorder of glycogen metabolism (Hers, 1963). It is caused by mutations in the gene encoding the lysosomal enzyme α-glucosidase (GAA) and results in the progressive accumulation of glycogen in the endosome-lysosome system (Hirschhorn and Reuser, 2001). Patients with Pompe disease develop a progressive muscular dystrophy that leads to premature death. The disorder was first described in 1932 by J.C Pompe, a Dutch pathologist who observed a seven year old girl presenting with idiopathic hypertrophy of the heart (Pompe, 1932). Pompe was the first to observe the accumulation of glycogen within vacuoles in the heart and other tissues.

1.2.1: Incidence

The incidence of Pompe disease in Australia has been reported to be 1 in 201,000 live births (Meikle *et al*., 1999). The incidence reportedly varies between different countries and ethnic groups (Raben *et al*., 2002); for example, the prevalence of Pompe disease in the Dutch population (Ausems *et al*., 1999) is three-fold higher than the African-American population (Martiniuk *et al*., 1998). Newborn screening pilot studies for Pompe disease, which have led to improved patient identification, reported an incidence of 1 in 8,684 live births in Austria (Mechtler *et al*., 2012), 1 in 33,000 live births in Taiwan (Chien *et al*., 2008) and 1 in 138,000 in The Netherlands (Wang *et al*., 2011).

1.2.2: Clinical manifestations

Pompe disease is characterised by a spectrum of clinical severity that ranges from rapid (infantile-onset) to slowly progressive (adult-onset). There are two forms of infantile-onset Pompe disease, classic and non-classic. The classic infantile-onset form is characterised by rapidly progressive muscle weakness, cardiomegaly, hypotonia, and less marked hepatomegaly (Hirschhorn and Reuser, 2001). The 'floppy baby' appearance is the first clinical indication of a classic phenotype and is related to the weakening of the musculature (**Figure 1.4**). Within the first months of life there is a failure to thrive, feeding problems and respiratory difficulties (van den Hout *et al*., 2004). Over time the cardiomegaly progressively worsens, with left ventricular thickening that eventually obstructs left ventricular flow, ultimately causing death. The life expectancy of a patient with classic infantile-onset Pompe disease is less than two years. The non-classic infantile-onset form is characterised by rapidly progressive

muscular pathology, without cardiac involvement (Pascual, 2009). Patients typically present within the first six months of life and survival can exceed two years of age.

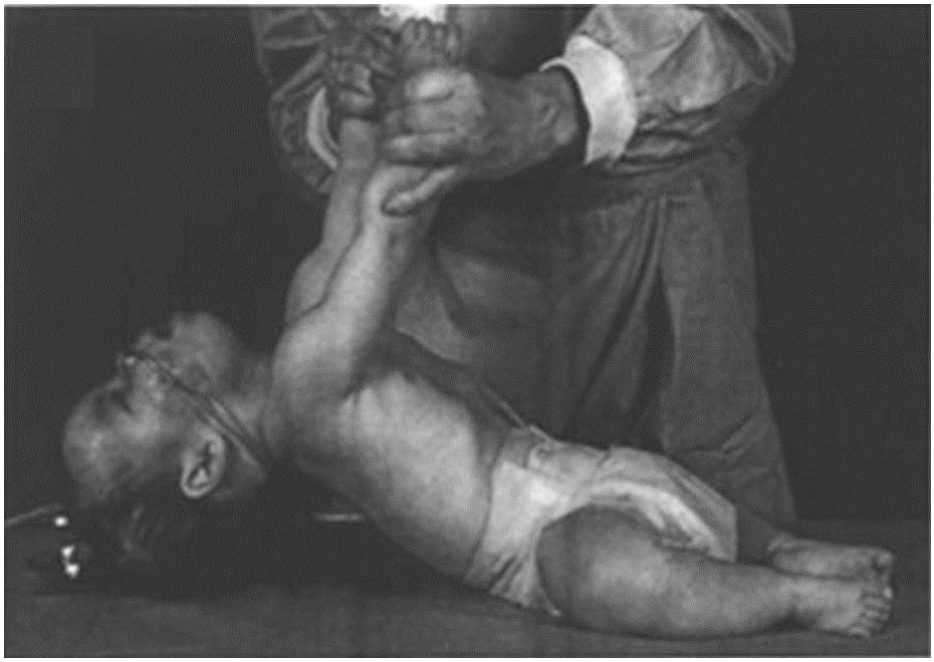

Figure 1.4: Infant-onset Pompe disease. An eight month old female Pompe patient displaying floppy baby and head lag. Figure from Neufeld and Muenzer, 2001.

The disease course in adult-onset Pompe patients is less progressive than infantile-onset and cardiomyopathy is absent in most cases (Winkel *et al*., 2005), with diagnosis sometimes into their sixth decade of life. Juvenile-onset is a form of the disorder with intermediate clinical severity, and diagnosis typically between five and 18 years of age (van Capelle *et al*., 2010). Juvenile- and adult-onset Pompe disease is suspected in patients who demonstrate proximal muscular weakness in combination with

respiratory insufficiency in the absence of cardiac pathology (Kishnani *et al*., 2006). A respiratory tract malfunction is a key component of the worsening pathology, but other symptoms include orthopnoea, morning headache, somnolence, exertional dyspnoea and even disruptive sleep apnoea (Margolis *et al*., 1994). Patients eventually become wheelchair- and ventilator-dependent, with respiratory failure the major contributor to premature death (van Capelle *et al*., 2010).

1.2.3: Genetics

Pompe disease is caused by mutations in the GAA gene (MIM# 606800), which is localised to the long arm of human chromosome 17q25.2-q25.3, and is approximately 28 kb in length, contains 20 exons and encodes a precursor protein of 952 amino acids (Martinuik *et al*., 1986). Despite being ubiquitously expressed, studies have revealed quantitative differences in GAA expression between tissue types and during stages of development (Ponce *et al*., 1999). These differences in GAA expression indicate gene regulation at a transcriptional level, but differences in post-transcriptional regulation may also play a role.

More than 372 sequence variations have been identified in the GAA gene, with 248 proven pathogenic mutations (Kroos *et al*., 2012a). GAA gene mutations comprise missense and nonsense base pair changes, variously sized deletions or insertions and splicing defects. These mutations are located across the entire sequence of the GAA gene but are particularly prevalent on exon 14, which has a large number of missense mutations (Huie *et al*., 1998).

The phenotype of Pompe patients is typically dependent on the amount of residual GAA activity. Less than 1% of normal is considered indicative of an infantile-onset phenotype (Kemper *et al*., 2007), whilst one to 30% of normal is suggestive of juvenile- and adult-onset disease (Tager *et al*., 1987). An infantile-onset Pompe phenotype typically involves mutations in both alleles (Kroos *et al*., 2012b). For example, p.Glu176ArgfsX45 (c.525delT) and the deletion of exon 18 (p.Gly828_Asn882del; c.2482_2646del) are predominantly associated with infantile-onset Pompe, with one study in a Dutch population showing the deletion of exon 18 in 10/39 patients (Van der Kraan *et al*., 1994). The Arg854X nonsense mutation is also common in infantile-onset patients of African or African-American descent (Becker *et al*., 1998).

Juvenile- and adult-onset Pompe disease typically result from various combinations of other mutations in alleles (Tager *et al*., 1987). For example, c.336-13T>G results in a leaky splice site that only partially reduces GAA activity (Hermans *et al*., 2004; Montalvo *et al*., 2006), and this correlates with an adult-onset phenotype. The IVS1 -13T-->G transversion in the acceptor splice site was found on one allele in over two thirds of adult-onset Pompe patients (Huie *et al*., 1994).

There is evidence of genotype-phenotype correlation for some common mutations, but genotype-phenotype correlations are not always possible; for example, clinical diversity has been observed within a large cohort of patients with the same genotype and c.-32-13C > T haplotype (Kroos *et al*., 2012). The combination of the Gly643Arg and Arg725Trp mutations in one patient resulted in an infantile-onset phenotype, but led to an adult-onset phenotype in another (Hermans *et al*., 1993). Other genetic and

epigenetic factors are therefore suspected of being involved in the disease process but have not been fully elucidated.

1.2.4: Diagnosis

Suspicion of Pompe disease is typically based on a combination of clinical history, selected tests for cardiomyopathy, including chest radiographs, electrocardiograms, and echocardiograms, and elevated serum levels of creatine kinase, aspartate aminotransferase and alanine aminotransferase; general markers of myopathy (Kemper *et al*., 2007). Following clinical suspicion, Pompe disease is diagnosed by the analysis of GAA activity in blood or tissues, including fibroblasts (Kishnani *et al*., 2006), followed by molecular testing (Bodamer and Dajnoki, 2012).

Fluorometric and mass spectrometry methods for enzyme analysis and detection of analytes in dried blood spots are being progressively used to aid in diagnosis, as these permit high-throughput screening of both newborns and high risk populations. One such screening program in Taiwan, which tested 132,538 newborns using a fluorometric assay, demonstrated that newborn screening was feasible, allowing earlier diagnosis than conventional methods (Chien *et al*., 2008). Mass spectrometric analysis of blood and urine samples have been used to determine the presence of specific tetrasaccharides, which are derived from partially degraded glycogen, as these are elevated in close to 100% of individuals with infantile-onset disease (An *et al*., 2005). However, these tetrasaccharides are not elevated in some juvenile- and adult-onset patients, which limits the usefulness of this technique as a monitor of clinical progression.

1.2.5: Lysosomal acid α-glucosidase

The GAA protein (EC.3.2.1.20) belongs to a group of enzymes known as glycosyl hydrolases (Henrissat, 1998), and specificity acts at the non-reducing end of glycogen to hydrolyse both α -1,4 and α -1,6 glycosidic linkages, liberating glucose (Koster and Slee, 1977). GAA has a pH optimum of 5.1 (Palmer, 1971), making it suited to the acidic environment of the lysosome.

GAA is synthesised as a 100 kDa enzyme in the endoplasmic reticulum (Hoefsloot *et al*., 1988). It has been reported to contain seven N-linked carbohydrate chains (Kroos *et al*., 2008) with a hydrophobic N-terminus where the signal peptide sequence resides. The signal peptide sequence is cleaved at the second potential cleavage site between glycine 28 and histidine 29, after which GAA is termed the precursor form (Oude Elferink *et al*., 1984). The resultant 110 kDa protein is extensively glycosylated and all seven potential glycosylation sites are used (Hermans *et al*., 1993). GAA is then trafficked from the endoplasmic reticulum to the Golgi complex where high mannose-type oligosaccharide side-chains are phosphorylated (Von Figura and Hasilik, 1986), enabling it to bind to the mannose-6-phosphate receptor and traffic to the endosome (**Figure 1.5**). The low pH in late endosomes dissociates GAA from the mannose-6-phosphate receptor and, while the receptor is recycled back to either the trans-Golgi network (Riederer *et al*., 1994) or the cell surface, GAA is targeted to the lysosome.

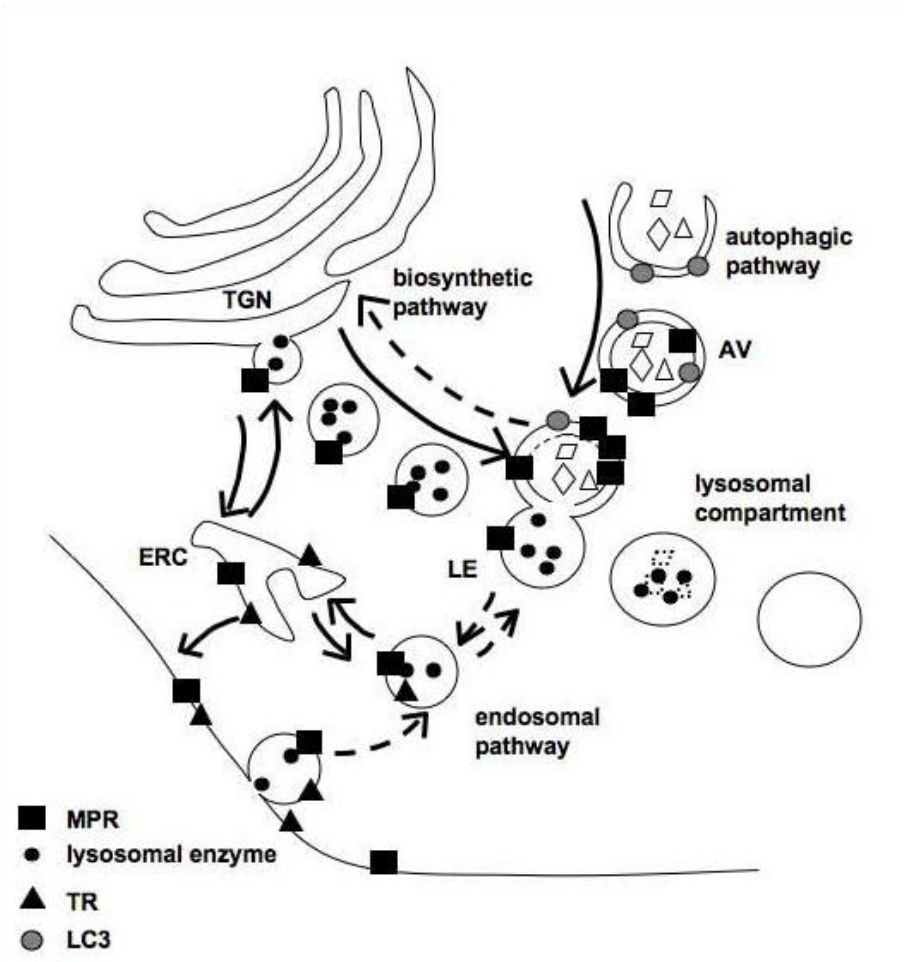

Figure 1.5: Schematic representation of lysosomal enzyme trafficking in cells. Newly synthesised lysosomal hydrolases (i.e. GAA) are trafficked from the trans-Golgi network to late endosomes and finally to the lysosomal compartment. Clathrin independent-mannose-6-phosphate receptors are required for the delivery of lysosomal proteins to the late endosome, with these vesicles maturing into lysosomes. The high acidity of the endosomal/lysosomal compartment results in the mannose-6-phosphate receptor dissociating from the lysosomal protein and being trafficked either to the cell surface or back to the trans-Golgi network. Abbreviations in this figure are trans-Golgi network (TGN), late endosome (LE), autophagosome (AV), endosome recycling centre (ERC), mannose-6-phosphate receptor (MPR) and transferrin receptor (TR). Image from Cardone *et al.*, 2008.

Proteolytic processing occurs in the lysosome to produce mature species of both 76 and 70 kDa (Wisselaar *et al*., 1993). The mature form has a half-life of five- to eight-days (Hirschhorn and Reuser, 2001), in contrast to the precursor form, with an intracellular half-life of only two hours, reflecting the time taken to process and traffic GAA to the lysosome. Catalytic activity of the mature form is seven-fold greater than the 110 kDa precursor, and the 95 kDa form has an intermediate value (Wisselaar *et al*., 1993). The need for proteolytic processing for optimal catalytic activity could relate to a conformational change, which would allow the large substrate, glycogen better access to the catalytic site (Hirschhorn and Reuser, 2001).

1.2.6: Glycogen synthesis and metabolism

Nutritional uptake in animals is only an episodic phenomenon, but the utilisation of glucose proceeds at a relatively constant rate. It is therefore essential to store glucose within the cell, when abundant, for times of high energy expenditure (exercise) or periods of fasting (sleep). Glycogen, also known as β-glycogen, is a polysaccharide of glucose that provides an energy store for the cell. Each glycogen unit, known as a granule, is composed predominantly of glucose, but also contain a number of proteins related to glycogen metabolism, including glycogenin, glycogen synthase and glycogen phosphorylase (Shearer and Graham, 2002). Glycogen enables glucose to be stored in a relatively densely packed conformation, unlike unbound glucose, but permits glucose to be liberated in an energy-efficient manner (Scott and Still, 1970).

The basic structure of glycogen involves layered branched chains of glucose (Marchand *et al*., 2002; **Figure 1.6**). The glucosyl chains are arranged in 12 layers, the

outermost layer lacking branch points and therefore preventing further granule expansion (Elsner *et al*., 2002). Fully expanded and partially completed glycogen structures are found in each cell (Parker *et al*., 2007; Takeuchi *et al*., 1978). The size of purified glycogen granules in a cell can therefore vary widely, and have been reported to range between 10 nm and 80 nm in diameter (Parker *et al*., 2007; Takeuchi *et al*., 1978). Glycogen granules derived from hepatocytes have been found to bind together to form large spherical complexes known as α-particles or α-rosettes, which have a diameter up to 200 nm (Ryu *et al*., 2009). These α-particles have not been observed in other tissue types.

Although glycogen stores are reported in all tissue types in healthy individuals, the concentration varies for each. The main stores of glycogen are localised to the liver and skeletal muscle (Alonso *et al*., 1995), with limited stores in the brain (Cryer *et al*., 2003). The liver contains relatively large stores of glycogen compared to other tissues to provide an energy reserve for other tissues (Alonso *et al*., 1995). In fact, hepatocytes are unique in their ability to traffic glucose to the outside of the cell for use by other tissues (intestinal lumina and kidney cells are the only other exceptions; van Schaftingen and Gerin, 2002). Skeletal muscle has a greater turnover of glycogen than many other tissues as it has a higher energy demand (i.e. for muscle contraction).

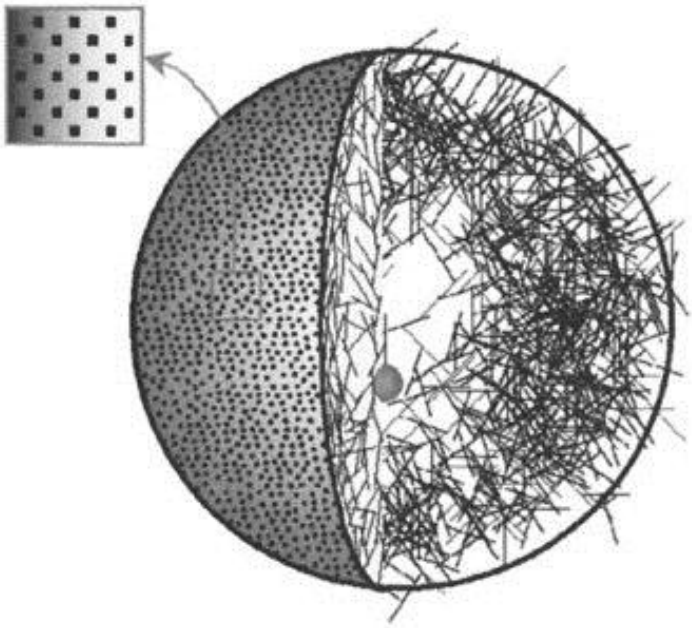

Figure 1.6: Simplified structure of an individual glycogen granule. Each line represents a polysaccharide chain containing multiple glucose residues. The grey sphere in the centre of the glycogen granule represents the primer protein, glycogenin. Image from Meléndez *et al*., 1999.

1.2.6.1: Glycogen synthesis

Extracellular glucose can be trafficked across cell membranes and into the cell, a process requiring the GLUT-4 transporter (Robinson *et al*., 1992). Upon entering the cytosol, glucose is phosphorylated to produce glucose-6-phosphate (G6P). G6P is either metabolised through the pentose-phosphate pathway, trafficked through the Kreb's cycle or converted to glycogen (glycogenesis; Newsholme *et al*., 2003; **Figure 1.7**). The 37

kDa primer protein, glycogenin, initiates glycogen formation from glucose in the cytosol (Hurley *et al*., 2006). Glycogenin undergoes a process of self-glycosylation resulting in glucose attachment. The enzyme glycogen synthase (UDP-glucose-glycogen glucosyltransferase) is responsible for the addition of further glucose molecules and results in an elongation of the polysaccharide chain. When six to 11 glucose residues are linked, the enzyme amylo-1,4 to 1,6-transglucosidase acts to branch the glycogen granule. Through this mechanism large quantities of glucose become attached to the glycogen granule, which will continue to expand until the 12th layer, as the addition of a 13th layer would add a theoretically impossible density of glucose residues to the granule (Goldsmith *et al*., 1982; Roach *et al*., 2012).

Glycogen synthesis is controlled by protein phosphatase-1, which removes the phosphoryl group from glycogen synthase-b, the inactive form of glycogen synthase. This enzymatic reaction contributes to the conversion of glycogen synthase-b into glycogen synthase-a, the active form, leading to glycogen synthesis. Importantly, the pathway for glycogen breakdown is inhibited at the same time that glycogen is synthesised, with phosphorylase kinase and phosphorylase-a being dephosphorylated by protein phosphatase-1 (Berg *et al*., 2002). Protein phosphatase-1 therefore regulates glycogen in an energy efficient manner by preventing its simultaneous synthesis and catabolism.

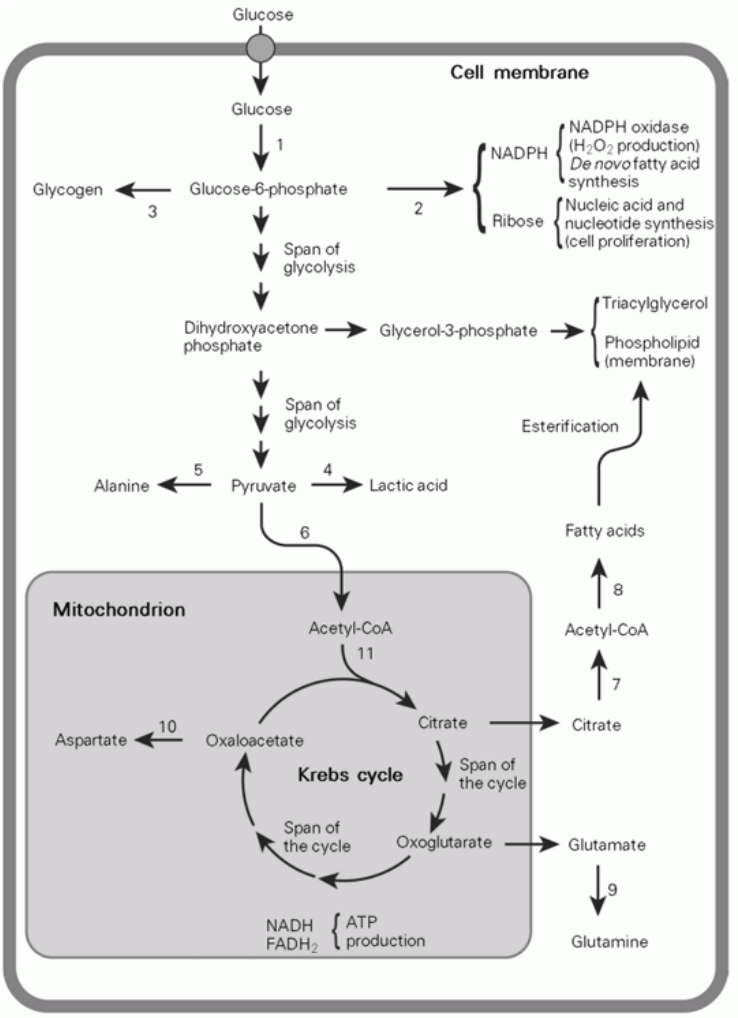

Figure 1.7: An overview of glucose metabolism in mammalian cells. Glucose is converted into G6P after entry into cells (except hepatocytes). G6P is then either converted to glycogen, is metabolised through the pentose-phosphate pathway or is incorporated into the Kreb's cycle. 1, hexokinase/glucokinase; 2, pentose-phosphate pathway; 3, glycogen synthesis; 4, lactate dehydrogenase; 5, alanine aminotransferase; 6, pyruvate dehydrogenase; 7, ATP-citrate lyase; 8, fatty acid synthesis; 9, glutamine synthetase; 10, aspartate aminotransferase; 11, citrate synthetase. Image from Newsholme *et al*., 2003.

1.2.6.2: Glycogen catabolism

Glycogen is catabolised by a number of enzymes, either intra- or extracellularly (Ugorski *et al*., 1983), with intracellular degradation occuring in endosome-lysosome network (discussed further in section 1.2.6.3) or in the the cytosol (Wisselaar *et al*., 1993). The functional role of lysosomal glycogen catabolism is not entirely clear. In the cytosol, glycogen is catabolised by a debranching enzyme and glycogen phosphorylase, with the resultant liberation of glucose contributing to the energy requirements of the cell (Watanabe *et al*., 2008). Neutral α-glucosidase has also been demonstrated to catabolise glycogen in the cytosol (Lavrenova and Presnova, 1994), although the specific role for this soluble amylase with a neutral pH optimum remains unknown (Andersson *et al*., 2004). Extracellular glycogen is catabolised by circulating amylases (Ugorski *et al*., 1983), which have been demonstrated through the presence of partially degraded glycogen in the plasma and urine of healthy individuals (Rozaklis *et al*., 2002).

The majority of cellular glycogen is catabolised in the cytosol and is hormonally triggered in response to either an energy requirement (i.e. muscle) or to raise blood glucose (liver only). Protein phosphatase-1 activates phosphorylase kinase and phosphorylase-a through a phosphorylation reaction, leading to increased glycogen catabolism (Berg *et al*., 2002). The release of glucose from glycogen granules is not a simple reversal of glycogenesis. Debranching enzyme and glycogen phosphorylase are required in concert to catabolise glycogen (Watanabe *et al*., 2008). The major product from the action of these enzymes is glucose-1-phosphate. In the liver, glucose-1-phosphate is converted to G-6-P and then glucose by the action of phosphoglucomutase and glucose-6-phosphatase. In other tissues, glucose-6-phosphatase is only present at

very low concentrations thereby limiting the conversion of G-6-P to glucose. Cytoplasmic G-6-P is then utilised for either glycogen synthesis or as an energy source.

1.2.6.3: Autophagy and lysosomal degradation of glycogen

Autophagy is the mechanism responsible for the delivery of cytosolic glycogen to the endosome-lysosome network. In healthy cells cultured using standard nutrient-rich medium conditions, five to 10% of the total cell glycogen is autophagocytosed (Calder and Geddes, 1989; Kotoulas *et al*., 2004). The reason for glycogen autophagy remains unclear, but may be a way of sensing energy stores in the cell. Glycogen autophagy could provide a rapid and specific glycogen degradation process linked to glucose requirement during high energy demand. Evidence for this comes from the postnatal period, a period of high energy expenditure, where glucose is liberated from liver glycogen in large quantities in a tightly regulated fashion (Kotoulas *et al*., 2004). Alternatively, there may be random autophagic sequestration of cytosolic content, inadvertently capturing glycogen which therefore needs to be degraded. In the course of glycogen turnover, degradation is incomplete, resulting in the accumulation of residual glycogen particles. The autophagic uptake of glycogen may therefore permit the degradation of old glycogen granules that have amassed structural errors over time.

In healthy cells, there is a balance between the autophagosomal uptake of cytosolic glycogen and subsequent catabolism, thereby keeping the amount of vesicular glycogen low. However, the lysosomal catabolism of glycogen has been reported to occur at a lower rate than expected (<1% of the expected maximum rate; Brown *et al*., 1978), which may be partly due to the time taken to deliver the autophagocytosed glycogen to

the phagolysosome (Knecht and Hernández, 1978). The observation of periodic acid-Schiff-stained inclusion bodies (i.e. glycogen granules) within autophagosomes supports this (**Figure 1.8**; Kondomerkos *et al*., 2004). The endosome-lysosome network within healthy cells therefore appears to contain a pool of partially degraded glycogen.

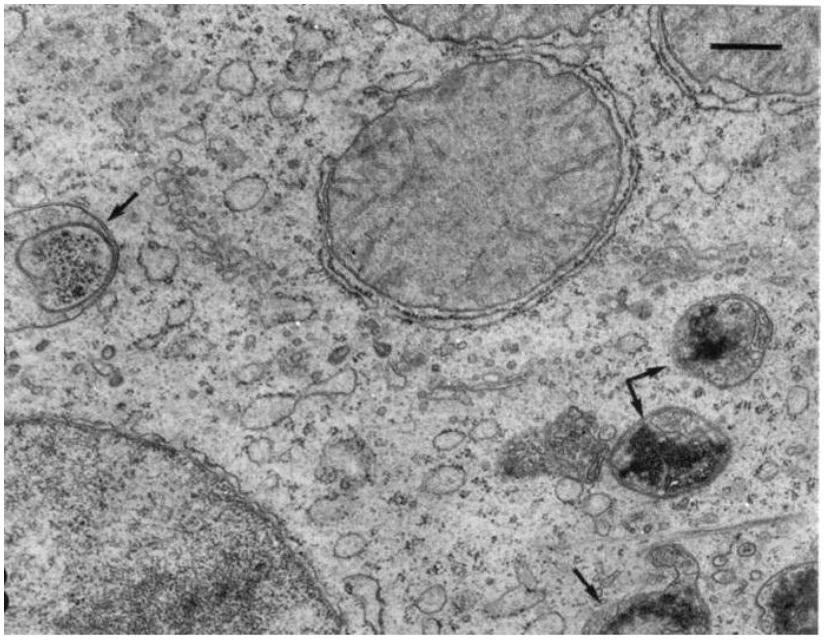

Figure 1.8: Glycogen autophagy in rat hepatocytes during the post-natal period. Electron micrograph images of a rat hepatocyte containing autophagosomes (arrows). Electron-dense inclusion bodies (glycogen) can be visualised inside these autophagosomes. Scale bar equivalent to 0.5 µm. Image from Kotoulas *et al*., 2004.

1.2.7: Glycogen accumulation in Pompe disease

Glycogen accumulation has been observed in a number of Pompe tissues, including skeletal muscle (Lynch *et al*., 2005), cardiac muscle (Raben *et al*., 2005), brain tissue and the cervical spinal cord (DeRuisseau *et al*., 2009). Using a mass spectrometry based glycogen quantification assay, glycogen stores were significantly elevated in type I muscle, type II muscle, heart, brain, skin and diaphragm tissues derived from a mouse model of Pompe disease (GAA knockout; representative of infantile-onset disease), when compared to healthy control tissues (Fuller *et al*., 2012). Type I and type II skeletal muscle had the largest storage of glycogen, with intermediate amounts in the heart and brain. Cultured skin fibroblasts from Pompe patients have also been reported to contain elevated glycogen, with approximately six-fold more vesicular glycogen than that observed in healthy controls (Umapathysivam *et al*., 2005).

In Pompe cells, glycogen can be detected in a number of different compartments, including lysosomes (Raben *et al*., 2005), autophagosomes and late endosomes (Cardone *et al*., 2008; **Figure 1.9**). In most tissues, the relative proportion of glycogen that accumulates in each of these compartments has not been characterised. However, there is a build-up of glycogen-filled autophagosomes in type II skeletal muscle fibres isolated from Pompe mice (Shea and Raben, 2009). In older mice, these glycogen-filled autophagosomes occupy almost 40% of the cellular space (Fukuda *et al*., 2006b). The autophagosomal accumulation of glycogen in type II muscle fibres is expected to disrupt the contractile apparatus, contributing to muscular decay, a hallmark of the pathology in Pompe patients.

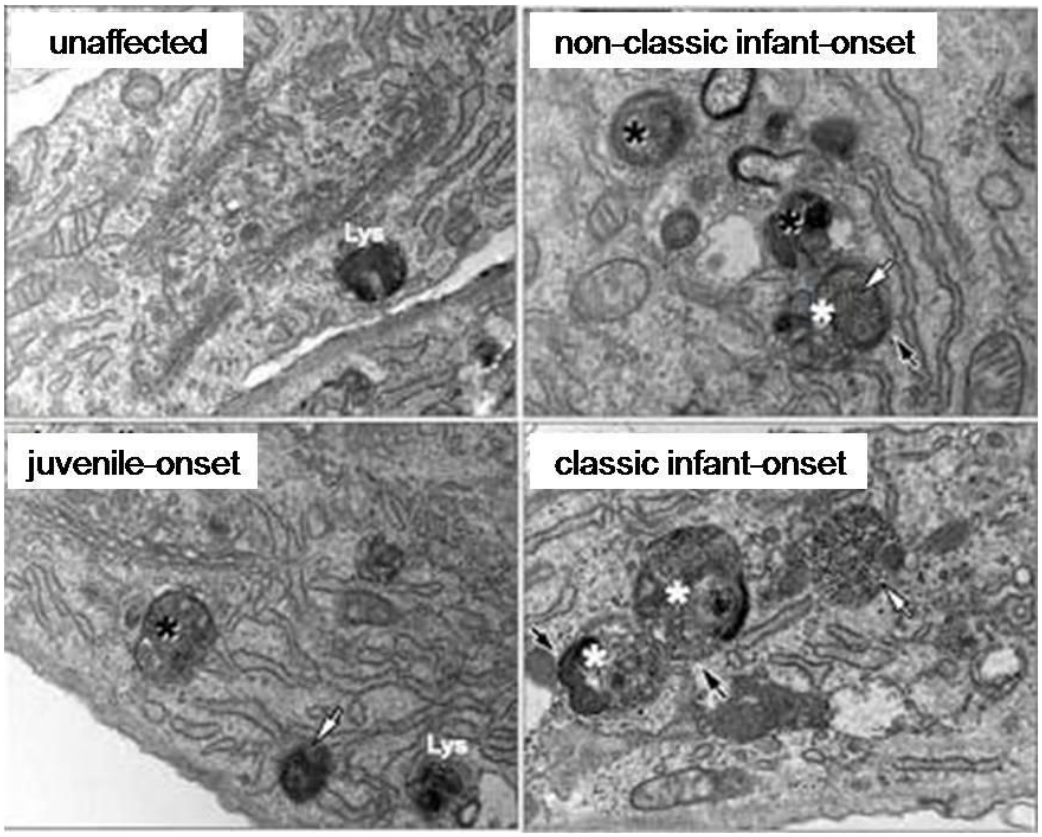

Figure 1.9: The accumulation of glycogen in vesicles from Pompe cells. Electron microscopy of a juvenile, non-classic infantile, classic infantile-onset Pompe and unaffected control human fibroblast. Classic and non-classic infant-onset Pompe skin fibroblasts show increased numbers of glycogen-filled autophagosomes or autolysosomes (white asterisks) which are characterised by double membranes (black arrows). Pompe skin fibroblasts also show an increase in glycogen-filled multivesicular bodies (black asterisks) and lysosomes (white arrows), when compared to the unaffected control. Image adapted from Cardone *et al*., 2008.

1.2.8: Treatment of Pompe disease

Although there is no cure, therapies are available and/or in development for Pompe disease. Current therapies for LSDs typically involve either the replacement of defective enzyme with a functional version or aim to prevent the accumulation of substrate (Vellodi, 2005). Each of these treatments, which include gene therapy (Kyosen *et al*., 2010), chaperone therapy (Parenti *et al*., 2007) and enzyme replacement therapy (ERT; Kishnani *et al*., 2010), has limitations associated with effectiveness.

1.2.8.1: Gene therapy

The direct transduction of all affected cells/tissues with a functional GAA gene (gene therapy) is potentially the most optimal therapy for Pompe disease; but this remains technically difficult and is therefore a longer-term prospect. The transduction of only a limited pool of cells/tissues may also be adequate for a therapeutic effect because transduced cells may release GAA, which can then be delivered to and internalised into peripheral tissues, a process known as cross-correction (Byrne *et al*., 2011).

Two different gene therapy strategies have been employed for Pompe disease; (1) the direct administration of recombinant vectors into target tissues; and (2) autologous transplantation of transfected or transduced cells (fibroblasts, progenitor cells, muscular cells; Sun *et al*., 2010). The direct administration of recombinant vectors that contain the functional GAA gene into target tissues, including lung and liver (Beck, 2010), has been reported to provide transgene expression and subsequent cross-correction in a number of tissues, including cardiac and skeletal muscle in Pompe mice (Sun *et al*., 2008). Other studies in Pompe mice have demonstrated; sustained GAA

activity for up to 24 weeks in cardiac and skeletal muscle and a reduction in glycogen storage within these tissues (Kyosen *et al*., 2010); a significant increase in GAA activity and reduced glycogen content in diaphragm and skeletal muscle (Sun *et al*., 2005, Cresawn *et al*., 2005); and a 70% reduction in cardiac glycogen content one year after treatment (Mah *et al*., 2005). The direct administration of recombinant vectors is therefore promising.

Autologous transplantation involves the transplantation of the patients' own stem cells back into the body once transfected with a functional copy of GAA. In one study, autologous transplantation in Pompe mice resulted in glycogen clearance in heart, diaphragm, spleen, and liver (van Til *et al*., 2010). Respiratory function, skeletal muscle strength, and motor performance were also improved, indicating some correction of central nervous system pathology. However, the clinical efficacy of hematopoietic stem cell transplantation in this study was only partial and cannot completely ameliorate the progression of pathology. Moreover, overcoming the high rate of transplant-related morbidity and mortality remain significant hurdles. Many important issues regarding the safety and efficacy of gene therapy therefore need to be addressed before large-scale clinical trials can be initiated (Beck, 2010).

1.2.8.2: Chaperone therapy

In Pompe disease, as in other LSDs, missense mutations, where a point mutation leads to a single nucleotide change and results in a codon that codes for a different amino acid, have been reported to interfere with the folding, transport and post-translational modification of lysosomal proteins (Okumiya *et al*., 2007). These incorrectly folded

lysosomal proteins can be degraded in the cell by an endoplasmic reticulum-associated process (Flanagan *et al*., 2009), which functions by targeting misfolded proteins for ubiquitination and subsequent degradation by the proteasome system (Lord *et al*., 2005). Despite incorrect folding, these lysosomal enzymes may retain some enzyme activity if trafficked to the lysosome. Chaperones have been reported to increase protein stability (Flanagan *et al*., 2009), by rescuing incorrectly folded proteins from degradation. The treatment of Pompe cells with chemical chaperones was therefore identified as a potential therapeutic strategy.

In cultured human Pompe skin fibroblasts, the chemical chaperone N-butyldeoxynorjirimycin (NB-DNJ; an analogue of the substrate that binds to the active site) has been shown to improve the transport and enhance the stability of the mutant GAA protein (Okumiya *et al*., 2007; Parenti *et al*., 2007). However, a number of adverse effects are associated with NB-DNJ and the effect of its use long-term remain unknown (Porto *et a*l., 2009). Moreover, because only certain mutations can respond to this treatment (Flanagan *et al*., 2009) only about 10 to 15% of patients are expected to benefit (Porto *et al*., 2009). Taken together, these two factors suggest that either alternative chemical chaperones or other therapeutic strategies are required.

1.2.8.3: Enzyme replacement therapy

Enzyme replacement therapy involves the intravenous administration of functional GAA into patients. The infused enzyme, which contains mannose phosphate, can bind to mannose-6-phosphate receptors on the cell surface, thereby allowing endocytic uptake

into the endosome-lysosome network and degradation of the stored substrate (Zhu *et al*., 2009).

In 1991, ERT was first evaluated in the Pompe mouse; demonstrating that GAA was taken-up into muscle and glycogen storage was reduced (van der Ploeg *et al*., 1991). Later, in 2000, ERT was evaluated in infantile-onset Pompe patients and demonstrated prolonged survival, reversal of cardiomyopathy, and motor gains (Van den Hout *et al*., 2004). Clinical trials in infantile-onset patients (Van den Hout *et al*., 2000; Kishnani *et al*., 2006; Kishnani *et al*., 2007) have shown that treatment significantly prolonged ventilator-free survival and overall survival in patients compared with an untreated historical control population (Kishnani *et al*., 2007). FDA approval for alglucosidase alpha (*Myozyme*®; CHO cell derived recombinant human GAA), was granted in 2006 and is the gold standard of infantile-onset Pompe disease treatment.

Despite its beneficial clinical effect, not all Pompe patients displayed reduced glycogen storage or improved muscle architecture in response to ERT (Winkel *et al*., 2003). Possible reasons for this may be elucidated from mouse studies; in one study, administered enzyme did not effectively clear glycogen from type II skeletal muscle, one of the primary sites of pathology (Raben *et al*., 2005). There is evidence of impaired GAA uptake into glycogen-filled autophagosomes (Shea and Raben, 2009), possibly due to an absence of mannose-6-phosphate receptors in late-stage type II muscle fibres (Raben *et al*., 2007). A strong correlation has been demonstrated between the capillary density of muscle fibres and glycogen clearance post-ERT, suggesting that type II fibres may be less accessible to the administered GAA than type I fibres and other tissues (Hawes *et al*., 2007). Glyco-engineering of GAA has been demonstrated to improve

enzyme affinity for the mannose-6-phosphate receptor, and the efficacy of endocytic uptake (Zhu *et al*., 2009). In Pompe mice, this strategy partially improved GAA delivery into muscles, increased glycogen clearance and improved muscular function and strength (Parenti *et al*., 2007).

The development of neutralising antibodies against infused GAA has been reported in approximately 20% of infantile-onset patients (Kishnani *et al*., 2010). Patients who develop antibodies to GAA therapy have a reduction in overall survival, invasive ventilator-free survival and have poorer clinical outcomes (DeRuisseau *et al*., 2009). Neutralising antibodies are typically observed in patients that are cross-reactive immunological material (CRIM)-negative (Kishnani *et al*., 2010); deficient in any residual endogenous GAA protein, with no/little GAA exposure and therefore more likely to recognise GAA as foreign. Conversely, CRIM-positive patients usually have some residual GAA protein.

Efficacy of enzyme replacement is also reduced in infantile-onset patients who commence treatment after excessive accumulation of glycogen has already accumulated (Kishnani *et al*., 2006). Initiation of ERT later than six months of age is associated with a reduced chance of survival, increased heart size, and there are significant reductions in motor skill acquisition, when compared to patients who were treated earlier (Kishnani *et al*., 2007). Early treatment has therefore been identified as a key step in improving the efficacy of ERT for Pompe disease.

The widespread application of ERT is also limited by the high costs associated with both drug manufacture, the clinical care associated with weekly/fortnightly infusions and the relatively high amount of enzyme required; the recommended dose for

Pompe patients is 20 to 40 mg/kg body weight (Kishnani *et al*., 2010); in comparison, the recommended dose for MPS VI patients is 1 mg/kg (Harmatz *et al*., 2010) and Fabry patients is 0.2 mg/kg (Whybra *et al*., 2009). Alternative or adjunct treatment options for Pompe disease are therefore required.

The clearance or prevention of autophagic build-up has been identified as a target for future therapies (Orlikowski *et al*., 2011; Fukuda *et al*., 2006a). The induction of exocytosis, a cellular mechanism expected to release glycogen from the endosome-lysosome network to the outside of Pompe cells, may be one possibility to reduce the amount of glycogen storage in Pompe cells. Exocytosis will therefore be investigated in section 1.3.

1.3: Exocytosis

Exocytosis is a ubiquitous cellular process whereby intracellular vesicles are trafficked to the cell surface, allowing vesicle-plasma membrane fusion and the extracellular release of vesicle content (**Figure 1.10**). Exocytosis is a normal and vital aspect of cellular function and is involved in regulatory and signaling functions, neurotransmission (Calì *et al*., 2009), plasma membrane repair (Gerasimenko *et al*., 2001), melanosome transfer to endothelial cells (Stinchcombe *et al*., 2004), and in maintaining cell surface area during cytokinesis, the process of cell division that divides the cytoplasm of a parent cell into two daughter cells (Boucrot and Kirchhausen, 2008). Exocytosis also functions in the release of vesicular contents such as undegraded waste products, toxins, amino acids, hormones, hydrolases and neurotransmitters.

Two main types of exocytic triggers have been reported in mammalian cells; (1) non-Ca^{2+}-triggered constitutive exocytosis (Ca^{2+}-independent); and (2) Ca^{2+}-triggered non-constitutive exocytosis (Ca^{2+}-dependent; Khvotchev *et al*., 2003). Ca^{2+}-independent exocytosis is not well characterised due to an inability to artificially trigger the process, but is thought to primarily contribute to trafficking newly synthesized proteins from the biosynthetic compartment (Schmoranzer *et al*., 2000). Ca^{2+}-dependent exocytosis has been well characterised, particularly in nerve cells and is known to exocytose lysosomes (Rodríguez *et al*., 1997; Sugo *et al*., 2006). Importantly, Ca^{2+}-dependent exocytosis has been implicated in the release of the primary storage products in metachromatic leukodystrophy (sulphatide; Klein *et al*., 2005) and Niemenn-Pick type C (cholesterol; Chen *et al*., 2010) cells. The defect in GAA leading to an inability to catabolise

vesicular glycogen suggested that Ca^{2+}-dependent exocytosis could release glycogen and may provide a novel therapeutic intervention for Pompe disease.

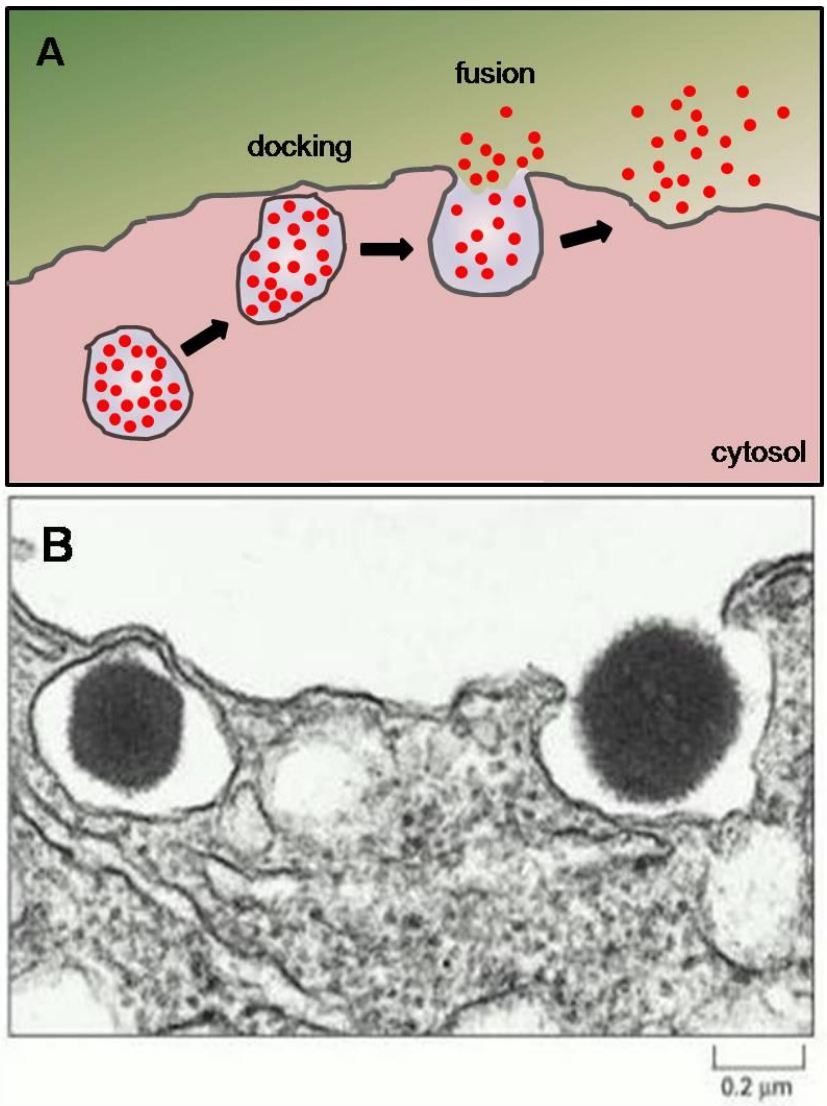

Figure 1.10: The exocytosis of vesicular content. (A) Schematic image of a vesicle fusing with the cell surface and exocytosing content (red circles) into the extracellular milieu. (B) Electron micrograph of a vesicle during the exocytic discharge of electron-dense material (insulin) to the outside of a pancreatic β-cell. Image adapted from Orci *et al*., 1988.

1.3.1: Ca^{2+}-dependent exocytosis

Ca^{2+}-dependent exocytosis has been reported in normal rat kidney (NRK) cells (Rodríguez *et al*., 1999), fibroblasts (Jaiswal *et al*., 2004), skeletal muscle (Kuncl *et al*., 2003), Chinese hamster ovary cells (Jaiswal *et al*., 2002), macrophages (Yogalingam *et al*., 2008) and dendrocytes (Becker *et al*., 2009). Ca^{2+}-dependent exocytosis is involved in hormone release from mast cells (Sagi-Eisenberg, 2007), plasma membrane repair (McNeil, 2002), and the release of lysosomal hydrolases from fibroblasts (Sugo *et al*., 2006).

Ca^{2+}-dependent exocytosis is induced by increasing the cytosolic concentration of Ca^{2+} (Rodríguez *et al*., 1997), with Ca^{2+} derived from either organelle stores (Launikonis *et al*., 2010) or extracellularly (Low *et al*., 2010). In muscle cells, Ca^{2+}-dependent exocytosis can be induced through the release of Ca^{2+} from the sarcoplasmic reticulum; a process responsible for muscle contraction (Launikonis *et al*., 2010). There is a concentration gradient of Ca^{2+} between the cytosol (10^{-4} mM) and the extracellular milieu (1 to 2 mM; Alberts *et al*., 2000). Cell surface plasma membrane damage allows an influx of extracellular Ca^{2+} into the cytosol, leading to Ca^{2+}-dependent exocytosis. Exocytosis then functions to transfer membrane from the vesicle to the cell surface in order to repair the wound (McNeil, 2002). Ca^{2+}-dependent exocytosis is also induced in response to an influx of Ca^{2+} into the cell through voltage-gated Ca^{2+} channels on the plasma membrane (Rizzuto and Pozzan, 2006; Low *et al*., 2010). Cell stimulation and de-polarisation lead to the opening of voltage-sensitive Ca^{2+} channels, and this leads to an influx of Ca^{2+} into the cytosol (Thorn, 2012). Ca^{2+} then diffuses into the cytosol

before being cleared by plasma membrane pumps and transporters (Klingauf and Neher, 1997; Juhaszova *et al*., 2000).

Ca^{2+}-dependent exocytosis operates through different mechanisms. In putative parvalbumin-containing basket cells in the hippocampus, cell surface Ca^{2+} channels and the site of exocytosis are in close proximity, localised within specific nano-domains (Bucurenciu *et al*., 2008). When the Ca^{2+} channels are open the Ca^{2+} concentration in the nano-domains can exceed 100 μM (Oheim *et al*., 2006). This close proximity permits a rapid and efficient induction of the exocytic response (Stanley, 1993). In retinal bipolar cells, Ca^{2+} channels are not associated with nano-domains, leading to a much slower exocytic response (Beaumont *et al*., 2005).

The intracellular messenger, cyclic AMP (cAMP), is a key modulator of Ca^{2+}-dependent exocytosis (Rodríguez *et al*., 1999). Exocytic events involving neurotransmitter release from neurons, hormone secretion from endocrine and neuroendocrine cells, and the secretion of various enzymes from exocrine cells, have each been reported to be modulated by cAMP (Seino and Shibasaki, 2005). An increase in the intracellular cAMP concentration results in a concurrent increase in cytosolic Ca^{2+}concentration, a process regulated by either protein kinase A or the cAMP-sensing protein, cAMP-GEFII (also known as Epac; Ma *et al*., 2005; Seino *et al*., 2009). Other targets of cAMP have also been reported, including exchange proteins activated directly by cAMP, which mobilise Ca^{2+} from the endoplasmic reticulum (Holz *et al*., 2006), cyclic nucleotide-gated channels, hyperpolarisation-activated cyclic nucleotide-gated channels, and cAMP-specific guanine nucleotide exchange factors/exchange proteins, which also mediate Ca^{2+} influx (Seino and Shibasaki, 2005).

The transcription factor, bHLH-leucine zipper transcription factor EB (TFEB), has also been demonstrated to regulate Ca^{2+}-dependent exocytosis (Sardiello and Ballabio, 2009). TFEB functions by inducing the release of intracellular Ca^{2+} through its target gene MCOLN1 and by increasing the population of lysosomes ready to fuse with the cell surface plasma membrane (Sardiello *et al*., 2009). Modulation of TFEB expression has been found to alter the extracellular release of lysosomal cargo, including stored product (Medina *et al*., 2011).

1.3.2: Exocytic mechanism

Vesicles destined for exocytosis are trafficked to the cell surface along the cytoskeletal network by motor proteins such as myosin I α (Raposo *et al*., 1999). The exocyst, an octameric protein complex, mediates the tethering of the vesicle to the plasma membrane, positioning the vesicle at approximately half the diameter of the vesicle from the cell surface (He and Guo, 2009). Rab27a and synaptotagmin (Syt)-like protein 1 (SLP1) or SLP2 mediate the docking of the vesicle at the cell surface, where the two membranes are positioned within a bi-layer's distance of one another (de Saint Basile *et al*., 2010). The vesicle interacts with the cell surface-docking complex, composed of MUNC18-2 and syntaxin 11, and switches syntaxin 11 from a closed to an open conformation. Soluble N-ethylmaleimide-sensitive factor attachment protein (SNAP; possibly SNAP-23) and SNARE proteins (possibly Vamp7 and Vamp8) are associated with the fusion of the vesicle with the cell surface (de Saint Basile *et al*., 2010). The exocyst may also interact with SNARE proteins, thereby allowing SNARE assembly

(He and Guo, 2009). Finally, MUNC18-2 clasps across the zippering four-helix SNARE complex bundle to complete the fusion reaction.

During the fusion process exocytic pores open to permit the release of components from inside the vesicle into the extracellular milieu. Two types of exocytic release events have been described; (1) all-or-none, which involves the complete fusion of vesicles to the plasma membrane; and (2) cavicapture, which involves only a partial fusion between the vesicle and the plasma membrane (**Figure 1.11**; Larina *et al*., 2007).

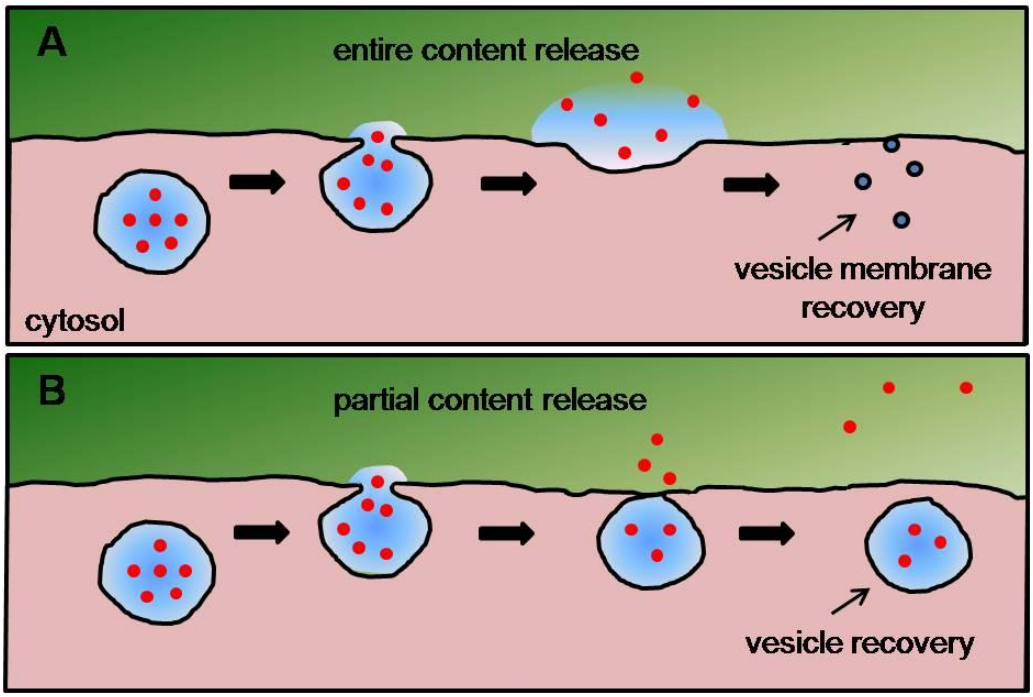

Figure 1.11: The two models for secretion of vesicular content. (A) During all-or-none exocytosis, the vesicle is completely incorporated into the plasma membrane of the cell surface and all of the vesicle content (red) is released from the cell. (B) During cavicapture (graded or partial exocytosis), an exocytic pore opens transiently to permit the release of some of the soluble content. Figure adapted from Thorn, 2009.

1.3.3: All-or-none exocytosis

All-or-none exocytosis is the classical model of exocytic release. The vesicle membrane is fully incorporated into the cell surface, enabling the release of its entire contents (Thorn, 2009). Vesicular membrane proteins are also incorporated into the cell surface and have been reported to provide a vesicle regulatory and intracellular signaling function (Chieregatti and Meldolesi, 2005).

The transfer of plasma membrane from the vesicle to the cell surface contributes to an overall increase in the surface area of the cell (Barg and Machado, 2008). However, the cell surface area is tightly regulated (Chen, 1981), necessitating the induction of endocytosis to internalise membrane and restore the cell surface area to its original size (Barg and Machado, 2008). This maintenance of cell surface area is seen during cell migration in fibroblasts, where an increase in exocytosis at the leading edge of the cell was balanced by an equivalent amount of endocytosis at its trailing edge (Sesaki and Ogihara, 1997), thereby providing an efficient mechanism for cultured cells to migrate with no change in cell surface area. There is, therefore, a regulated balance between the amount of all-or-none exocytosis and the amount of endocytosis.

1.3.4: Cavicapture

Unlike all-or-none exocytosis, cavicapture involves only a transient opening of a pore at the cell surface (Thorn, 2009), enabling the limited release of vesicle content from the cell with little to no membrane transference to the cell surface (Larina *et al*., 2007). Cavicapture has been reported in pancreatic islet β-cells (Rutter *et al*., 2006; Tsuboi *et al*., 2004), endocrine PC-12 cells (Taraska *et al*., 2003) and anterior pituitary cells

(Ferraro *et al*., 2005). The size of the exocytic pore has been reported to vary between different cell types (Larina *et al*., 2007); moreover, the pore diameter and the time the pore remains open has been reported to vary within each cell type (Thorn, 2009). The amount of vesicular material that is exocytosed is therefore dependent on the size of the cargo, the diameter of the exocytic pore and the length of time that the pore remains open.

1.3.5: The contribution of all-or-none exocytosis and cavicapture to the overall amount of exocytosis

The relative contribution of all-or-none exocytosis and cavicapture to the overall release of vesicular content from cultured cells has not been determined (Larina *et al*., 2007), but a number of factors thought to affect fusion pore dynamics have been reported. Ca^{2+} can accelerate fusion pore expansion (Scepek *et al*., 1998) and enhance vesicle content release (Fernández-Chacón and Alvarez de Toledo, 1995); protein kinase C regulates fusion pore expansion (Scepek *et al*., 1998); syt VII, a Ca^{2+}-binding protein, may have multiple roles in the regulation of exocytosis, including being a trigger (Geppert *et al*., 1994), an inhibitor of asynchronous release (Yoshihara and Littleton, 2002), a retriever of vesicular membrane following exocytosis (Jorgensen *et al*., 1995) and an inhibitor of fusion pore dilation (Wang *et al*., 2001); dynamin contributes to clathrin-dependent membrane recovery and may also be involved in the modulation of the fusion pore (Tsuboi *et al*., 2004).

The creation of an F-actin network around the vesicle following fusion has been identified as a possible regulatory control for the dynamics of the exocytic pore (Larina

et al., 2007). F-actin regulates exocytosis by forming a barrier to block SNARE complex formation but also provides transportation tracks for vesicles to traffic to the cell surface (Wang and Thurmond, 2009). When exocytosis is triggered, there is a transient re-organisation of F-actin to allow the vesicle access to the cell surface. F-actin may also regulate the interaction between the vesicle and the cell surface by stabilising the vesicle shape during exocytosis (Sokac *et al*., 2003). Other factors reported to affect pore dynamics include Munc18, which forms a complex with syntaxin-1 (Jewell *et al*., 2011), cysteine string proteins and the SNARE complex-binding protein, complexin II (Jackson and Chapman, 2008), although the detailed mechanism is yet to be fully elucidated.

One study in chromaffin cells has reported that exocytosis can be directed towards cavicapture by increasing the cytosolic Ca^{2+} concentration (Alés *et al*., 1999). The treatment of skin fibroblasts with the Ca^{2+} ionophore, calcimycin, which artificially increases the cytosolic concentration of Ca^{2+}, led to the induction of cavicapture (Jaiswal *et al*., 2004). This may indicate that Ca^{2+}-dependent exocytosis is responsible for cavicapture, whilst all-or-none exocytosis is Ca^{2+}-independent. Cellular components of the exocytic machinery can therefore be manipulated to up-regulate exocytic release.

1.3.6: Evidence for the exocytosis of glycogen in Pompe disease

Although the hallmark of Pompe disease is the accumulation of lysosomal glycogen, a glucose tetrasaccharide (Glc_4) has been observed in both the urine and blood of Pompe patients (Rozaklis *et al*., 2002). This glycogen breakdown product is presumed to arise from circulating amylase digestion (Kumlien *et al*., 1989), implying the release of

glycogen from affected cells into circulation. One possible explanation for this extracellular glycogen is cell death, and there is some evidence for apoptosis in the advanced stages of Pompe disease (Hesselink *et al*., 2003). However, the amount of circulating tetrasaccharide in Pompe appears to be similar in both early- and late-stage disease (An *et al*., 2005), suggesting that cell death is only a partial explanation. An alternative/additional explanation is the release of stored glycogen from muscle and other cells by exocytosis. There is some evidence that the induction of exocytosis results in an overall reduction in glycogen storage in cultured Pompe cells (Medina *et al*., 2011).

1.4: Hypothesis and aims

Exocytosis is a natural process by which content located within the endosome-lysosome network can be released from the cell (Sugo *et al*., 2006). The first hypothesis was that there is a basal level of exocytosis in Pompe cells, some vesicular glycogen is released, and that the identification of a mechanism able to release stored glycogen from Pompe cells could provide an alternative therapeutic target.

The amount of exocytosis in cultured cells is modulated by a number of drugs/compounds, each targeting specific components of the exocytic machinery (Pan *et al.,* 2006; Jaiswal *et al.,* 2002). The second hypothesis was that increased exocytosis from Pompe cells may result in an elevated release of glycogen.

These hypotheses were addressed by the following specific aims:

1. Quantify glycogen exocytosis in Pompe skin fibroblasts.
2. Determine whether exocytosis is impaired in cultured Pompe skin fibroblasts.
3. Determine whether glycogen exocytosis is modulated by culture conditions and define the amount of glycogen that is exocytosed from Pompe skin fibroblasts.
4. Evaluate glycogen exocytosis in Pompe skin fibroblasts with compounds known to increase exocytosis as a therapeutic strategy for Pompe disease.

Chapter 2:

Materials and Methods

2.1: Materials

2.1.1: Solvents, chemicals and reagents

Acetonitrile (HPLC grade)	Unichrom, Ajax Finechem, Auburn, Australia
Amyloglucosidase from *Aspergillus niger*	Sigma Chemical Co., St. Louis, USA
Arachidonic acid	Sigma Chemical Co., St. Louis, USA
Araldite 502	Sigma Chemical Co., St. Louis, USA
BAPTA-AM	Invitrogen, Carlsbad, USA
BD PrecisionGlide™ 23 Gauge needle	BD, Franklin Lakes, USA
Bicinchoninic acid microassay kit	Thermo Scientific, Rockford, USA
BCA protein standards	Thermo Scientific, Rockford, USA
Bovine serum albumin	Sigma Chemical Co., St. Louis, USA
$^{13}C_6$ Glucose	CDN Isotopes, Pointe-Claire, Canada
Calcimycin A23187	Sigma Chemical Co., St. Louis, USA
Carbon film	Obtained from Lyn Waterhouse, Adelaide Microscopy

Chloroform, 1% (v/v) ethanol; HPLC grade	AnalaR, BDH Lab. Supplies, Poole, England
Colchicine	Sigma Chemical Co., St. Louis, USA
Collodion grids	Obtained from Lyn Waterhouse, Adelaide Microscopy
DDSA	Sigma Chemical Co., St. Louis, USA
D-glucose anhydrous	Ajax Chemicals, Auburn, Australia
DMP-30	Sigma Chemical Co., St. Louis, USA
Eicosapentaenoic acid	Sigma Chemical Co., St. Louis, USA
Epoxy embedding medium	Sigma Chemical Co., St. Louis, USA
Filter paper	Obtained from Lyn Waterhouse, Adelaide Microscopy
Fluorophore 488 conjugated goat α-mouse antibody	Invitrogen, Carlsbad, USA
Formic acid, 96% (v/v), analytical grade	Ajax Chemicals, Auburn, Australia
Forskolin	Sigma Chemical Co., St. Louis, USA

Glucagon	Sigma Chemical Co., St. Louis, USA
Glutaraldehyde	Sigma Chemical Co., St. Louis, USA
Hydrochloric acid	Unilab, AnalaR Chemical Co., St Louis, USA
Ionomycin	Sigma Chemical Co., St. Louis, USA
Lead citrate	Sigma Chemical Co., St. Louis, USA
Lysophosphatidylcholine	Avanti Polar Lipids, Alabaster, USA
Membra-Cel dialysis membrane	Serva Electrophoresis, Heidelberg, Germany
4-Methylumbelliferyl-iduronide	Sigma Chemical Co., St. Louis, USA
4-Methylumbelliferyl-2-acetamido-2-deoxy-β-D-glucopyranoside	Sigma Chemical Co., St. Louis, USA
4-Methylumbelliferone standard	Sigma Chemical Co., St. Louis, USA
3-Methyl-1-phenyl-5-pyrazolone	Tokyo Kasei Kogyo Co. Ltd., Tokyo, Japan

Mouse α-LAMP-1 monoclonal antibody clone BB6	provided by SR. Carlsson, Umea, Sweden
Nitrogen	Obtained from Lyn Waterhouse, Adelaide Microscopy
Nonidet (NP-40)	Amersham Life Science, Buckinghamshire, UK
Non-binding 96-well micro-plates	Greiner Bio-One, Frickenhausen, Germany
Osmium tetroxide	Sigma Chemical Co., St. Louis, USA
Paraformaldehyde	Sigma Chemical Co., St. Louis, USA
Phorbol 12-myristate 13-acetate	Sigma Chemical Co., St. Louis, USA
Phosphatidylcholine	Avanti Polar Lipids, Alabaster, USA
Procure 812	ProSciTech, Kirwan, Australia
Prolong Gold nuclear stain	Invitrogen, Carlsbad, USA
Propidium iodide	Sigma Chemical Co., St. Louis, USA
Propylene oxide	Sigma Chemical Co., St. Louis, USA

RNAse I	Sigma Chemical Co., St. Louis, USA
Sphingosine-1-phosphate	Sigma Chemical Co., St. Louis, USA
Sucrose	Ajax Chemicals, Auburn, Australia
Texas-red conjugated fluospheres	Invitrogen, Carlsbad, USA
Texas-red conjugated dextran beads	Sigma Chemical Co., St. Louis, USA
TOX-7 *In Vitro* Toxicology Assay Kit	Sigma Chemical Co., St. Louis, USA
Triton X-100	Sigma Chemical Co., St. Louis, USA
Type IX bovine liver glycogen	Sigma Chemical Co., St. Louis, USA
Un-endcapped C18 solid phase (25 mg/mL) extraction columns	United Chemical Technologies, Bristol,USA
Uranyl acetate	Sigma Chemical Co., St. Louis, USA

2.1.2: Cell culture

Basal Eagle medium	Sigma Chemical Co., St. Louis, USA

Bovine fibroblast growth factor	Sigma Chemical Co., St. Louis, USA
Cell culture flasks (25 and 75 cm^2)	Nunc, Roskilde, Denmark
Cell culture 6-well plates	Nunc, Roskilde, Denmark
Disposable plastic pipettes (5 mL and 10 mL)	Greiner Labortechnik, Frickenhausen, Germany
Dulbecco's modified Eagle's medium	Sigma Chemical Co., St. Louis, USA
Fetal bovine serum	JRH Biosciences, Lenexa, USA
F10 medium	Sigma Chemical Co., St. Louis, USA
Glucose-free Dulbecco's modified Eagle's medium	GIBCO BRL Life Technologies Inc., Grand Island, USA
Penicillin (10^3 units/mL)/streptomycin (10 mg/mL)	Sigma Chemical Co., St. Louis, USA
Phosphate buffered saline, pH 7.2	Sigma Chemical Co., St. Louis, USA
Trypan blue	Cytosystems, Castle Hill, Australia
Trypsin (0.5% v/v)	JRH Biosciences, Lenexa, USA

2.1.3: Buffers and solutions

KH_2PO_4/Na_2HPO_4 buffer	10 mM KH_2PO_4 and 10 mM Na_2HPO_4/HCl, pH 6.5

BCA reagent	50% (v/v) of BCA reagent A; 48% (v/v) of BCA reagent B; and 2% (v/v) of BCA reagent C
Carrying solvent	50% (v/v) acetonitrile/0.025% (v/v) formic acid in H_2O
Complete medium	BME supplemented with 10% (v/v) of FBS
Elution buffer	50% (v/v) acetonitrile and 0.025% (v/v) formic acid in water
Extract buffer	20 mM of Tris/HCl containing 0.5 M of NaCl, pH 7.0
Fixative	methanol/acetone (1:1 ratio)
Glycine buffer	0.2 mol/L sodium glycine, pH 10.3
Glycogen digestion buffer	0.5 mg/mL of amyloglucosidase in 100 mM of sodium acetate, pH 5.0
Heat-inactivated fetal bovine serum	Fetal bovine serum heated for 1 hr, at 70°C
β-Hexosaminidase substrate (0.62 mmol/L)	4.7 mg of 4-methylumbelliferyl-N-acetyl-β-D-glucosaminide in 10 mL of citrate phosphate buffer, pH 4.8
α-L-iduronidase substrate (0.5 mmol/L)	2.3 mg of 4-methylumbelliferyl-iduronide in 10 mL of citrate phosphate buffer, pH 4.8

Internal standard $^{13}C_6$ glucose	2 µg of $^{13}C_6$ glucose in 20 mM CH_3COONa, pH 5.0
Lysis buffer	1 mM of EDTA, 0.1% (v/v) NP-40 and 10 mM of Hepes in sucrose buffer, pH 7.0
Myoblast medium	F10 supplemented with 20% (v/v) of fetal bovine serum, 0.25% (v/v) of bovine fibroblast growth factor and 1% (v/v) of penicillin/streptomycin
3-Methyl-1-phenyl-5-pyrazolone solution A	436 mg of 3-methyl-1-phenyl-5-pyrazolone(250 mM) in 275 µL of 28% ammonia (v/v) and 9.725 mL of water, pH 9.1
3-Methyl-1-phenyl-5-pyrazolone solution B	436 mg of 3-methyl-1-phenyl-5-pyrazolone (250 mM) in 5 mL of methanol, 4.2 mL of sodium hydroxide and 0.8 mL of water, pH 9.1
Propidium iodide solution	0.5% (v/v) of Triton-X 100, 250 µg/mL of propidium iodide and 250 µg/mL of RNAse in phosphate buffered saline

Sucrose buffer	0.25 M of sucrose containing 1 mM of EDTA and 10 mM of Hepes, pH 7.0
Sucrose (25%; w/v)	6.6 g of sucrose in 40 mL of sucrose buffer
Sucrose (50%; w/v)	16.6 g of sucrose in 40 mL of sucrose buffer
Sucrose (75%; w/v)	26.6 g of sucrose in 40 mL of sucrose buffer
Trypan blue (0.1%; v/v)	0.5% (v/v) of trypan blue in water
Uranyl acetate solution	2% (v/v) of uranyl acetate in water

2.1.4: Software and equipment

Alltima C18 3 µm (50 x 2.1 mm) high pressure liquid chromatography column	Alltech, Deer field, USA
Analyst 1.4.1	Applied Biosystems, MDS Sciex, Toronto, Canada
AnalySIS	Soft Imaging System GmbH, Munster, Germany
API 3000 triple quadrapole mass spectrometer	PE SCIEX, Foster City, USA
Autosampler AS90/AS91	Perkin Elmer, Connecticut, USA
Benchtop Biofuge Fresco centrifuge	Thermo Scientific, Waltham, USA
Biohazard hood	Gelman Science, Australia

CellQuest software	BD Biosciences, Franklin Lakes, USA
Dry block heater	Ratek Instruments Pty. Ltd., Boronia, Australia
FACScalibur flow cytometer	BD Biosciences, Franklin Lakes, USA
Haemocytometer	Blau Brand, Wertheim, Germany
Homogeniser	Ratek Instruments Pty. Ltd., Boronia, Australia
HPLC system	Agilent, Santa Clara, USA
Luminescence FL WINLAB version 3	Perkin Elmer, Connecticut, USA
Optima L-100K Ultracentrifuge	Beckman Coulter Inc., Fullerton, USA
Philips CM100 SIS MegaviewII Image Capture Transmission Electron Microscope	FEI Company, Hillsboro, USA
Plate shaker	Ratek Instruments Pty. Ltd., Boronia, Australia
Polyvinylchloride (96-well) plates	Costar, Cambridge, USA
Sciex quantification software	Applied Biosystems, Carlsbad, USA
Slides	Menzel-Glaser, Braunscheig, Germany
Spectral scanning confocal microscope	Leica Microsystems Pty Ltd., North Ryde, Australia

Spectrophotometer	Amersham Biosciences, Buckinghamshire, England
Sterile coverslips	Menzel-Glaser, Braunscheig, Germany
Stirrer	Industrial Equipment and Control Pty. Ltd., Australia
Ultracentrifuge rotor (Ti70)	Beckman Coulter Inc., Fullerton, USA
Victor^3 plate reader	Perkin Elmer, MA, USA
VV-225 Ultrasonic processor	Misonix Inc., Farmingdale, USA
Work Out 2.0 software	Dazdaq Solutions, Brighton, United Kingdom

2.2: Methods

2.2.1: Cell culture

De-identified Pompe and mucopolysaccharidosis type I (MPS I) skin fibroblasts were derived from skin biopsies referred to the National Referral Laboratory for Lysosomal, Peroxisomal and Related Genetic Disorders (Women's and Children's Hospital, Adelaide, Australia) and used in accordance with Women's and Children's Human Research Ethics Committee approval 668/4/2009. Unaffected skin fibroblasts were derived from skin biopsies from apparently healthy volunteers. C2C12 myoblasts were obtained from the American Type Culture Collection (ATCC; CRL-1772).

To revive cells from liquid nitrogen storage, each 1 mL frozen vial of cell suspension was incubated in a 37°C water bath. The cell suspension was resuspended in 9 mL of culture medium that had been pre-warmed to 37°C and was then transferred to a 75 cm^2 culture flask. The culture medium was either Basal modified Eagle's medium (BME) supplemented with 10% (v/v) of fetal bovine serum (FBS; complete culture media; skin fibroblasts) or F10 supplemented with 20% (v/v) of FBS, 0.25% (v/v) of bovine fibroblast growth factor and 1% (v/v) of penicillin/streptomycin (myoblast culture medium; myoblasts). Cells were cultured in 75 cm^2 tissue culture flasks containing 10 mL of complete medium (skin fibroblasts) or myoblast medium (myoblasts) and incubated at 37°C in a humidified atmosphere with 5% CO_2. After seven days of culture (skin fibroblasts) or every four days (myoblasts) the culture medium was decanted from each flask and replaced with 10 mL of fresh medium.

Myoblasts were cultured to a maximum of 70% confluence to prevent differentiation into myotubes.

Skin fibroblasts and myoblasts were sub-cultured by aspirating the culture medium, washing the monolayer twice with 12 mL of phosphate buffered saline (PBS), and then disrupting the cells by incubation with 3 mL of trypsin for 5 minutes at 37°C. Cell suspensions were then transferred to new 75 cm^2 culture flasks (2.5 x 10^5 cells per 75 cm^2 culture flask for skin fibroblasts, and 1 x 10^5 cells per 75 cm^2 culture flask for myoblasts) containing 10 mL of complete or myoblast culture medium and incubated at 37°C.

To deplete the skin fibroblast cultures of cytoplasmic glycogen, cells were cultured in FBS- and glucose-free culture medium. For depletion, the complete culture medium was first decanted from the cells. The cells were then washed twice with 12 mL of PBS to remove residual FBS and then cultured in FBS-free BME containing for 24 hrs at 37°C. After discarding this culture medium, the cell monolayer was washed with 12 mL of PBS (three times) and cultured in glucose-free DMEM for 24 hrs at 37°C.

2.2.2: Preparation of cell extracts

Cells were harvested and resuspended in 10 mL of PBS and centrifuged at 200 *g* for 5 mins. This step was repeated twice before the resultant cell pellet was resuspended in 200 μL of extract buffer. Cells were lysed by sonication for 20 sec at 4°C (continuous, dry cycle 20-30%, output control 3 on a VV-225 Ultrasonic processor). The cell debris was removed by centrifugation (13,000 *g* for 5 mins at 4ºC) and the resulting supernatant (cell extract) recovered and stored at -20ºC until analysis.

2.2.3: Protein quantification

The protein concentration of cell extracts was determined using a bicinchoninic acid (BCA) microassay as previously described (Smith *et al*., 1985). Briefly, for the calibration curve, BSA (0, 2, 4, 6, 8, 10, 15 and 20 μg) was diluted in water to make a total volume of 100 μL in a non-binding 96-well plate (in duplicate). Cell extracts (2 and 5 μL aliquots) were added to individual wells of the 96-well plate, and the volume of each well was made up to 100 μL with H_2O. A 100 μL volume of BCA reagent was then added to each well. For the colour reaction to proceed, the 96-well plate was incubated for 2 hrs at 37^{o}C. The OD_{562} of each well was measured using a Victor^3 plate reader. The amount of protein in each sample was quantified by interpolation through the calibration curve using Work Out 2.0 software.

2.2.4: Cell surface immune-fluorescence

Skin fibroblasts were seeded onto sterile coverslips in 6-well plates at approximately 1 x 10^4 cells/mL (each well containing 2 mL of complete culture medium). Cells were cultured to either 20% to 50% confluence (3.4 to 8.5 x 10^4 cells/well) or confluence (1.7 x 10^5 cells/well). Each well was washed three times with 4 mL of PBS for 5 mins at 4°C on a plate shaker. One hundred μL of mouse α-LAMP-1 monoclonal antibody clone BB6 was then added to each well (diluted to 2.2 μg/mL in complete culture medium) and incubated for 1 hr at 4°C. Wells were then washed three times with 4 mL of PBS for 5 mins at 4°C on a plate shaker. Each well was then aspirated and 100 μL of Fluorophore 488 conjugated goat α-mouse antibody (diluted to 1:1000 in complete

culture medium) was added and incubated in the dark for 1 hr at 4°C. All wells were washed three times with 3 mL of PBS for 5 mins at 4°C on a plate shaker, in the dark. To stain the nucleus, 50 μL of Prolong Gold nuclear stain, containing 4', 6-diamidino-2-phenylindole (DAPI), was added to each coverslip. The coverslip was then inverted onto a microscope slide. Coverslips/cells were stored in the dark at 4ºC until examined on a Leica SP5 spectral scanning confocal microscope at 100X magnification. Fluorescence intensity per unit area was determined using AnalySIS software.

2.2.5: Intracellular immune-fluorescence

To visualise the intracellular location of LAMP-1 in skin fibroblasts, cells were permeabilised and stained by immune-fluorescence using a procedure similar to that described in section 2.2.4. To fix and permeabilise the cells, 1 mL of fixative was added to each well (coverslip) and then incubated for 10 mins at –20°C. Each well was then aspirated and air-dried for 20 mins at 20°C. To prevent non-specific antibody binding, 1 mL of PBS containing 5% (w/v) BSA was added to each well and incubated for 1 hr at 20°C on a plate shaker. Each well was aspirated and 100 μL of monoclonal LAMP-1 antibody (diluted to 2.2 μg/mL in 5% (w/v) BSA in PBS) was added and incubated for 1 hr at 20°C. Each well was washed three times with 4 mL of PBS for 5 mins at 4°C on a plate shaker. One hundred μL of Fluorophore-488 conjugated donkey α-mouse secondary antibody (diluted to 1:200 in 5% (w/v) BSA in PBS) was added to each well and incubated in the dark for 1 hr at 20ºC. All wells were washed three times with 4 mL of PBS for 5 mins at 20°C on a plate shaker, in the dark. To stain the nucleus, 50 μL of Prolong Gold nuclear stain was added to each coverslip; the coverslip was then inverted

onto a microscope slide. Coverslips/cells were stored in the dark at 20ºC until examined on a Leica SP5 spectral scanning confocal microscope at 100X magnification.

2.2.6: Phagocytosis and exocytosis of fluorescent beads in skin fibroblasts

Skin fibroblasts were incubated with fluorescent beads of different sizes to permit phagocytosis and trafficking of the beads into the cell. Cells were cultured to 30% confluence on coverslips in 6-well plates and then washed twice with 3 mL of PBS. Cultures were incubated in the presence of 2.4 nm, 20 nm, 40 nm, 0.1 μm, 0.5 μm, 1 μm and 2 μm beads (texas-red conjugated; diluted 1:1000 in complete medium) and incubated for 4 hrs at 37°C in 5% CO_2. To remove non-internalised beads, each well was washed four times with 4 mL of PBS for 1 min at 20ºC, in the dark on a plate shaker. Cells were treated with the pharmacological compounds described in Chapter 6, section 6.2.1, then fixed and mounted on slides as described in section 2.2.4. Coverslips/cells were examined on a Leica SP5 spectral scanning confocal microscope at 100X magnification, with the number of bead-containing vesicles recorded in at least 20 cells per treatment group. This method required a period of optimisation for Pompe and unaffected skin fibroblasts, including the identification of which sized-beads were able to be phagocytosed, and the evaluation of cell viability in response to bead internalisation (see **Supplementary data A**)

2.2.7: Trypan blue cell viability

To evaluate the viability of cultured cells at harvest, a 20 μL aliquot of cell suspension was mixed with an equal volume of 0.1% (v/v) trypan blue and incubated for 5 mins at

20°C. A 20 µL aliquot of the resultant cell suspension was transferred to a haemocytometer and examined at 100X magnification. Greater than 100 cells were counted within five 1 mm^2 grid squares of the haemocytometer. Non-viable cells were stained blue due to uptake of trypan blue into the cell. Culture viability was evaluated as the percentage of total cells that did not stain blue. Data were not collected from control fibroblast cultures with <90% trypan blue exclusion (Takashima, 2001).

2.2.8: Lactate dehydrogenase assay

A 300 µL aliquot of glucose-free DMEM from cultured cells was mixed with 200 µL of lactate dehydrogenase (LDH) assay substrate, 200 µL of LDH cofactor and 200 µL of LDH dye solution, and incubated for 30 mins at 20°C in the dark, in accordance with the TOX-7 kit instructions. Each reaction was stopped by the addition of 90 µL of 1 N HCl and analysed spectrophotometrically at both 690 nm (background signal) and 490 nm. A sample of glucose-free DMEM was included as a negative control. For the positive control, 10 mL of LDH assay lysis solution (diluted 1:10 in glucose-free DMEM) was added to a flask of cells to release cellular LDH. All assays, including the positive control, were performed in triplicate. The amount of LDH in the culture medium was corrected for total cell protein and expressed as the percentage of LDH released per culture. Data were not collected from control fibroblast cultures with >5 µg/mg of total cell protein LDH release (Legrand *et al.*, 1992).

2.2.9: Glycogen quantification

To quantify glycogen, an electrospray ionisation-tandem mass spectrometry (ESI-MS/MS) assay was used. However, during the course of this study, the assay was adapted to include an in-line liquid chromatographic step (LC/ESI-MS/MS). The assay was altered to improve sample reproducibility and reduce the amount of labour required to prepare each sample (Fuller *et al*., 2012). **Supplementary data B** shows the development, optimisation and validation of the mass spectrometry assays for a range of biological samples, including cell extract and culture medium. Tomas Rozek and Stephen Duplock (Lysosomal Diseases Research Unit, Adelaide) contributed to the development of the ESI-MS/MS and LC/ESI-MS/MS assays and Philippa Davey (Lysosomal Diseases Research Unit, Adelaide) assisted with its validation.

2.2.9.1: Sample, standard and QC preparation

For the ESI-MS/MS assay, a 10-point glycogen calibration curve (final concentration of 0, 2.5, 5, 10, 25, 37.5, 50, 100, 150 and 200 µg/mL of type IX bovine liver glycogen) containing 2 µg/mL of BSA was prepared in water. For the LC/ESI-MS/MS assay, an eight-point glycogen calibration curve (final concentration of 0, 10, 20, 30, 40, 50, 75, and 100 µg/mL of type IX bovine liver glycogen) containing 2 µg/mL of BSA was prepared in water. Calibration curve samples were prepared from 1 mg/mL of glycogen stock prior to each assay, which were stored in 100 µL aliquots at -20^{o}C.

For the ESI-MS/MS assay, quality control (QC) samples of type IX bovine liver glycogen were prepared at low (7.5 µg/mL), medium (30 µg/mL), and high (150 µg/mL) concentrations in water containing 5 µg of C2C12 myoblast cell protein extract

(containing little or no detectable glycogen). For the LC/ESI-MS/MS assay, QC samples of glycogen were prepared at low (15 µg/mL), medium (35 µg/mL), and high (85 µg/mL) concentrations in water containing 0.1 µg of C2C12 myoblast cell protein extract.

To remove residual amylase activity from samples prior to analysis, cell extract and culture medium samples were heated for 15 mins at 100°C; for the ESI-MS/MS assay, samples of culture medium (250 µL) and cell extract (5 µg made up to 10 µL in water) were used; for the LC/ESI-MS/MS assay, samples of culture medium (100 µL) and cell extract (0.1 µg made up to 10 µL in water) were used.

To degrade glycogen to glucose, each standard (20 µL), QC (10 µL) and biological sample (10 µL to 250 µL) was incubated with equal volumes of digestion buffer and KH_2PO_4/Na_2HPO_4 buffer, and 10 µL of internal standard $^{13}C_6$ glucose, then incubated for 2 hrs at 37°C. To inactivate amyloglucosidase following the digestion step, each sample was heated for 5 mins at 100°C, cooled to 4ºC and then lyophilised. To determine background glucose, a separate incubation without amyloglucosidase was included with each sample analysed.

2.2.9.2: ESI-MS/MS analysis of glucose

The method of glucose analysis by ESI-MS/MS was adapted from Rozaklis *et al* (2002). Each sample, QC and standard was resuspended in 100 µL of 1-phenyl-3-methyl-5-pyrazolone (PMP) solution A and derivatised for 90 mins at 70°C. The incubation was terminated by the addition of 1 mL of 0.4 M formic acid. An equal volume of chloroform was added to each sample, mixed vigorously for 60 sec and then centrifuged

at 10,000 *g* for 5 mins. The aqueous layer was passed through a C18 solid phase column (25 mg/mL), pre-treated with 2 x 1 mL of ethanol; the sample was then desalted twice with 2 x 1 mL of H_2O and the column was allowed to dry at 20ºC for 30 mins. After 2 mL of chloroform was passed through the column, the PMP-derivatised sample was eluted with 3 x 200 µL of elution buffer (see Materials). The eluted samples were stored at -20°C until analysis.

One hundred µL of each sample was transferred to an individual well of a 96-well plate, and analysed on a PE SCIEX API 3000 triple quadrapole tandem mass spectrometer with a turbo ion spray source (400°C). The samples (20 µL) were injected using the Autosampler AS90/AS91. Glucose and $^{13}C_6$ glucose internal standard were analysed in positive ion mode using multiple reaction monitoring that measured transitions 511.5/175.0 and 517.5/175.0, respectively. Each ion pair was monitored for 200 ms with a resolution of 0.7 atomic mass units at half-peak height. Glucose concentrations were calculated by relating peak area to the peak area of the $^{13}C_6$ glucose internal standard using Analyst 1.4.2 quantification software.

The glycogen concentration in each sample and QC was calculated by interpolation of the amount of glucose through the glycogen calibration curve, which was then expressed as µg glycogen per mg of cell lysate protein. To exclude background glucose, the amount of glycogen in each sample was estimated by calculating the difference between the amount of glucose in the amyloglucosidase-digested and non-digested sample.

2.2.9.3: LC/ESI-MS/MS analysis of glucose

Each sample, QC and standard was resuspended in 100 µL of PMP solution B, and incubated for 45 mins at 70°C. The reaction was terminated by the addition of 400 µL of 200 mM formic acid. Excess PMP was removed with the addition of 500 µL of chloroform, vigorous shaking for 60 sec, centrifugation at 10,000 *g* for 5 mins, and then discarding the chloroform layer. This step was repeated twice to remove excess PMP. The PMP-derivatised sample was retained at -20°C until analysis.

Each sample (100 µL) was transferred to an individual well of a 96-well plate. Reverse-phase LC separation of PMP-glucose was performed on a 3 µm Alltima C18 column (50 x 2.1 mm) with the sample injected (20 µL) into the column using a Gilson 233 auto-sampler. The HPLC gradient program was 100% mobile phase A from zero to 0.5 mins, 0.5 to 6.4 mins, with a linear ramp to 50% mobile phase B, 6.5 to 7.0 mins at 100% mobile phase B, and 7.01 to 9.0 mins at 100% mobile phase A. A Valco 10-port post-column valve diverted the column flow to waste from zero to 4.1 mins. The retention time for glucose was approximately 6.5 mins. Samples were then analysed as described in section 2.2.9.2.

2.2.10: Dialysis of heat-inactivated fetal bovine serum

Membra-Cel dialysis membrane with a low molecular weight cut-off (14,000) was rehydrated in water for 5 mins at 4°C. The dialysis tubing was sealed at one end with a clamp and filled with 20 mL of heat-inactivated FBS, then sealed at the other end, ensuring no air bubbles remained inside the tubing. To dialyse the heat-inactivated FBS, the membrane was transferred into 500 mL of PBS and incubated for 6 hrs at 4°C with

continual stirring. The PBS was replaced twice during the dialysis at 2 hr intervals. The dialysed heat-inactivated FBS was decanted from the tubing and stored at 4°C until use.

2.2.11: β-Hexosaminidase and α-L-iduronidase activity

Ten μL of cell extract or culture medium was incubated with either 10 μL of α-L-iduronidase substrate (Clements *et al*., 1985) or 100 μL of β-Hexosaminidase substrate (Leaback and Walker, 1961) for 1 hr at 37°C. The reaction was quenched by the addition of 1.6 mL glycine buffer. The liberated 4-methylumbelliferyl (4-MU) in each sample was measured fluorometrically at an excitation wavelength of 358 nm and an emission wavelength of 438 nm. The fluorescence value of the substrate blank was subtracted from that of the samples, and enzyme activity was calculated by relating the fluorescence of the samples to that of the 2.84 nmol 4-MU standard in the same volume of glycine buffer.

2.2.12: Evaluation of cell division in skin fibroblasts

Cultured skin fibroblasts were harvested and washed as described in section 2.2.2. Approximately $1x10^6$ cells were resuspended in 220 μL of propidium iodide solution and incubated in the dark for 30 mins at 20°C. Different stages of the cell cycle were distinguished by the relative proportion of propidium iodide incorporated into the nucleus of each cell (Givan, 2001). To remove excess propidium iodide solution, cells were washed with 1 mL of PBS for 1 min on a plate shaker before final re-suspension in 1 mL of PBS. Cells were then injected into a FACScalibur flow cytometer and the

amount of propidium iodide intercalated into each cell was evaluated using CellQuest software; 20,000 cells were counted for each culture.

2.2.13: Extraction of glycogen from cultured skin fibroblasts

Two 75 cm^2 flasks of Pompe and unaffected skin fibroblasts were cultured to 3 wks post-confluence and then harvested, as described in section 2.2.2. The cells were re-suspended in 1 mL of sucrose buffer (4ºC) and passed through a 23G needle to break up the cells. The cells were then lysed by hypobaric shock (x 6) and centrifuged at 400 *g* to remove cell debris but without breaking the vesicles. The supernatant was decanted and retained at 4ºC until use. To lyse the vesicles present in the supernatant, 5 µL of lysis buffer was added to the supernatant and incubated for 10 mins at 4°C. The supernatant, which contained lysed vesicles, was then layered above a step-wise sucrose gradient (25% (top), 50% and 75% (bottom; v/v)) and centrifuged at 300,000 *g* for 2 hrs at 4ºC. Glycogen was decanted from both the interface of each sucrose layer and the pellet (resuspended in 100 µL of Tris buffer). Samples containing glycogen were stored at -20ºC until analysis. This method was adapted from a protocol provided by Dr. David Stapleton (Department of Biochemistry and Molecular Biooogy, University of Melbourne; Parker *et al*., 2007), with **Supplementary data C** showing the method development for glycogen extraction from a vesicular pool.

2.2.14: Size evaluation of glycogen by electron microscopy

The size of the glycogen granules extracted from cultured skin fibroblasts was determined by electron microscopy (Parker *et al*., 2007). Briefly, mesh collodion grids

were coated with thin carbon film and glow-discharged in nitrogen. Approximately 20 μg/mL of glycogen (prepared in section 2.2.13) was added to each grid and incubated for 30 secs at room temperature. Filter paper was used to draw off excess glycogen and the grids were stained with three/four drops of uranyl acetate buffer; excess buffer was drawn off with filter paper and the grid was allowed to dry for 5 mins at room temperature. Each grid was then examined with a Philips CM100 SIS MegaviewII Image Capture Transmission Electron Microscope. The diameter of at least 600 individual glycogen granules was recorded for each sample.

2.2.15: Electron microscopy of cultured skin fibroblasts

Seventy five cm^2 flasks of Pompe and unaffected skin fibroblasts were cultured to 3 wks post-confluence and then harvested, as described in section 2.2.2. The cell pellet was fixed by immersion in 2% (v/v) paraformaldehyde/2.5% (v/v) glutaraldehyde, buffered in 0.2 M cacodylate, for 4 hrs at 4°C (Glauert and Lewis, 1998). The cell pellet was washed three times in 0.1 M cacodylate (5 mins/wash) and then post-fixed in 2% (v/v) aqueous Osmium tetroxide/0.2 M cacodylate for 2 hrs at 4°C. After three further washes in 0.1 M cacodylate, cells were dehydrated by successive incubations with increased concentrations of ethanol (35, 50, 70, 95 and 100% (v/v)) and then propylene oxide for 15 mins at 20°C. Cells were then embedded by incubation in a 1:1 ratio of propylene oxide/epoxy embedding medium for 12 hrs at 4°C, followed by 100% epoxy embedding medium for 3 hrs at 20°C, then cured for 12 hrs at 60°C. Ultra-thin sections (70 nm) were cut, transferred to mesh collodion grids, stained with uranyl acetate for 2 hrs, then

lead citrate for 5 mins at 20°C. Each grid was examined with a Philips CM100 SIS MegaviewII Image Capture Transmission Electron Microscope.

2.2.16: Statistical analysis

Statistical analysis was performed in consulatation with Nancy Briggs (Data Management and Analysis Centre, Discipline of Public Health, University of Adelaide). Differences between two independent groups of data with a normal distribution were determined by the student T-test, and the significance defined by a P value of <0.05. Data with different sources of variation utilised analysis of variance (ANOVA). In this instance, a repeated measures ANOVA was used and the P-values were adjusted by the Holm's Stepdown Bonferroni procedure.

Chapter 3:

Glycogen Exocytosis in Cultured Skin Fibroblasts

3.1: Introduction

In cultured kidney cells derived from metachromatic leukodystrophy patients, the release of the primary storage substrate, sulphatide, into the culture medium, has been reported (Klein *et al*., 2005). In other studies, exocytosis was induced in Niemenn Pick type C (Chen *et al*., 2010), multiple sulphatase deficiency, MPS type-IIIA and neuronal ceroid lipofuscinoses cells (Medina *et al*., 2011), and was linked to reduced storage product. There is therefore evidence that storage material is exocytosed from cultured LSD cells.

Exocytosis is detected in cultured cells by the extracellular release of soluble acid hydrolases, including β-hexosaminidase (fibroblasts; Sugo *et al*., 2006), N-acetyl-β-D-glucosaminidase (fibroblasts; La Plante *et al*., 2006) and β-glucuronidase (macrophages; Yogalingam *et al*., 2008). LAMP-1 at the cell surface (i.e. in cells not permeabilised by fixation) has also been used as a marker of exocytosis (Qureshi *et al*., 2007), with the luminal domain of LAMP-1 being detected at the cell surface as vesicles interact and fuse with the cell surface. Together, these techniques can be used to monitor exocytosis in a range of cultured cell types.

The amount of exocytosis in cultured cells is modulated by specific media and culturing conditions. Divalent Ca^{2+} ions (Rodríguez *et al*., 1999), protein (Barg and Machado, 2008), lipids/fatty acids (Amatore *et al*., 2006) and hormones (Dyachok and Gylfe, 2004), which are present in culture media, have each been reported to induce exocytosis. The process of exocytosis is increased in cultures at pre-confluence (Roederer *et al*., 1989). The precise reason for the reduction in exocytosis as cultures reach confluence is presumably related to cell-cell contact inhibition (Chen, 1981),

leading to a reduction in the rate of both cell division and migration (Barg and Machado, 2008; Sesaki and Ogihari, 1997).

Pompe skin fibroblasts contain an excess of glycogen in phago-lysosomal compartments (Umapathysivam *et al*., 2005). It was proposed that inducing exocytosis may promote glycogen release from these cells. Lysosomes and late endosomes are known to release soluble content following the induction of Ca^{2+}-dependent exocytosis (Chen *et al*., 2010), suggesting that vesicular glycogen may be released. There is some evidence it results in an overall reduction in glycogen storage in Pompe cells (Medina *et al*., 2011).

Current methods to detect glycogen include digital histomorphometry (Raben *et al*., 2003) and the colourimetric detection of liberated glucose following amyloglucosidase digestion of glycogen (Umapathysivam *et al*., 2005). Recently, a mass spectrometry based glycogen quantification assay has been developed (Fuller *et al*., 2012; see **Supplementary data B**) with greater sensitivity than existing methods. The mass spectrometry based assay can measure as little as 0.1 µg of glycogen in tissue extracts, and may therefore be sensitive enough to detect glycogen that has been released from cells into the culture medium.

The first aim of this chapter was to determine the amount of exocytosis from cultured Pompe skin fibroblasts, and to compare this to another LSD (MPS I, which accumulates glycosaminoglycans) and unaffected fibroblasts (a non-storage control). Two markers of exocytosis were measured; LAMP-1 on the cell suface was used as a marker of cell surface-vesicle interaction and β-hexosaminidase was used as a marker of lysosomal content release from cultured fibroblasts. The amount of exocytosis was

characterised in Pompe skin fibroblasts for culture conditions that were expected to have the greatest influence on exocytosis, namely Ca^{2+} concentration and culture confluence. The second aim of this chapter was to determine whether glycogen was exocytosed from Pompe skin fibroblasts. The amount of glycogen exocytosis was evaluated for Pompe skin fibroblasts by comparing the amount of glycogen in cell extracts with the amount released into the culture medium. The skin fibroblasts were depleted of cytoplasmic glycogen to provide a measure of vesicular glycogen release (>90% cytoplasmic glycogen depletion; Umapathysivam *et al*., 2005). The capacity for culture conditions to influence the release of glycogen was evaluated for Pompe and unaffected fibroblasts.

3.2: Results

3.2.1: Cell surface LAMP-1 staining in non-permeabilised cultured skin fibroblasts

To measure the amount of exocytosis, LAMP-1 staining was evaluated on the surface of infantile Pompe, MPS I and unaffected control fibroblasts. Each of the cultured fibroblast lines used had a similar rate of growth and was limited to less than nine sub-cultures. As shown in **Figures 3.1 A, B and C**, cell surface (external plasma membrane) LAMP-1 fluorescence was observed as small punctate vesicular staining in Pompe, MPS I and unaffected cells, but no difference was observed between the fluorescence intensity or the cell surface distribution of LAMP-1 punctae. Pompe, MPS I and unaffected cells treated with colchicine, a cytoskeletal destabiliser that inhibits exocytosis, demonstrated a 130% reduction in cell surface LAMP-1 fluorescence intensity compared to untreated cells ($P < 0.005$; **Figure 3.1 D, E and F**). There was no difference between the cell surface LAMP-1 fluorescence intensity of colchicine-treated Pompe, MPS I and unaffected cells. The absence of DAPI nuclear staining indicated that the cells were not permeabilised. To confirm this, LAMP-1 staining pattern in Pompe, MPS I and unaffected cells was compared to cells permeabilised by fixation. Permeabilised cells displayed a more extensive staining pattern with larger LAMP-1-positive vesicular structures (**Figures 3.1 G, H and I**), and also demonstrated the presence of DAPI nuclear staining.

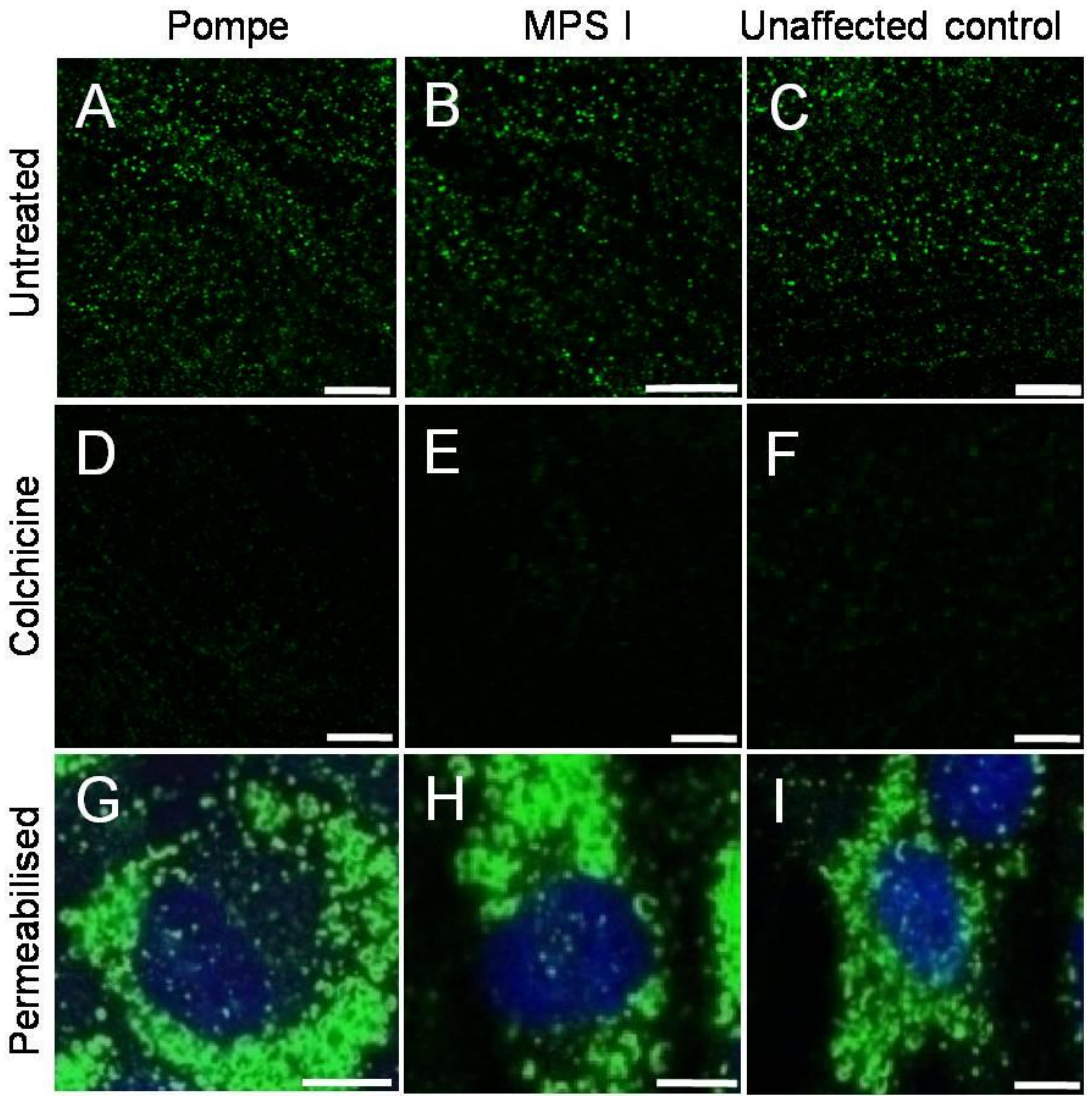

Figure 3.1: Cell surface and intracellular LAMP-1 in cultured skin fibroblasts. Cell surface LAMP-1 staining was performed in non-permeabilised Pompe (A), MPS I (B) and unaffected (C) cells, and Pompe (D), MPS I (E) and unaffected (F) cells that had been pre-incubated in the presence of 1 nM of colchicine for 2 hrs at 37^{o}C. Intracellular LAMP-1 staining of permeabilised Pompe, MPS I and unaffected cells are shown in panels (G), (H) and (I), respectively. Images are an overlay of LAMP-1 fluorescence using the 488 channel (green) and DAPI (blue). Each image is representative of $\geq$ 20 images with each experiment performed in triplicate. Bar is equivalent to 20 nm.

3.2.2: β-Hexosaminidase release from cultured skin fibroblasts

As a second marker of exocytosis, the extracellular release of β-hexosaminidase was determined in Pompe, MPS I and unaffected cells. Cells were cultured to confluence and either depleted of cytoplasmic glycogen (referred to as depleted; see section 2.2.1) or not depleted of cytoplasmic glycogen (referred to as non-depleted). As shown in **Figure 3.2**, there was no difference in the amount of intracellular β-hexosaminidase in any of the depleted cells, when compared to non-depleted cells. β-Hexosaminidase was 2-fold higher in Pompe and 3.5-fold higher in MPS I than unaffected cells. There was rapid extracellular release of β-hexosaminidase from Pompe, MPS I and unaffected cells in the first 30 minutes of culture, which then plateaued over the next 1.5 hours (**Figure 3.3A**). Significantly more β-hexosaminidase was released from Pompe (2.2 +/- 0.4 nmol/min/mg) and MPS I (3.8 +/- 1.9 nmol/min/mg) cells than unaffected control cells (0.9 +/- 0.4 nmol/min/mg; $P < 0.05$). However, when the amount of β-hexosaminidase released was expressed as a percentage of total (i.e. the extracellular amount as a percentage of the combined total amount of intracellular and extracellular β-hexosaminidase), Pompe, MPS I and unaffected cells released the same amount (approximately 2%; **Figure 3.3B**). Cell viability for each cell line was similar, with trypan blue exclusion ≥ 90% and LDH release <5 μg/mg of total cell protein.

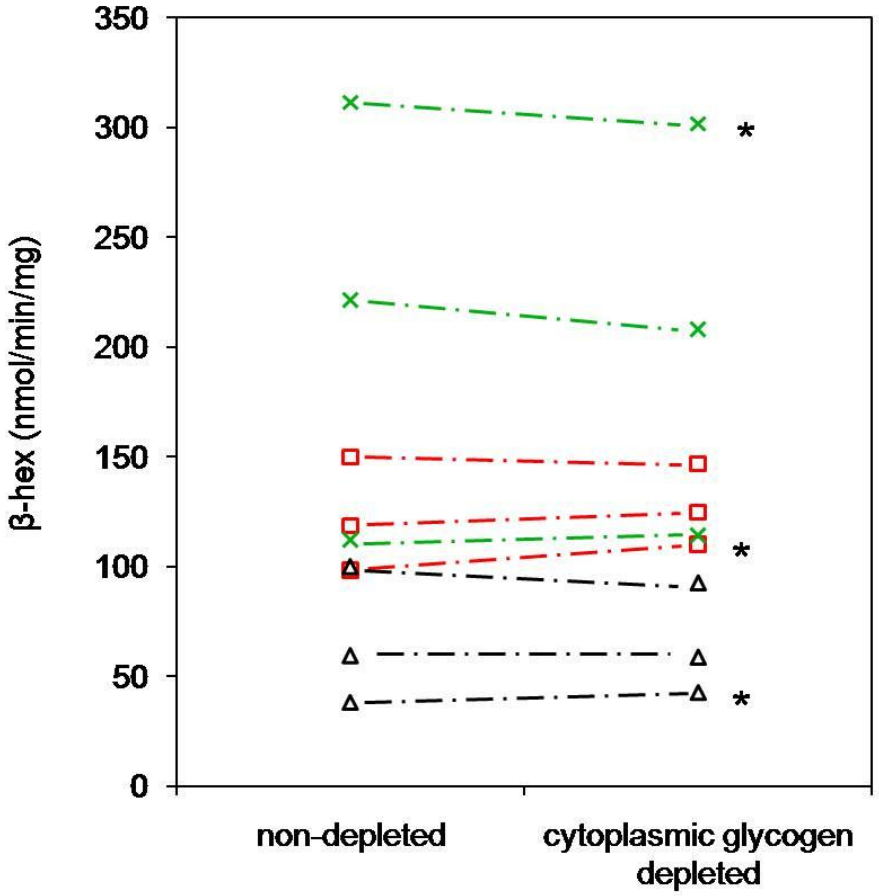

Figure 3.2: Intracellular amounts of β-hexosaminidase in cultured skin fibroblasts. The amount of β-hexosaminidase was determined in cell extracts derived from non-depleted and depleted Pompe (□), MPS I (×) and unaffected (Δ) cells (n=3 cell lines). The activity of β-hexosaminidase is presented as nmol/min/mg of total cell protein. *Indicates cell lines used in all further experiments.

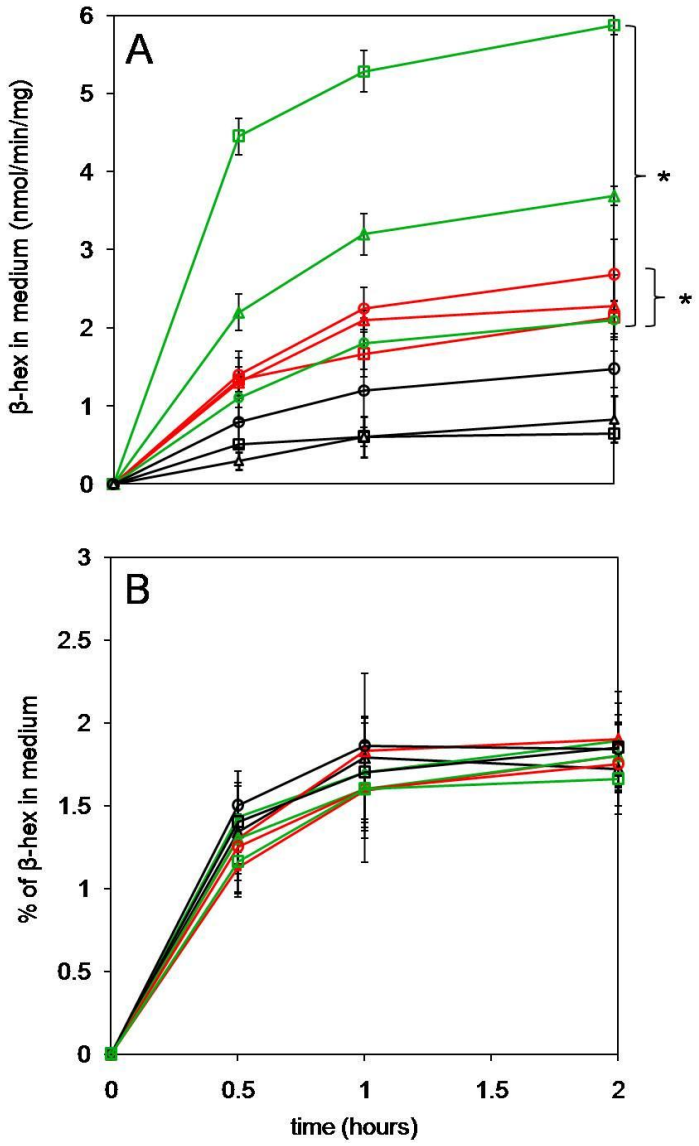

Figure 3.3: β-Hexosaminidase release from cultured skin fibroblasts. The release of β-hexosaminidase (β-hex) was determined from glycogen-depleted Pompe (red), MPS I (green) and unaffected (black) cells (n=3 cell lines; (□), (○) and (Δ)). All cells were cultured in glucose-free DMEM from t = 0 to 2 hrs. In panel (A), results are expressed as nmol/min/mg of β-hex activity released into the culture medium (mean +/- standard deviation (n=3)). In panel (B) results are expressed as the percentage of total β-hex activity in the culture medium (mean +/- standard deviation (n=3)). *Significant difference ($P < 0.05$) when compared to unaffected cells.

3.2.3: Glycogen release from cultured skin fibroblasts

Figure 3.4 shows that there were similar amounts of total cellular glycogen in non-glycogen-depleted Pompe, MPS I and unaffected cells. In the depleted cells, containing predominantly vesicular glycogen, Pompe cells contained the highest amount of glycogen (88 +/- 5 µg/mg) relative to MPS I (47 +/- 11 µg/mg) and unaffected cells (20 +/- 5 µg/mg; $P < 0.05$ for all comparisons). The amount of glycogen released from depleted Pompe cells was 1.4-fold greater than depleted MPS I ($P < 0.05$) and 2.7-fold greater than unaffected cells ($P < 0.005$). Although releasing significantly higher amounts of glycogen, the total percentage of glycogen released from Pompe cells was >70% less than that observed for MPS I ($P < 0.05$) and unaffected control cells ($P < 0.005$; **Figure 3.5B**).

3.2.4: Glycogen and β-hexosaminidase release from colchicine-treated skin fibroblasts

Colchicine-treated Pompe, MPS I and unaffected cells (depleted) showed a ≥ 20% reduction in the release of β-hexosaminidase and glycogen into the culture medium after 2 hrs, when compared to untreated cells ($P < 0.03$; **Figure 3.6**). Trypan blue exclusion was ≥ 90% and LDH release <5 µg/mg of total cell protein for each treatment group.

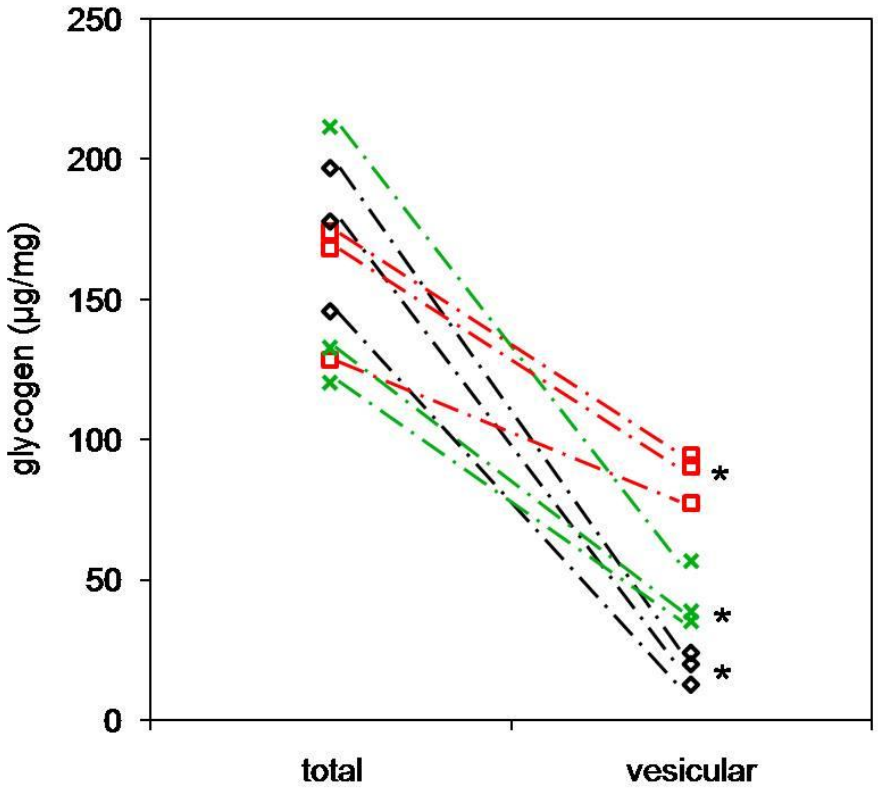

Figure 3.4: Intracellular amounts of glycogen in cultured skin fibroblasts. The amount of glycogen was determined in cell extracts derived from cytoplasmic glycogen-depleted and non-depleted Pompe (□), MPS I (×) and unaffected (Δ) cells (n=3 cell lines). The amount of glycogen is presented as µg/mg of total cell protein. *Cell lines used in all further experiments.

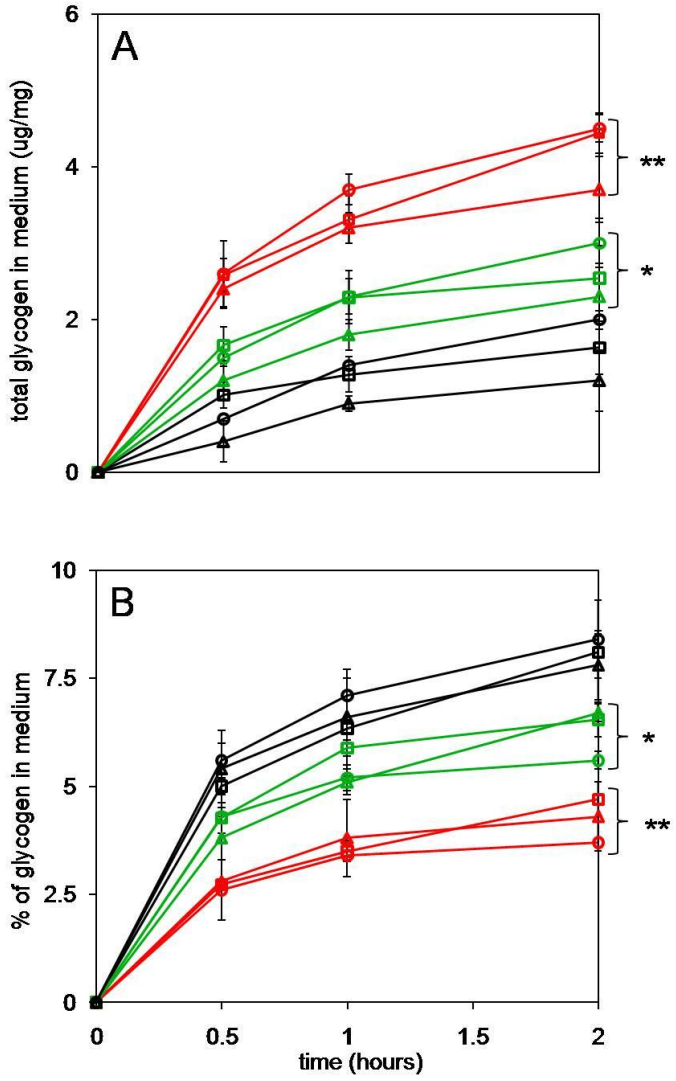

Figure 3.5: Glycogen release from cultured skin fibroblasts. Glycogen release was determined from cytoplasmic glycogen-depleted Pompe (red), MPS I (green) and unaffected (black) cells (n=3 cell lines; (□), (○) and (Δ)). All cells were cultured in glucose-free DMEM from t = 0 to 2 hrs. In panel (A), results are expressed as µg/mg of glycogen released into the culture medium (mean +/- standard deviation (n=3)). In panel (B), results are expressed as the percentage of total glycogen in the culture medium (mean +/- standard deviation (n=3)). *Significant difference ($P < 0.05$) when compared to unaffected cells. **Significant difference ($P < 0.005$) when compared to unaffected cells.

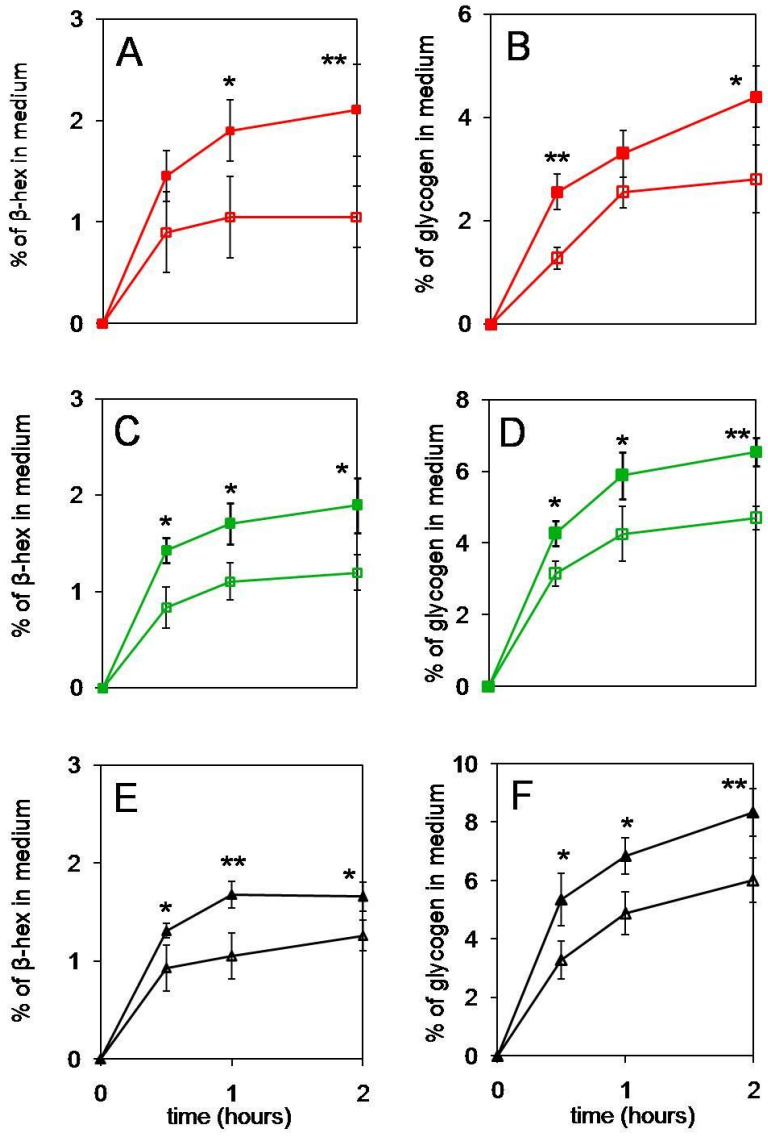

Figure 3.6: Effect of colchicine on the release of β-hexosaminidase and glycogen from cultured skin fibroblasts. The release of β-hexosaminidase (β-hex) and glycogen was determined from cytoplasmic glycogen-depleted Pompe (A and B; red), MPS I (C and D; green) and unaffected (E and F; black) cells. Cells were treated with 1 nM of colchicine in glucose-free DMEM for 2 hrs at 37°C (□) or untreated (■). Results are expressed as the percentage of β-hex/glycogen in the culture medium (mean +/- standard deviation (n=3)). *Significance P <0.05 when compared to untreated controls. **Significance P <0.005 when compared to untreated controls.

3.2.5: The effect of Ca^{2+} on cell surface LAMP-1 staining, and β-hexosaminidase and glycogen release from Pompe skin fibroblasts

The ability of Ca^{2+} to alter the amount of exocytosis and glycogen release in Pompe cells was evaluated; approximately 2-fold more glycogen was released into the culture medium with 2.3 mM of extracellular Ca^{2+} compared to 1.8 mM ($P < 0.05$; **Figure 3.7A**). **Figure 3.7B** shows an increase in the amount of β-hexosaminidase released into the culture medium of Pompe cells treated with 2.3 mM of extracellular Ca^{2+}, but this was not significant when compared to 1.8 mM ($P > 0.05$). Trypan blue exclusion was ≥ 90% and LDH release was <5 µg/mg of total cell protein for Ca^{2+} concentrations of 1.8 mM and 2.3 mM. The amount of LDH release was variable with 2.3 mM Ca^{2+} treatment (3.2 +/- 2.5 µg/mg), as was trypan blue exclusion (93.8 +/- 3.6% of total cells) compared to 1.8 mM Ca^{2+} treatment (93.3 +/- 1.3% of total cells). Pompe cells treated with 3.6 mM Ca^{2+} displayed increased cell permeability, suggesting some cell death, with LDH release at 10.1 +/- 2.1 µg/mg and trypan blue exclusion at 79.2 +/- 4.4% of total cells.

Pompe skin fibroblasts treated with the Ca^{2+} chelator, 1,2-Bis(2-aminophenoxy)ethane-N,N,N′,N′-tetraacetic acid tetrakis -acetoxymethyl ester (BAPTA-AM), which decreases cytosolic Ca^{2+} concentration, showed a ≥ 65% reduction in the amount of glycogen (**Figure 3.8A**) and β-hexosaminidase (**Figure 3.8B**) released into the culture medium, when compared to untreated cells ($P < 0.05$ at 2 hrs). There was no significant difference in the amount of LDH released into the culture medium (3.1 +/- 0.6 µg/mg) or trypan blue exclusion (93.8 +/- 2.4% of total cells) in cells treated with BAPTA-AM, compared to untreated cells. **Figures 3.8C and D** shows that BAPTA-AM-treated cells demonstrated an 80% reduction in the fluorescence

intensity of external plasma membrane LAMP-1 staining compared to untreated cells ($P < 0.05$), while DAPI nuclear staining was similar.

3.2.6: The effect of culture confluence on cell surface LAMP-1, β-hexosaminidase and glycogen release from Pompe skin fibroblasts

The amount of exocytosis and glycogen release was evaluated in Pompe cells at different stages of confluence. Cell cultures at pre-confluence contained a higher percentage of dividing cells, when compared to Pompe cells at confluence (**Figure 3.9**). The percentage of dividing cells remained at 5% for Pompe cells from 90% confluence through to three weeks post-confluence. There was a >3.6-fold increase in the amount of glycogen released into the culture media in cells that had not yet reached confluence (40% and 70%) compared to one week post-confluence ($P < 0.001$ at 2 hrs; **Figure 3.10A**). A greater than 6-fold increase in the amount of β-hexosaminidase released from cells at 40% confluence and 70% confluence was also observed compared to cells at one week post-confluence ($P < 0.001$ at 2 hrs; **Figure 3.10B**). Cell viability was measured at each stage of confluence with trypan blue exclusion ≥ 90% and LDH release <5 µg/mg of total cell protein.

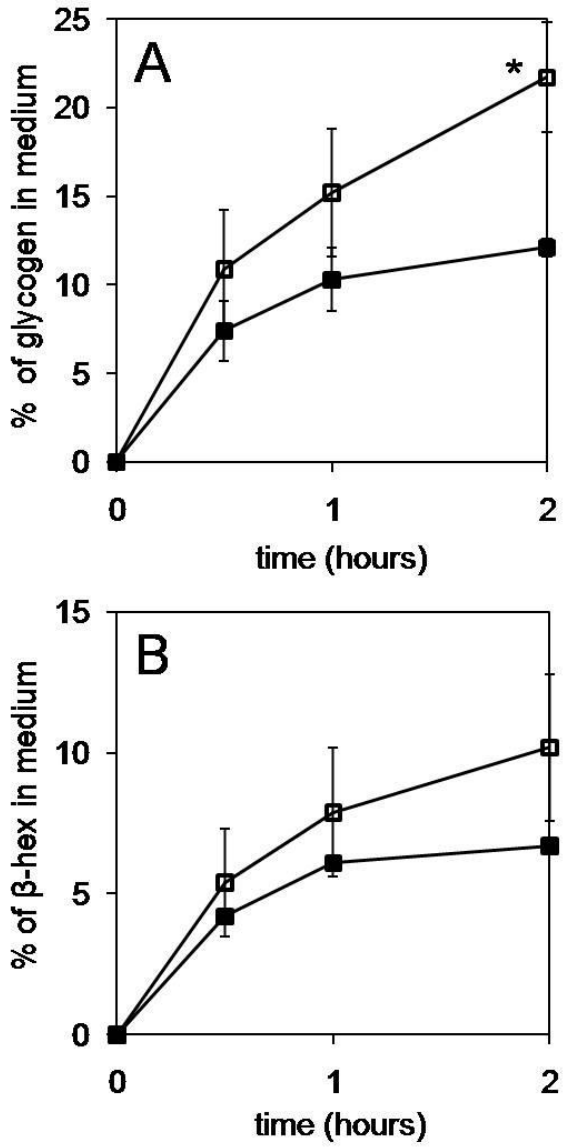

Figure 3.7: The effect of extracellular Ca^{2+} on exocytosis in Pompe skin fibroblasts. Non-glycogen-depleted cells were treated with glucose-free DMEM containing 1.8 mM (■) and 2.3 mM (□) of $CaCl_2$. $CaCl_2$ supplemented DMEM was added to the cells at t = 0; cells were then incubated for 2 hrs. The release of β-hexosaminidase (β-hex; panel A) and glycogen (panel B) was measured and results are expressed as the total percentage released into the culture medium (mean +/- standard deviation (n=3)). *Significance P <0.05 compared to untreated control cells.

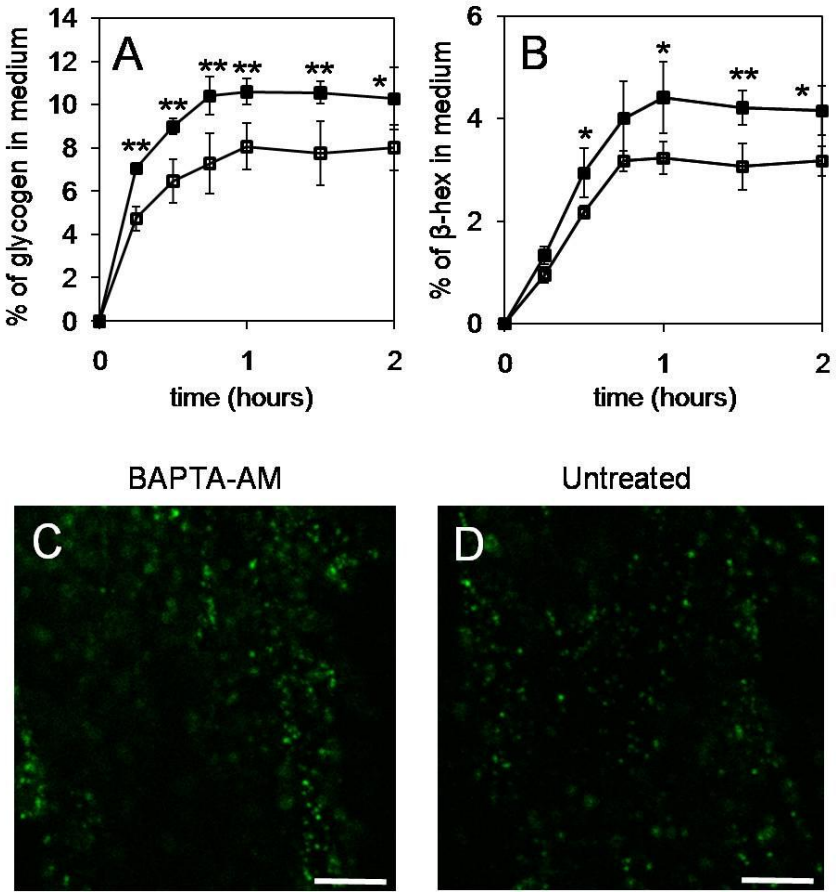

Figure 3.8: The effect of intracellular Ca^{2+} on exocytosis in Pompe skin fibroblasts. Non-glycogen-depleted cells were treated with 10 µM of BAPTA-AM. The BAPTA-AM-supplemented DMEM was added to the cells at t = 0 and cells were incubated for 2 hrs. The release of glycogen (A) and β-hexosaminidase (β-hex; B) into the culture medium of BAPTA-AM-treated (□) and untreated (■) cells was determined. All results are expressed as the percentage of total glycogen and total β-hex released into the culture medium (n=3). Cell surface LAMP-1 fluorescence of non-permeabilised BAPTA-AM-treated and untreated cells is shown in panels (C) and (D), respectively. Images are an overlay of LAMP-1 fluorescence (green) and DAPI (blue). Each image is representative of >20 images. Size bar equivalent to 25 nm. *Significance P <0.05 when compared to untreated controls. **Significance P <0.005 when compared to untreated controls.

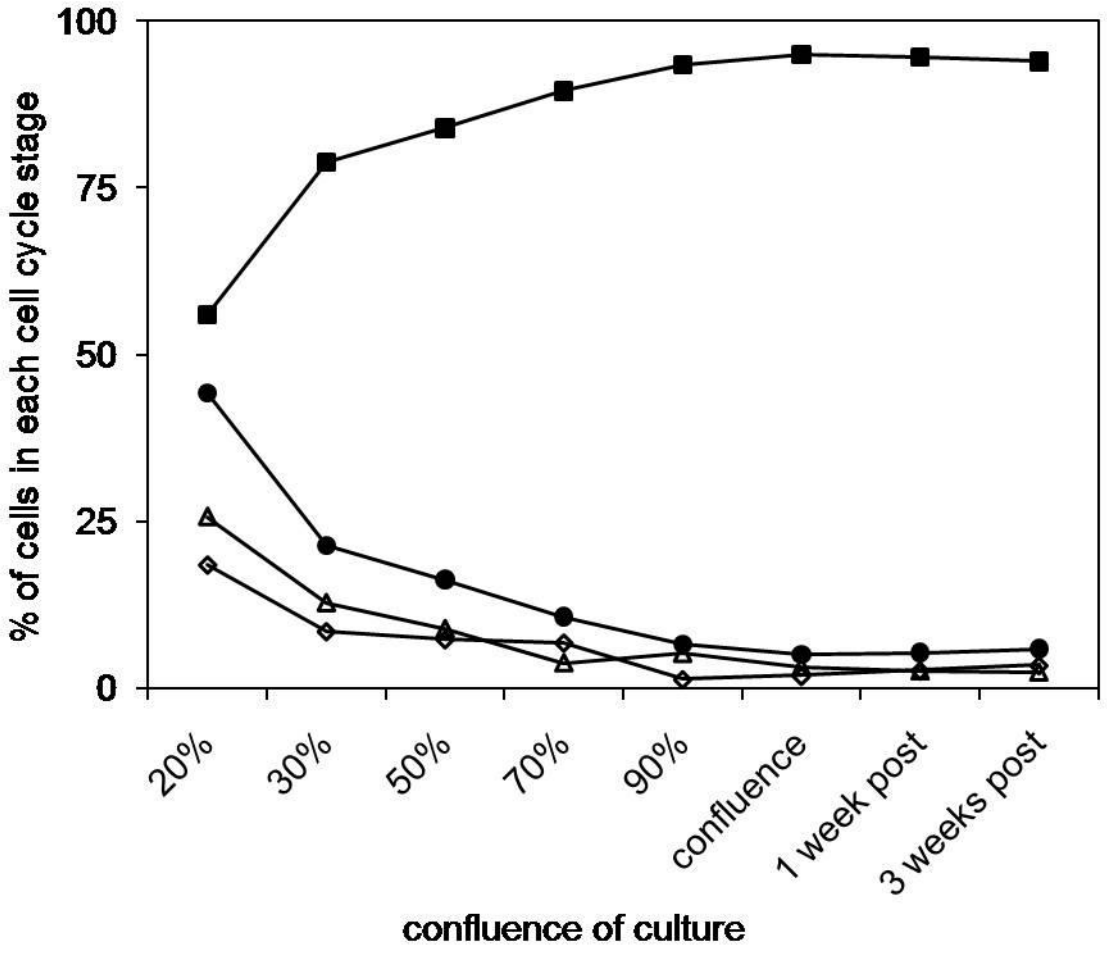

Figure 3.9: Measure of cell division in Pompe skin fibroblast cultures. The percentage of Pompe cells at each stage of the cell cycle was determined for cells from 20% confluence to three weeks post-confluence. Non-glycogen-depleted cells were cultured in DMEM (10% FBS) until harvested. The percentage of Pompe cells in the G0/G1 phase (■; senescent), S phase (◊; growth phase) and G2/M phase (Δ; growth phase) is shown. Data for stages S and G2/M were also combined to provide a total percentage of cells in the growth phase (●). Each data point was evaluated from the measure of 20,000 Pompe cells by flow cytometry.

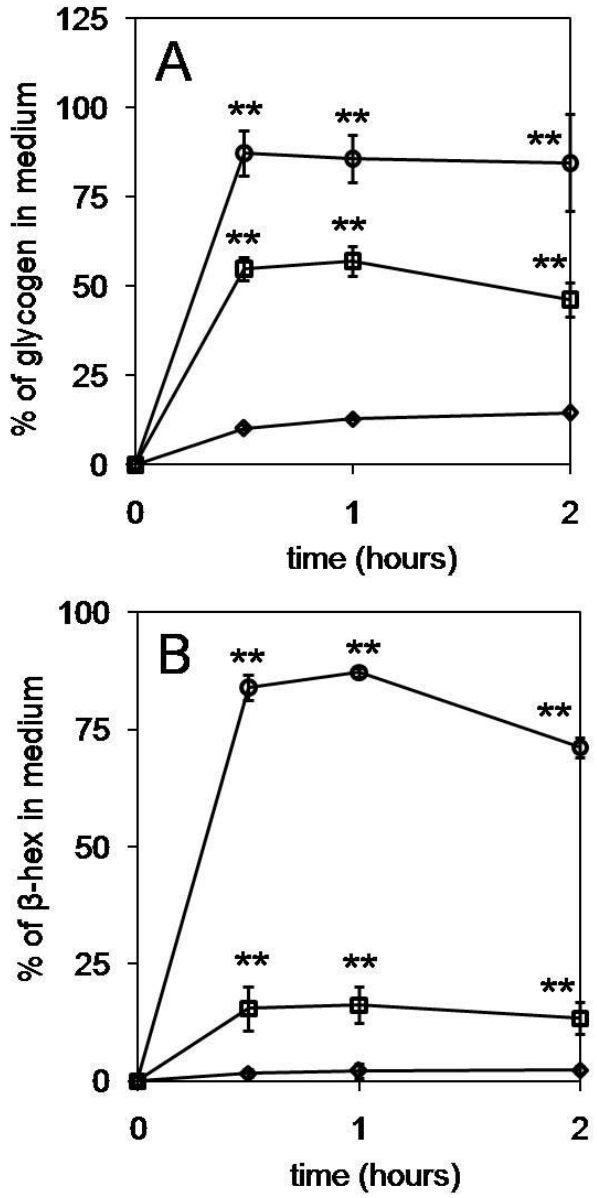

Figure 3.10: The effect of Pompe skin fibroblast culture confluence on exocytosis. The release of glycogen (A) and β-hexosaminidase (β-hex; B) was evaluated in non-glycogen-depleted Pompe cells at 40% confluence (○), 70% confluence (□) and one week post-confluence (◊). Glucose-free DMEM was added to the cells at t = 0 and cells were incubated for 2 hrs. Results are expressed as the mean +/- standard deviation (n=3). **Significance P <0.005 when compared to cells at confluence.

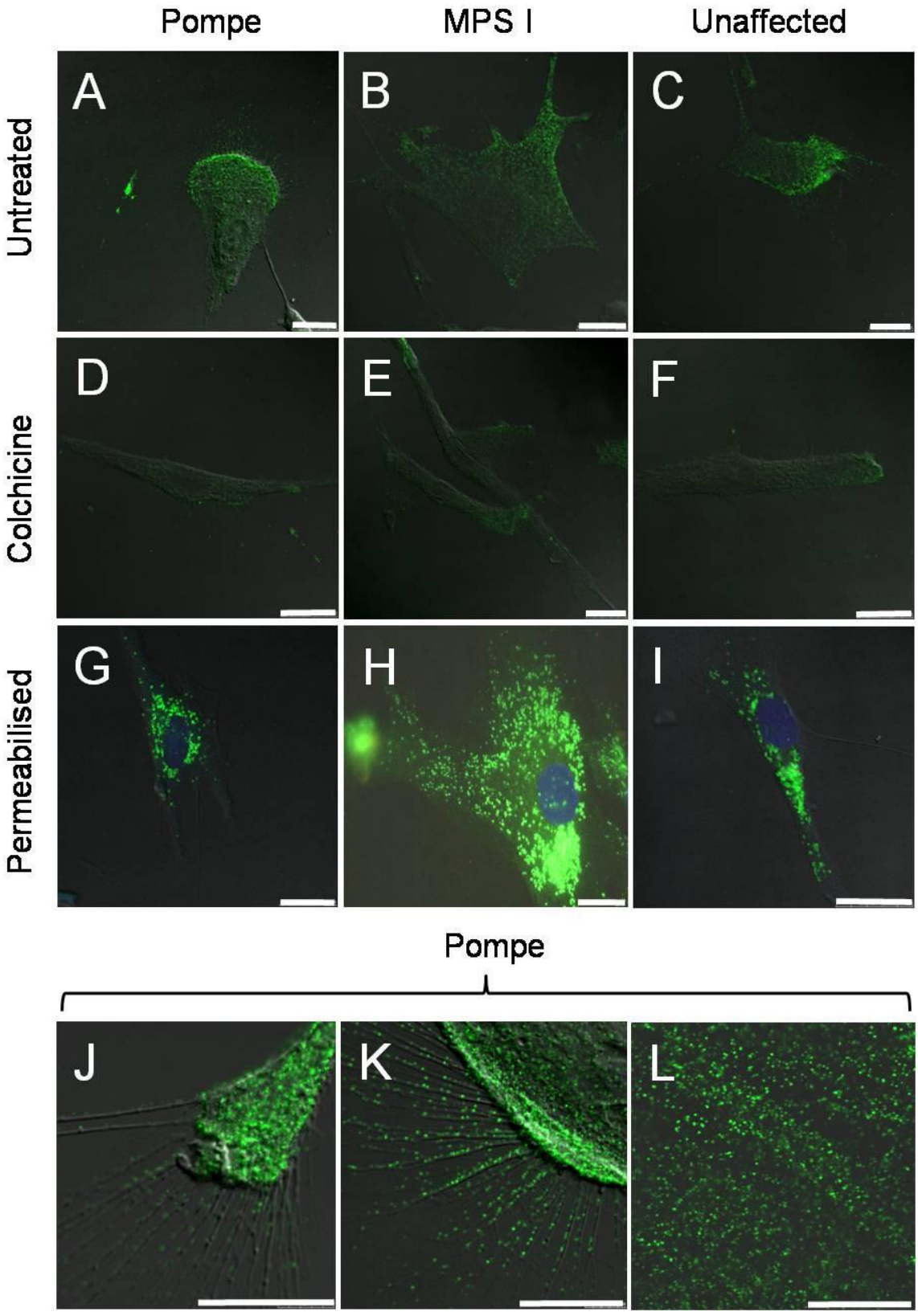
Pompe
MPS I
Unaffected
Untreated
Colchicine
Permeabilised
A
B
C
D
E
F
G
H
I
Pompe
J
K
L

Figure 3.11: The effect of confluence on cell surface LAMP-1 staining. LAMP-1 staining was evaluated in non-permeabilised (cell surface) and permeabilised (intracellular) Pompe, MPS I and unaffected cells at 40% confluence. Cells were non-glycogen-depleted and cultured in DMEM (10% FBS) until harvested. Cell surface LAMP-1 staining was evaluated in Pompe (A, J, K), MPS I (B) and unaffected (C) cells at 40% confluence. Cell surface LAMP-1 staining was also measured in colchicine-treated (1 nM) Pompe (D), MPS I (E) and unaffected (F) cells at 40% confluence (10 min incubation only). Intracellular LAMP-1 fluorescence was determined in permeabilised Pompe (G), MPS I (H) and unaffected (I) cells at 40% confluence. Cell surface LAMP-1 staining of Pompe (L) skin fibroblasts at confluence (i.e. cell-to-cell contact) is also presented. Images are an overlay of LAMP-1 fluorescence (green), DAPI (blue) and DIC. Each picture represents >20 images with each experiment performed in triplicate. Size bar equivalent to 25 nm.

Pompe, MPS I and unaffected cells at 40% confluence displayed punctate cell surface LAMP-1 staining that was localised to distinct areas of each cell (**Figures 3.11A, B and C**) which was associated with ruffling and filopodia (also known as microspikes; **Figures 3.11J and K** for Pompe cells). The amount of cell surface LAMP-1 staining in Pompe, MPS I and unaffected cells at 40% confluence was 1.6-fold higher when compared to cells at confluence ($P < 0.05$; **Figure 3.11L** for Pompe cells). Pompe, MPS I and unaffected cells at 40% confluence were permeabilised by fixation and displayed a more extensive staining pattern and larger vesicular structures than non-permeabilised cells (**Figures 3.11G, H and I**). Pompe, MPS I and unaffected cells at 40% confluence were also treated with colchicine, which showed a >110% reduction in the fluorescence intensity of cell surface LAMP-1 punctae in colchicine-treated (10 mins), when compared to untreated cells ($P < 0.05$; **Figures 3.11D, E and F**). The release of β-hexosaminidase and glycogen from colchicine treated cells at 40% confluence could not be evaluated for ≥ 30 minutes because of a significant reduction in cell viability (≥ 6.9 µg/mg LDH and ≤ 82.3% trypan blue exclusion). In non-permeabilised cells treated with colchicine for <30 mins, trypan blue exclusion was ≥ 90% and LDH release was <5 µg/mg of total cell protein.

3.3: Discussion

Two markers of exocytosis were evaluated in this study; cell surface LAMP-1 staining and the extracellular release of β-hexosaminidase. LAMP-1-positive punctae have been used to define Ca^{2+}-triggered exocytic events at the cell surface of non-permeabilised NRK cells, keratinocytes and fibroblasts (La Plante *et al*., 2006; Medina *et al*., 2011). Newly synthesised LAMP-1 is predominantly transported from the trans-Golgi network to endosomes/lysosomes via an intracellular route (Eskelinen *et al*., 2003). Surface expression of LAMP-1 primarily results from the recycling of endosomal/lysosomal membrane via the exocytic/endocytic pathways (Eskelinen *et al*., 2003). The activity of β-hexosaminidase in cell extracts and culture medium has been used to determine the amount of exocytosis in cultured cells (Sugo *et al*., 2006). β-Hexosaminidase is also released from the cell through the secretory pathway (Sagherian *et al*., 1994), however, based on the biosynthetic rate of β-hexosaminidase, the amount of enzyme release via this pathway is expected to be minimal (≤ 3% after 24 hours in culture; Von Figura and Weber, 1978).

The fluorescence intensity and cell surface distribution of LAMP-1 was similar in Pompe, MPS I and unaffected skin fibroblasts. While the amount of intracellular β-hexosaminidase varied between Pompe, MPS I and unaffected cells the percentage of total β-hexosaminidase released into the culture medium after 2 hrs was similar for all three cell lines (approximately 2%) and was consistent with previous reports on unaffected cultured fibroblasts (1.5 to 5%; Martinez *et al*., 2000; Rodríguez *et al*., 1997). The amount of exocytosis in Pompe, MPS I and unaffected cells was therefore similar,

as measured by two exocytic markers (cell surface LAMP-1 staining and the extracellular release of β-hexosaminidase).

Ca^{2+}-dependent exocytosis is capable of releasing lysosomal content from the cell (Sugo *et al*., 2006), with glycogen potentially released as part of this event. Pompe cells depleted of cytoplasmic glycogen, and therefore containing predominantly vesicular glycogen, released glycogen into the culture medium. Glycogen was also shown to be exocytosed from cytoplasmic glycogen-depleted MPS I and unaffected cells. However, cytoplasmic glycogen depleted Pompe cells, which contained ≥ 2-fold more vesicular glycogen than both depleted MPS I and unaffected cells, released more glycogen into the culture medium, indicating that glycogen in Pompe cells may be available for exoytic release.

The treatment of cultured cells with colchicine, a cytoskeletal destabiliser, has been reported to inhibit exocytosis through its action on microtubules and this is thought to impede vesicle traffic to the cell surface (Kuncl *et al*., 2003). Colchicine treatment of Pompe, MPS I and unaffected cells led to a >20% reduction in cell surface LAMP-1, β-hexosaminidase and glycogen release with no change in cell viability. This result for β-hexosaminidase release was similar to that observed in NRK cells, with colchicine treatment leading to a 15% reduction (Rodríguez *et al*., 1997). Treatment of fibroblast cells with colchicine therefore inhibits exocytosis and glycogen release.

In Pompe, MPS I and unaffected fibroblast cells, there was a rapid increase in the release of β-hexosaminidase and glycogen into the culture medium for the first 30 mins, followed by a plateau in β-hexosaminidase release between 30 and 60 mins in culture. In NRK cells (Rodríguez *et al*., 1997), fibroblasts (Chen *et al*., 2010) and mast cells

(Tiwari *et al*., 2008) exocytosis has also been reported to plateau after time in culture. Extracellular β-hexosaminidase can be re-internalised into fibroblasts by endocytosis (Von Figura and Weber, 1978) and may therefore contribute to this plateauing effect. In contrast to β-hexosaminidase, glycogen release did not plateau between 30 and 60 minutes in culture, although there was a reduction in the amount of release. There are no reports of glycogen endocytosis in cultured cells, but this may be responsible for the partial reduction in glycogen release after time in culture.

Two culture conditions, Ca^{2+} concentration and culture confluence, were used to modulate exocytosis and glycogen release in Pompe cells. Elevated concentrations of Ca^{2+} in the culture medium has been reported to increase the extracellular release of acid hydrolases from cells (Martinez *et al.,* 2000), whereas a decrease in Ca^{2+} resulted in a reduction (Li *et al*., 2008). Here, Ca^{2+} was demonstrated to be a minor contributor to the amount of exocytosis and glycogen release in Pompe skin fibroblasts. There was only a 70% increase in the release of β-hexosaminidase from Pompe cells cultured in high Ca^{2+}, whilst a 300% increase in β-hexosaminidase release has been reported in Ca^{2+}-treated NRK cells (Martinez *et al.*, 2000). Similarly, there was a 65% reduction in the release of β-hexosaminidase from Pompe cells when the intracellular concentration of Ca^{2+} was reduced with BAPTA-AM, whereas similarly treated NRK cells displayed a 200% reduction (Ito *et al.*, 2002). Cultured fibroblasts therefore appear to be less susceptible to exocytic induction with Ca^{2+} than other cell types.

In contrast to Ca^{2+} modulation, exocytosis and glycogen release varied significantly in cultures at different stages of confluence. Pompe cell cultures with a high percentage of dividing cells were shown to release >75% of the total cell β-

hexosaminidase and >85% of the glycogen into the culture medium after only 2 hrs of culture, which was >7-fold higher than that observed in confluent cells. The ability to release such a high percentage of total cell glycogen from non-depleted Pompe cells at pre-confluence was unexpected, as confluent cells only contain approximately 50% vesicular glycogen, with the remainder of glycogen localised to the cytoplasm. A potential explanation for this high percentage of glycogen release may be that during cell growth cytoplasmic glycogen is rapidly autophagocytosed to provide an energy source to drive these processes, thereby depleting the cytoplasmic stock of glycogen and providing a pool of vesicular glycogen that is susceptible to exocytic release. An increase in glycogen autophagy to provide an energy source has been demonstrated in liver cells during the post-natal period, a period of high energy demand (Kotoulas *et al.*, 2004).

Cell division and migration are elevated in cultures at pre-confluence (Boucrot and Kirchhausen, 2007). An increase in the amount of exocytosis has been reported during cell division, occuring at the cleavage furrow as cells divide (Goss and Toomre, 2008), but also during cell migration, localised to the leading edge of the cell (Sesaki and Ogihara, 1997). No increase in cell surface LAMP-1 staining was observed at the cleavage furrow of dividing Pompe cells. Golgi-derived vesicles, but not endosomal or lysosomal compartments, have been linked to increased exocytosis during cell division (Goss and Toomre, 2008), implicating Ca^{2+}-independent exocytosis. In sub-confluent, migrating Pompe cells, there was an increase in cell surface LAMP-1 staining at the leading edge of the cell, in areas of ruffling and filopodia. These structures are involved in the transfer of membrane from an intracellular location to the cell surface, thereby

enabling forward motion (Sesaki and Ogihara, 1997). The elevated exocytosis associated with sub-confluent Pompe skin fibroblasts, as measured by increased LAMP-1 staining and β-hexosaminidase release, may therefore be related to cell migration.

When expressed as a percentage of total cellular glycogen for each cell, Pompe cells released the lowest proportion of vesicular glycogen compared to MPS I and unaffected cells (**Figure 3.12**). However, the amount of exocytosis for each of these cell lines was similar, as determined by the presence of cell surface LAMP-1 staining and the release of β-hexosaminidase into the culture medium. This suggested the reduced glycogen release from Pompe (and to a lesser extent MPS I) cells was not due to impaired exocytosis per se. One possible explanation is that Ca^{2+}-induced exocytosis, which is the likely mechanism responsible for glycogen release, results in cavicapture (Jaiswal *et al*., 2004), the partial release of vesicle content through an exocytic pore. An explanation for this reduced glycogen exocytosis may be that the glycogen granules in Pompe cells may be larger in diameter than those in unaffected cells, and therefore limited in their ability to be exocytosed. Alternatively, the diameter of the exocytic pore in Pompe cells may be restricted, when compared to unaffected cells, which will also limit glycogen release. These two possible mechanisms for the reduced release of glycogen from Pompe cells will be examined in Chapter 4.

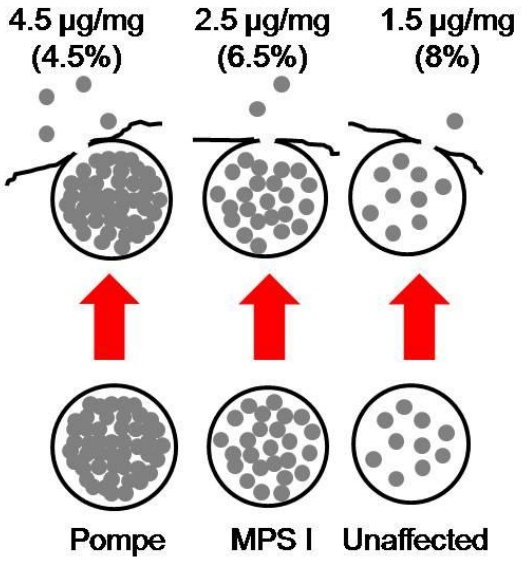

Figure 3.12: Exocytic release of glycogen from cultured skin fibroblasts. Comparison of the amount of vesicular glycogen (●) released from cytoplasmic glycogen-depleted Pompe, MPS I and unaffected cells. Data are presented as µg of glycogen in the culture medium per mg of total cell protein or the total percentage of glycogen released into the culture medium. The amount of lysosomal glycogen exocytosed from each cell line is representative of the data from **Figure 3.5**.

MPS I cells were included in this study as these accumulate different storage substrates to Pompe cells, namely glycosaminoglycans. However, MPS I cells were shown to contain more glycogen than unaffected cells, indicating elevated vesicular glycogen stores. While the defect in GAA explains increased glycogen in Pompe cells, a defect in α-L-iduronidase would not be expected to result in glycogen storage. It remains unknown as to why glycogen accumulates in MPS I cells, and further studies are required. However, it could be speculated that glycosaminoglycan storage in MPS I

cells either impairs the catalytic activity in endosome-lysosome compartments or limits lysosomal fusion and therefore degradation in autolysosomes.

In this chapter, we showed no impairment of exocytosis in Pompe cells as defined by cell surface LAMP-1 staining and β-hexosaminidase release. Glycogen was exocytosed from these cells. Importantly, glycogen release from Pompe fibroblasts was up-regulated by the culture conditions, presumably due to specific effects on the exocytic machinery. This provided proof of concept that glycogen may be triggered to rapidly re-locate from Pompe cells to the outside of the cell, opening the possibility for manipulating this process.

Chapter 4:

Induction of Glycogen Exocytosis in Pompe Skin Fibroblasts

4.1: Introduction

Exocytosis of stored substrate from LSD cells has been achieved with compounds that are capable of modulating the exocytic process or by the over-expression of proteins involved in the exocytic machinery. Kidney cells derived from metachromatic leucodystrophy patients treated with ionomycin demonstrated increased release of sulphatide (Klein *et al.,* 2005), when compared to untreated control cells, with a concomitant 5-fold increase in β-hexosaminidase release. In another study, transcription factor EB, a regulator of exocytosis, was over-expressed in cells derived from Pompe, multiple sulphatase deficiency, MPS IIIA and neuronal ceroidlipofuscinoses, leading to an increase in lysosomal exocytosis, as measured by the extracellular release of lysosomal enzymes and increased cell surface LAMP-1 staining (Medina *et al*., 2011). This increase in exocytosis led to an overall reduction in total cell storage, ranging from 20% (MPS IIIA) to 60% (multiple sulphatase deficiency), when compared to control cells. The culture medium and growth conditions investigated in chapter 3 had an effect on the exocytosis of both β-hexosaminidase and glycogen for Pompe skin fibroblasts. It was hypothesised that glycogen exocytosis could be induced with compounds previously shown to increase exocytosis (Santini and Beaven, 1993; Baram *et al.,* 1999).

Compounds that induce exocytosis in cultured cells do so by either a Ca^{2+}-dependent (Rodríguez *et al*., 1997) or a Ca^{2+}-independent (Amatore *et al.,* 2006) response. Ca^{2+}-dependent exocytosis has been well characterised and is known to release soluble enzyme content from lysosomes (Jaiswal *et al.,* 2002). Ca^{2+}-dependent exocytosis operates by increasing the cytosolic concentration of Ca^{2+} (Baram *et al.,*

1999), involving either the recruitment of extracellular Ca^{2+} (i.e. culture medium; Rodríguez *et al*., 1997) or liberation of Ca^{2+} from organelle stores (Pan *et al*., 2006). Calcium ionophores, including calcimycin and ionomycin, induce Ca^{2+}-dependent exocytosis by enabling a direct influx of Ca^{2+} into the cell across the plasma membrane (Rodríguez *et al*., 1997; Pressman, 1976). One study in mast cells demonstrated the release of approximately 15% of the total cellular β-hexosaminidase into the culture medium when treated with 1 µM calcimycin (Baram *et al.,* 1999). Sphingosine 1-phosphate (S-1-P) induces Ca^{2+}-dependent exocytosis by releasing Ca^{2+} into the cytosol from intracellular stores (Meyer ZuHeringdorf, 2004). The physiological function of S-1-P is mediated by specific G-protein coupled receptors, which are capable of activating a phospholipase C-dependent pathway, allowing Ca^{2+} liberation from organelle stores (Taha *et al*., 2004). In one study, the treatment of bovine chromaffin cells with S-1-P led to an increase in membrane capacitance in patch-clamp experiments, indicating elevated exocytosis (Pan *et al*., 2006).

Compounds that increase cytosolic cAMP concentration also induce Ca^{2+}-dependent exocytosis (Grapengiesser *et al*., 1991), with cAMP involved in vesicle recruitment and this can act directly on the exocytic machinery (Tengholm, 2012). Glucagon increases the secretion of insulin from pancreatic β-cells, with a Ca^{2+} stimulated elevation of cAMP, which is associated with a protein kinase A-dependent activation of inositol 1,4,5-trisphosphate receptors (Dyachok and Gylfe, 2004). Forskolin increases insulin secretion from pancreatic cells, raising cAMP concentration by activating adenylate cyclase (Kasai *et al*., 2005). Phorbol 12-myristate 13-acetate (PMA) induces enlargeosome exocytosis in PC-12 cells (derived from rat adrenal

medulla pheochromocytoma (Cocucci *et al.*, 2007)), which involves activating protein kinase C (Kasai *et al.*, 2005). However, in the Cocucci *et al* study, there was no apparent increase in cytosolic Ca^{2+} concentration, indicating that PMA may induce exocytosis by an alternative mechanism.

Ca^{2+}-independent exocytosis is up-regulated in cultured cells in response to the induction of endocytosis (Barg and Machado, 2008). One study showed an increase in exocytosis in macrophages cultured in the presence of albumin, a protein known to be internalized by receptor mediated endocytosis (Besterman *et al.*, 1983). The receptor-mediated uptake of protein from the culture medium leads to a reduction in the amount of plasma membrane at the cell surface (Barg and Machado, 2008), necessitating the induction of exocytosis to traffic plasma membrane back to the cell surface and maintain the surface area of the cell (Chen, 1981). Cells containing vesicles with a specific lipid composition also demonstrate an elevated amount of Ca^{2+}-independent exocytosis (Amatore *et al.*, 2006). The supplementation of culture medium with lysophosphatidylcholine (LPC), arachidonic acid (AA) and eicosapentaenoic acid (EPA), has been reported to trigger Ca^{2+}-independent exocytosis (Amatore *et al.*, 2006; Ong *et al.*, 2006). Exposure to these compounds in culture is thought to lead to their incorporation into vesicular membranes, thereby changing membrane curvature to a more suitable configuration for vesicle-plasma membrane fusion (Amatore *et al.*, 2006), but may also alter membrane fluidity, ion channel permeability and membrane-bound enzyme activity (Ong *et al.*, 2006).

The first aim of this chapter was to determine the amount of exocytosis and glycogen release from Pompe skin fibroblasts treated with modulators of both Ca^{2+}-

dependent and Ca^{2+}-independent exocytosis. S-1-P, calcimycin, ionomycin, glucagon, forskolin and PMA were selected as Ca^{2+}-dependent modulators of exocytosis. LPC, EPA, arachidonic acid and the recombinant lysosomal protein, α-L-iduronidase, that is rapidly internalised into cultured fibroblasts by receptor-mediated endocytosis (Unger *et al.*, 1994), were selected as modulators of Ca^{2+}-independent exoytosis. Phosphatidylcholine (PC) was used as a control for general lipid uptake as it was not expected to change membrane curvature. The second aim of this chapter was to determine the proportion of glycogen that can be released from Pompe cells treated with the most effective modulator of exocytosis.

4.2: Results

4.2.1: Toxicity assessment of compound-treated Pompe skin fibroblasts

Confluent Pompe cells depleted of cytoplasmic glycogen (i.e. containing predominantly vesicular glycogen) were treated with modulators of exocytosis at a range of concentrations to determine the threshold dose for toxicity, with the selected range based on previously published exocytosis studies (**Table 4.1**). **Table 4.2** (Ca^{2+}-dependent modulators) and **Table 4.3** (Ca^{2+}-independent modulators) show the concentration range for each compound that was evaluated. Cell viability did not change in Pompe cells treated for 2 hrs with each of the concentrations of S-1-P (0-80 µM), forskolin (0-200 µM), glucagon (0-100 µM), LPC (0-100 µM), PC (0-500 µM), PMA (0-1 µM) and α-L-iduronidase (0-1 µg/mL), when compared to the untreated controls (>90% trypan blue exclusion and <5 µg/mg LDH release). In Pompe cells treated with high concentrations of the calcium ionophores, calcimycin (2 to 3 µM) and ionomycin (0.5 to 3 µM) and the fatty acids, AA (0.1 µM) and EPA (100 µM), there was a reduction in cell viability (<90% trypan blue exclusion and >5 µg/mg LDH release), when compared to untreated controls. However, at lower concentrations no significant differences were observed in cell viability when compared to the untreated controls. Non-toxic doses of each compound were evaluated for glycogen release and markers of exocytosis, with the results for only the most effective concentrations of these compounds (i.e. largest difference to untreated controls) presented in section **4.2.2**.

Table 4.1: Compounds for the stimulation of glycogen exocytosis in Pompe skin fibroblasts

Compound	Concentration Range (μM)[1]	Proposed Mechanism of Exocytic Induction
Calcimycin	0-10	Ionophore; Ca^{2+}-dependent exocytosis (Jaiswal *et al.*, 2002)
Ionomycin	0-3	Ionophore; Ca^{2+}-dependent exocytosis (Rodriguez *et al.*, 1997)
S-1-P	0-80	Ca^{2+}-dependent exocytosis (Pan *et al.*, 2006)
Forskolin	0-200	Modulator of cAMP; Ca^{2+}-dependent exocytosis (Kasai *et al.*, 2005; Andrews, 2000)
Glucagon	0-100	Modulator of cAMP; Ca^{2+}-dependent exocytosis (Dyachok and Gylfe, 2004)
PMA	0-1	Modulator of cAMP; Ca^{2+}-dependent exocytosis (Cocucci *et al.*, 2007)
EPA	0-500	Vesicle membrane curvature; Ca^{2+}-independent exocytosis (Ong *et al.*, 2006)
LPC	0-100	Vesicle membrane curvature; Ca^{2+}-independent exocytosis (Amatore *et al.*, 2006)
AA	0-10	Vesicle membrane curvature; Ca^{2+}-independent exocytosis (Darios *et al.*, 2007)
α-L-iduronidase	0-1 μg/mL	Endocytosis; Ca^{2+}-independent exocytosis (Zhao *et al.*, 1997; Barg and Machado, 2008)

[1]Concentration range selected from the literature.

Table 4.2: The viability of Pompe skin fibroblasts following treatment with Ca^{2+}-dependent modulators of exocytosis

Compound	Concentration (µM)	Trypan blue exclusion (% of viable cells)[3]	LDH release (µg/mg)[3]	P value[1]
Calcimycin	0	92.3 +/- 2.3	3.2 +/- 1.1	-
	1	93.5 +/- 0.5	3.2 +/- 0.8	0.974
	2	90.7 +/- 2.4	6.5 +/- 1.7	0.048
	3	88.6 +/- 2.7	7.7 +/- 1.3	0.02
Ionomycin	0	94.4 +/- 2.2	3.2 +/- 0.9	-
	1	Cell death	Cell death	-
	2	Cell death	Cell death	-
	3	Cell death	Cell death	-
S-1-P	0	95.7 +/- 2.7	2.7 +/- 0.5	-
	0.1	91.7 +/- 2	2.6 +/- 0.8	0.863
	1	92.3 +/- 2.4	2.4 +/- 0.9	0.64
	10	91.7 +/- 1.3	2.5 +/- 0.3	0.584
Forskolin	0	95.6 +/- 1.8	2.5 +/- 0.3	-
	10	91.8 +/- 2	2.6 +/- 0.6	0.809
	50	93.3 +/- 1.1	2.7 +/- 0.9	0.733
	200	94 +/- 0.8	2.8 +/- 0.3	0.311
Glucagon[2]	0	93.4 +/- 1.8	2.6 +/- 0.6	-
	100	92.1 +/- 0.9	2.5 +/- 0.8	0.933
PMA	0	92.3 +/- 3.2	2.9 +/- 0.6	-
	0.03	93.7 +/- 1.5	2.8 +/- 0.5	0.835
	0.3	92 +/- 2.6	2.6 +/- 0.4	0.511
	1	93.3 +/- 1.5	2.8 +/- 0.7	0.86

[1]P-value calculated with the student's t-test.
[2]Only one concentration of glucagon evaluated due to the availability of the drug.
[3]Results are presented as mean +/- one standard deviation (n = 3).

Table 4.3: The viability of Pompe skin fibroblasts following treatment with Ca^{2+}-independent modulators of exocytosis

Compound	Concentration (µM)	Trypan blue exclusion (% of viable cells)[2]	LDH release (µg/mg)[2]	P value[1]
AA	0	91.3 +/- 2.5	3.3 +/- 0.6	-
	0.002	91.2 +/- 3.5	3.2 +/- 1	0.833
	0.01	91.3 +/- 2.1	3.3 +/- 0.3	1
	0.1	77.7 +/- 2.1	12.7 +/- 2.2	0.002
EPA	0	90.5 +/- 0.7	2.9 +/- 0.8	-
	20	92.5 +/- 1.6	3.1 +/- 0.8	0.775
	50	93.1 +/- 2.1	3.2 +/- 0.6	0.631
	100	75.3 +/- 4.7	13.3 +/- 2.1	0.001
LPC	0	92.5 +/- 0.5	3.2 +/- 0.6	-
	1	91.6 +/- 0.5	3.0 +/- 0.8	0.893
	2	93.6 +/- 2.1	3.3 +/- 0.4	0.848
	10	91.8 +/- 0.7	3.5 +/- 0.3	0.764
PC	0	94.1 +/- 1.8	2.4 +/- 0.7	-
	1	91.9 +/- 1.1	2.5 +/- 0.5	0.726
	5	94.1 +/- 1.9	2.9 +/- 0.7	0.353
	10	93.3 +/- 2.6	2.2 +/- 0.7	0.932
Idua[3]	0	94.1 +/- 1.8	3.4 +/- 0.7	-
	9 ng/mL	92.3 +/- 2.4	3.3 +/- 0.3	0.831
	72 ng/mL	93.1 +/- 2.1	3.6 +/- 0.5	0.708
	144 ng/mL	93.4 +/- 1.8	3.5 +/- 0.6	0.815
	1 µg/mL	93.5 +/- 0.5	3.3 +/- 0.5	0.85

[1]P-value calculated with the student's t-test.
[2]Results are presented as mean +/- one standard deviation (n = 3).
[3]α-L-Iduronidase

4.2.2: Compound-induced glycogen and β-hexosaminidase release from cultured Pompe skin fibroblasts

In Pompe cells treated with cytosolic Ca^{2+} concentration modulators; **Figure 4.1** shows that the treatment with 1 µM of calcimycin demonstrated a significant increase in the release of both glycogen (3-fold) and β-hexosaminidase (2.2-fold) into the culture medium, when compared to untreated controls ($P < 0.005$). There was no difference in glycogen and β-hexosaminidase release in Pompe cells treated with the other modulators of intracellular Ca^{2+} concentration (S-1-P, forskolin and PMA; all concentrations) compared to untreated controls. Although there was no change in glycogen release from glucagon-treated Pompe cells (100 µM), a 2-fold increase was observed in the amount of β-hexosaminidase released into the culture medium, when compared to untreated controls ($P = 0.002$).

Ca^{2+}-independent modulators of exocytosis resulted in increased β-hexosaminidase release from Pompe cells, with LPC producing a 1.8-fold increase in the release of both β-hexosaminidase and glycogen, when compared to untreated controls ($P < 0.005$). α-L-Iduronidase increased the release of both β-hexosaminidase (1.5-fold) and glycogen (1.4-fold) into the culture medium, when compared to untreated controls ($P < 0.005$). **Figure 4.2** shows that >90% of the α-L-iduronidase in the culture medium was internalised into Pompe cells after incubation for one hour. EPA-treated Pompe cells also demonstrated increased release of both β-hexosaminidase and glycogen (1.4-fold), but this was not significant due to the variability of the release, when compared to untreated controls. PC did not result in a change in β-hexosaminidase or glycogen release in Pompe cells when compared to untreated controls. In contrast to LPC and α-

L-iduronidase, arachidonic acid showed a significant reduction in both β-hexosaminidase and glycogen release when compared to untreated cells ($P < 0.05$).

4.2.3: Cell surface LAMP-1 staining, β-hexosaminidase and glycogen release from calcimycin-treated Pompe, MPS I and unaffected skin fibroblasts

Of the compounds tested, calcimycin produced the largest increase in glycogen exocytosis, and was therefore examined in greater detail. Firstly, the amount of glycogen and β-hexosaminidase release was determined over time (up to 2 hrs). β-Hexosaminidase (nmol/min released into the culture medium per mg of total cell protein) and glycogen (µg released into the culture medium per mg of total cell protein) were presented as both the amount of release and the percentage of total cell β-hexosaminidase/glycogen released from the cell. Cell surface LAMP-1 staining was also measured as an additional marker of exocytosis. Markers of exocytosis and glycogen release in calcimycin-treated Pompe cells were also compared to calcimycin-treated MPS I (glycosaminoglycan accumulation) and unaffected cells; cultured to confluence and depleted of cytoplasmic glycogen. **Figures 4.3A, C and E** show a 2-fold increase in β-hexosaminidase release in calcimycin-treated cells, when compared to untreated controls ($P < 0.005$). Calcimycin-treated Pompe and MPS I cells released more β-hexosaminidase (4 and 10 nmol/min/mg, respectively) after 2 hrs of culture than unaffected cells (2 nmol/min/mg). However, when expressed as a percentage of total cellular β-hexosaminidase, a similar amount of β-hexosaminidase was released in all cell lines (4% of total; $P < 0.005$; **Figures 4.3B, D and F**).

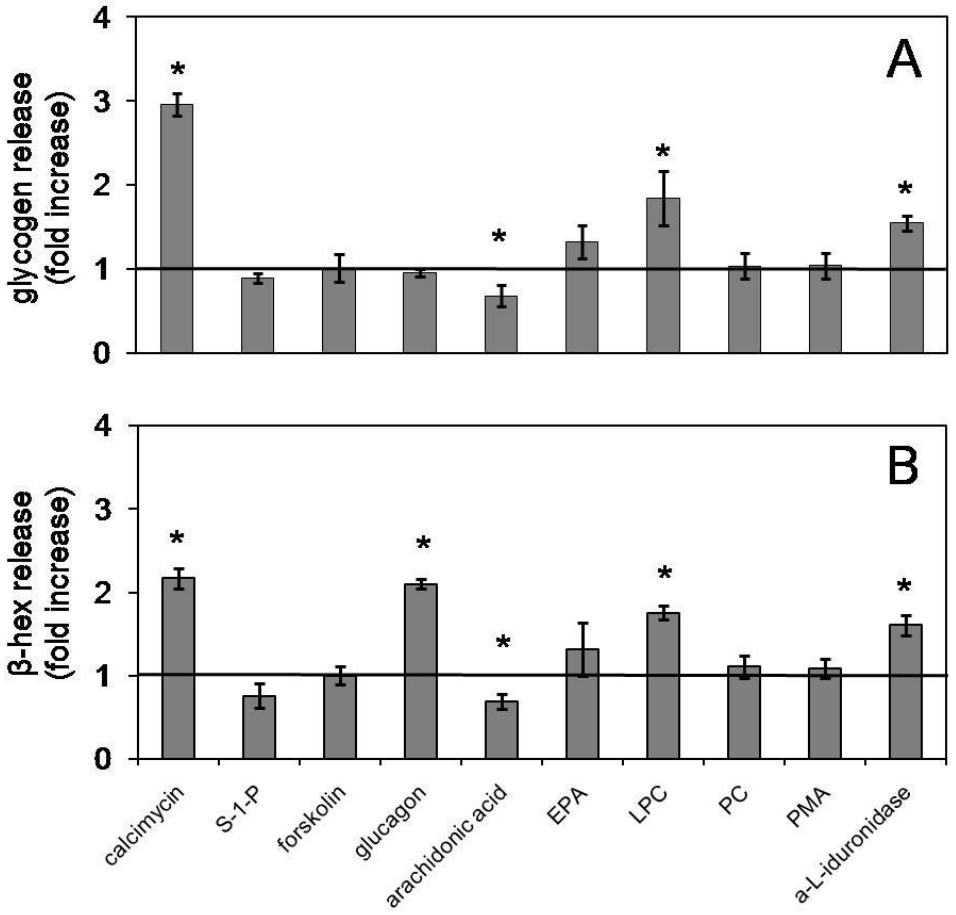

Figure 4.1: The effect of compounds on exocytosis in Pompe skin fibroblasts. The release of glycogen (A), and β-hexosaminidase (β-hex; B) was measured in Pompe cells depleted of cytoplasmic glycogen. Cells were treated with 1 µM of calcimycin, 10 µM of S-1-P, 200 µM of forskolin, 100 µM of glucagon, 0.1 µM of arachidonic acid, 50 µM of EPA, 2 µM of LPC, 1 µM of PC (negative control), 1 µM of PMA and 1 µg/mL of α-L-iduronidase for 2 hrs at 37^{o}C. Results are expressed as fold increase in the extracellular release of β-hex or glycogen (percentage of total released into the culture medium), when compared to untreated controls (mean +/- SD; n = 3). *Significance, when compared to untreated controls ($P < 0.05$).

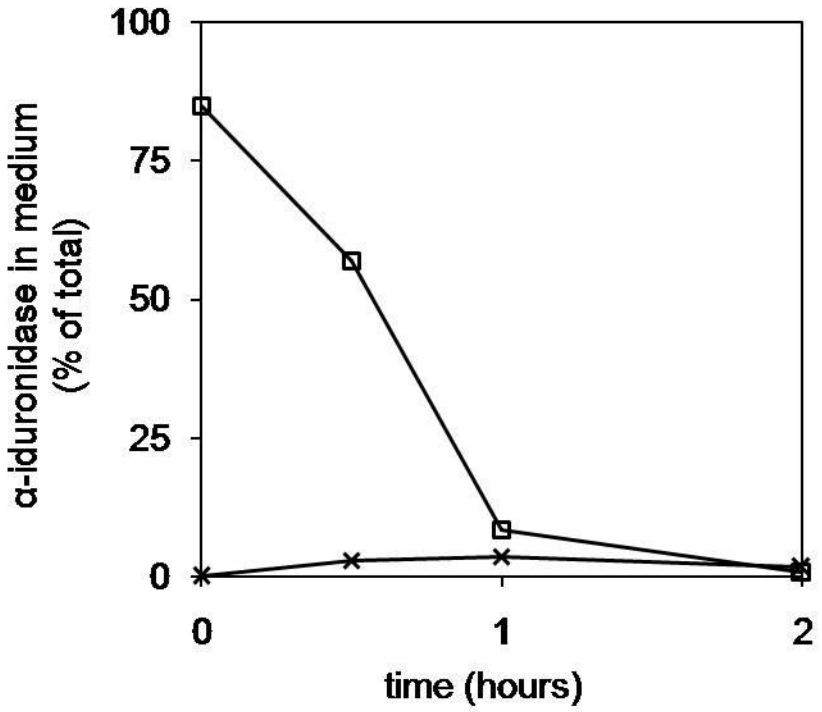

Figure 4.2: The uptake of α-L-iduronidase into cultured Pompe skin fibroblasts. Glycogen-depleted Pompe cells were cultured with α-L-iduronidase for 2 hrs at 37°C. Cells were treated with 1 μg/mL of α-L-iduronidase (□) or were untreated (×). Results are expressed as the total percentage of α-L-iduronidase in the culture medium of Pompe cells (mean +/- SD; n = 3).

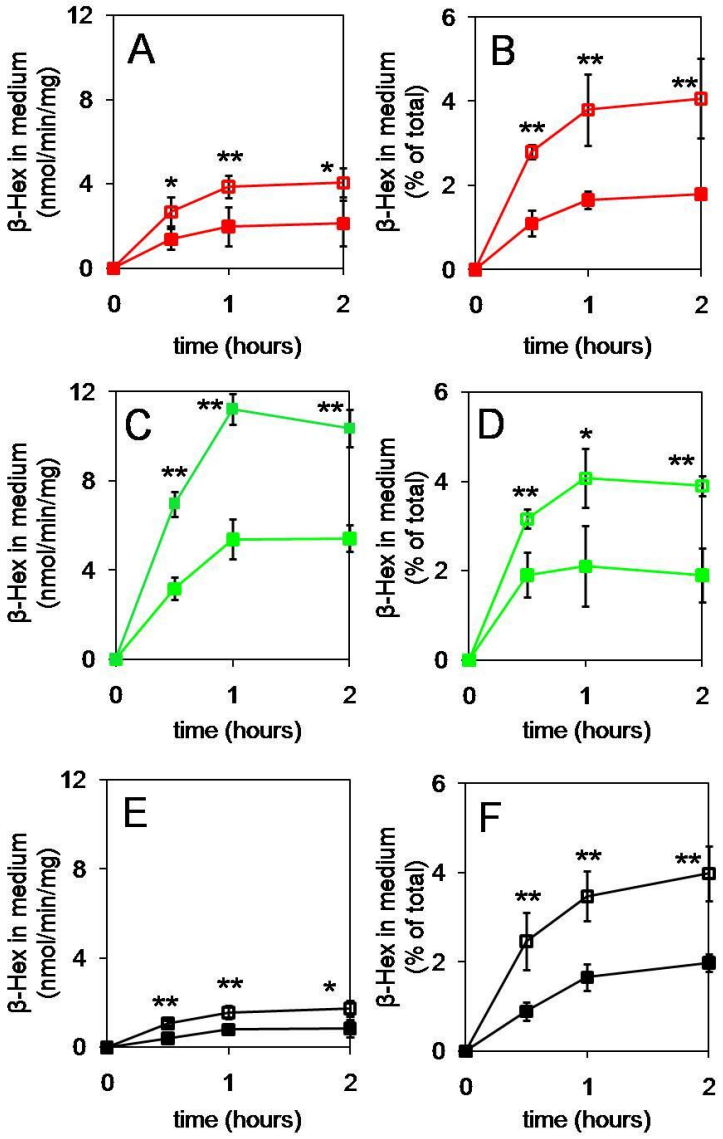

Figure 4.3: The effect of calcimycin on the release of β-hexosaminidase from skin fibroblasts. Glycogen-depleted Pompe (red), MPS I (green) and unaffected (black) cells were treated with 1 μM of calcimycin for 2 hrs at 37°C. Results are expressed as nmol/min of β-hexosaminidase per mg of total cell protein released into the culture medium (β-hex; A, C and E) or as the percentage of total β-hex (B, D and F) in the culture medium (mean +/- SD; n = 3). Calcimycin treated (□). Untreated (■). *Significance P <0.05 when compared to untreated controls. **Significance P <0.005 when compared to untreated controls.

Figures 4.4A, B and C show no difference between the number, the fluorescence intensity or the cell surface distribution of LAMP-1 punctae in either Pompe, MPS I or unaffected cells. Calcimycin-treated cells displayed a 2-fold increase in the fluorescence intensity of cell surface LAMP-1 punctae compared to untreated controls ($P < 0.005$; **Figures 4.4D, E and F)**. In cells permeabilised by fixation, the intracellular LAMP-1 staining pattern differed from the cell surface of the same cells, with evidence of a more extensive staining pattern, larger vesicular structures and DAPI nuclear staining (**Figures 4.4G, H and I**).

Calcimycin-treated Pompe, MPS I and unaffected cells displayed a significant increase in glycogen release (2.7-, 3.1- and 3.9-fold, respectively), when compared to the untreated controls ($P < 0.005$; **Figures 4.5A, C and E**). Pompe cells released the most glycogen into the culture medium in response to calcimycin treatment, when compared to MPS I and unaffected cells after 2 hrs in culture. The amount of glycogen in depleted cells was higher in Pompe (105 μg/mg of total cell protein) than MPS I (40 μg/mg of total cell protein) and unaffected cells (20 μg/mg of total cell protein). As a percentage of total cellular glycogen released after 2 hrs, Pompe cells showed the lowest release compared to MPS I cells and unaffected cells ($P < 0.005$; **Figures 4.5B, D and F**). Pompe, MPS I and unaffected cells treated with 1 μM of calcimycin did not show a difference in the amount of LDH released into the culture medium or the exclusion of trypan blue (>90% trypan blue exclusion and <5 μg/mg LDH release). Together, these results indicated that glycogen release from Pompe cells was impaired when compared to the control cells, necessitating further study to identify possible causes.

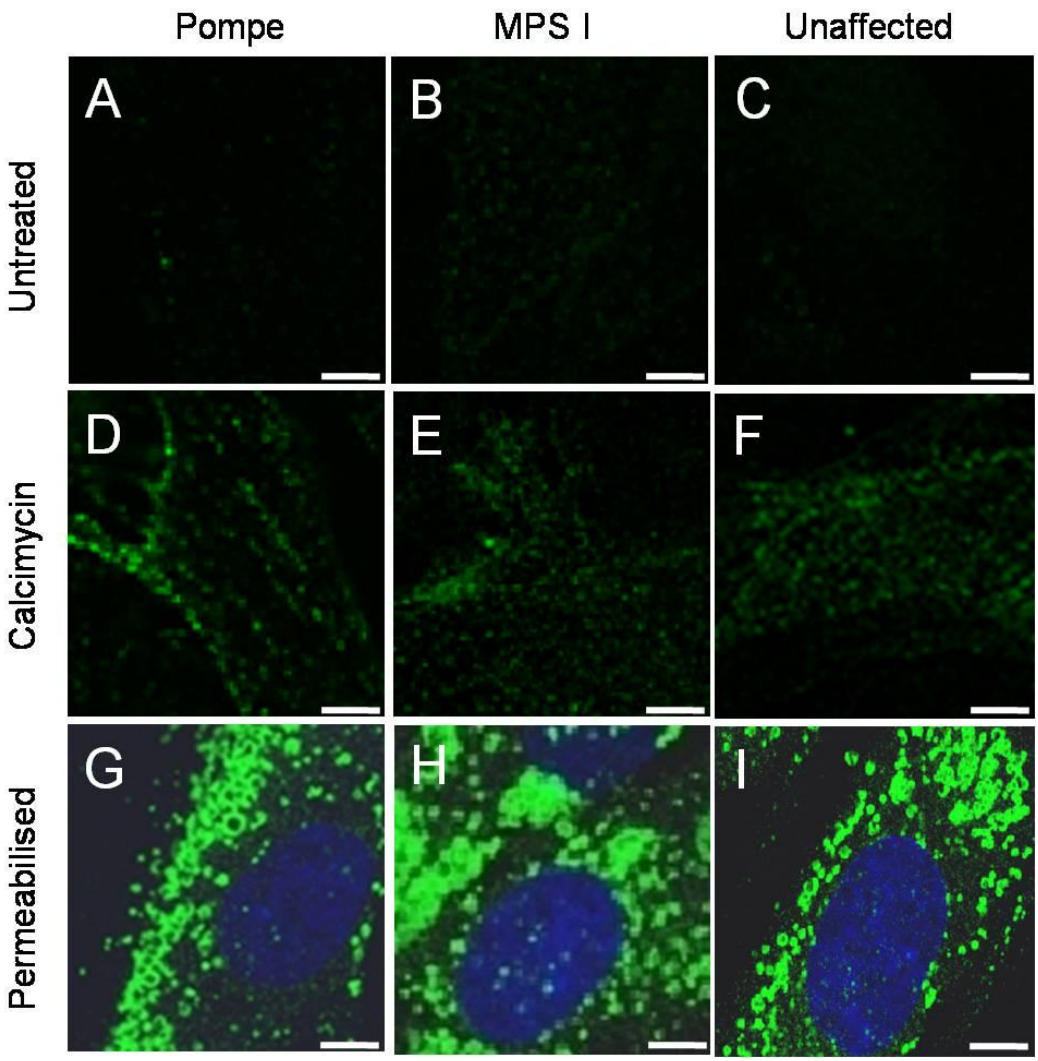

Figure 4.4: The effect of calcimycin on LAMP-1 staining of skin fibroblasts. Cell surface LAMP-1 fluorescence was evaluated in non-permeabilised untreated Pompe (A), MPS I (B) and unaffected (C) cells, and Pompe (D), MPS I (E) and unaffected (F) cells treated with 1 μM of calcimycin for 10 mins at 37°C. Intracellular LAMP-1 fluorescence was also measured in Pompe cells (G), MPS I (H) and unaffected (I) cells that were permeabilised by fixation. Cells were glycogen-depleted prior to experimentation. Images are an overlay of LAMP-1 fluorescence (green) and DAPI nuclear stain (blue). Each image is representative of greater than 20 images with each experiment performed in triplicate. Size bar equals 20 nm.

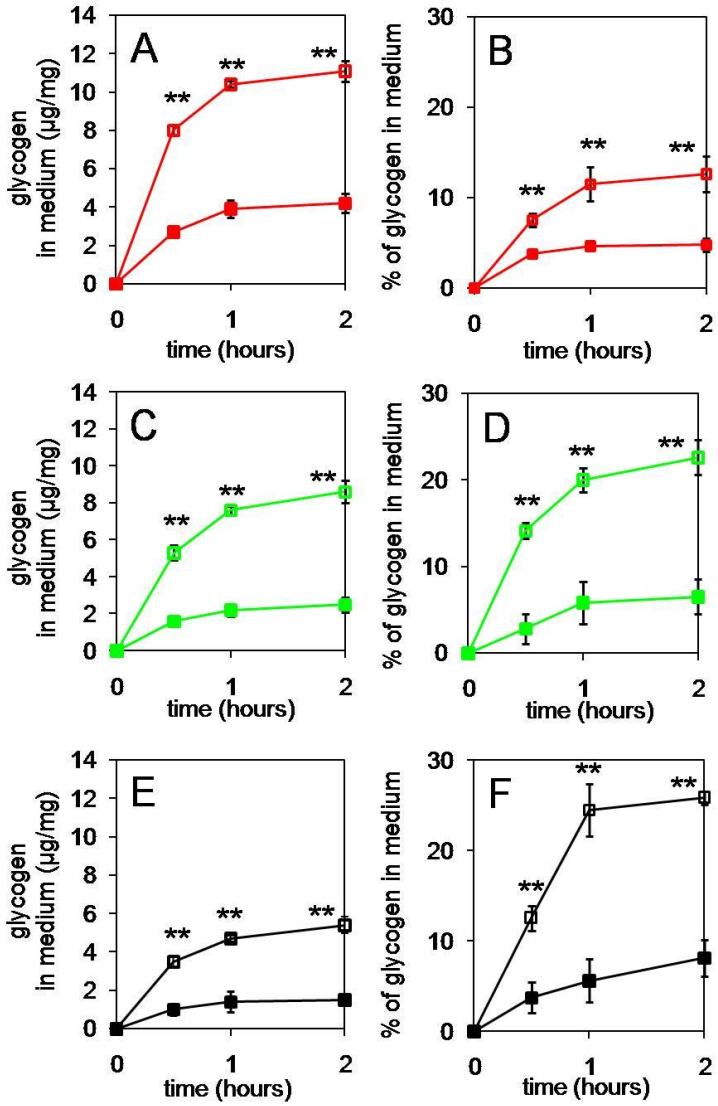

Figure 4.5: The effect of calcimycin on the release of glycogen from skin fibroblasts. Glycogen-depleted Pompe (red), MPS I (green) and unaffected (black) cells were treated with 1 µM of calcimycin for 2 hrs at 37°C. Results are expressed as µg of glycogen per mg of total cell protein in the culture medium (A, C and E) or as the percentage of total cell glycogen released into the culture medium (B, D and F; mean +/- SD; n = 3). All samples were measured in triplicate and the whole experiment was performed three times. Calcimycin-treated (□). Untreated (■). *Significance P <0.05 when compared to untreated controls. **Significance P <0.005 when compared to untreated controls.

4.2.4: The diameter of the calcimycin-induced exocytic pores in Pompe and unaffected skin fibroblasts

Whilst a reduction in the size of the exocytic pore may explain the decrease in glycogen release from Pompe compared to unaffected cells, it was necessary to investigate the maximum size of fluorescent beads capable of being released from the endosome-lysosome network in each of these cells. Fluorescent beads with a diameter of 2.4 nm, 20 nm, 40 nm and 100 nm were internalised into Pompe and unaffected cells. A significant increase in the release of 2.4 nm beads (≥ 30% increase) and 20 nm beads (≥ 24% increase) was observed for calcimycin-treated Pompe and unaffected cells, when compared to untreated control cells ($P < 0.005$; **Figures 4.6 and 4.7**). However, the 40 nm and 100 nm beads were not released. The uptake of beads and calcimycin treatment did not increase cell permeability, as measured by the amount of LDH released into the culture medium (<5 µg/mg LDH release).

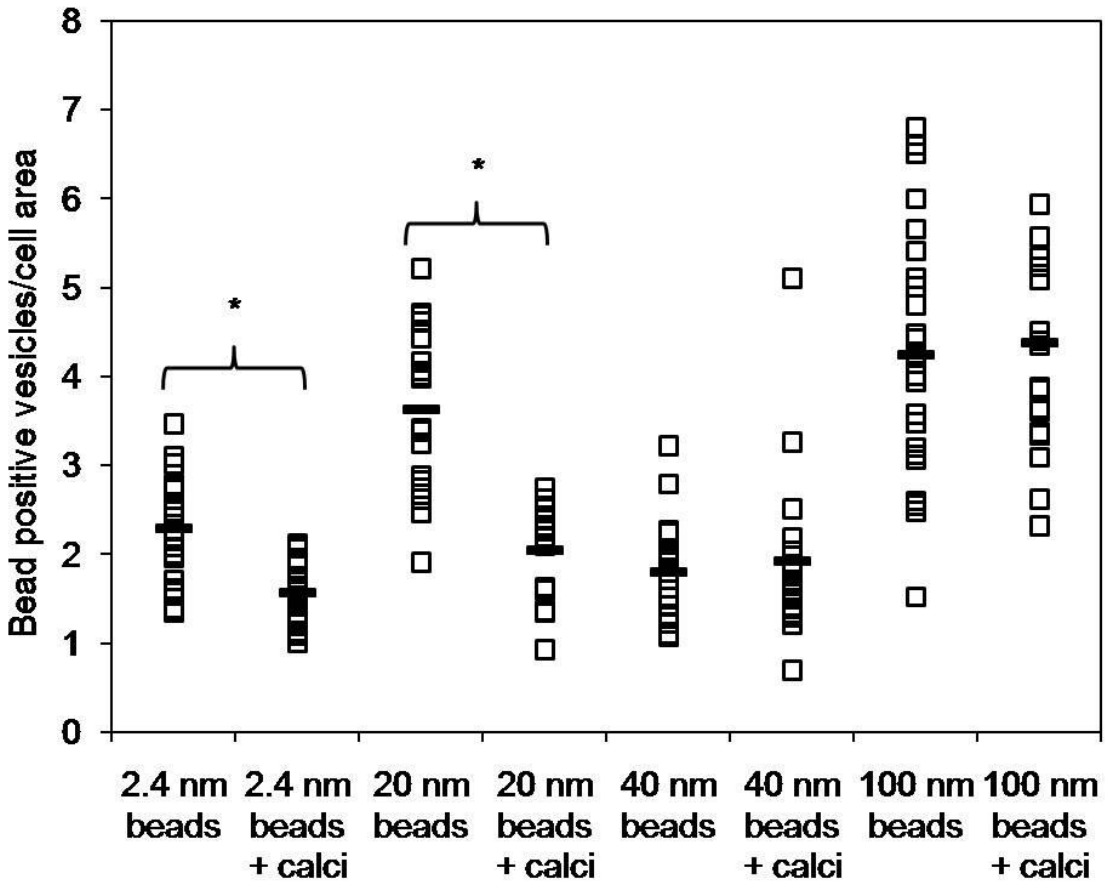

Figure 4.6: The release of fluorescent beads from calcimycin-treated Pompe skin fibroblasts. Pompe cells were incubated with fluorescent beads (2.4, 20, 40 and 100 nm in diameter) to allow internalisation into the endosome-lysosome network. Cells were calcimycin-treated and the amount of bead exocytosis was measured and then compared to untreated controls. Results are presented as the number of bead-positive vesicles per cell area (i.e. indicates the relative number of beads that could not be released from the cell). Greater than 20 cells were evaluated per treatment group. *Significance $P < 0.05$.

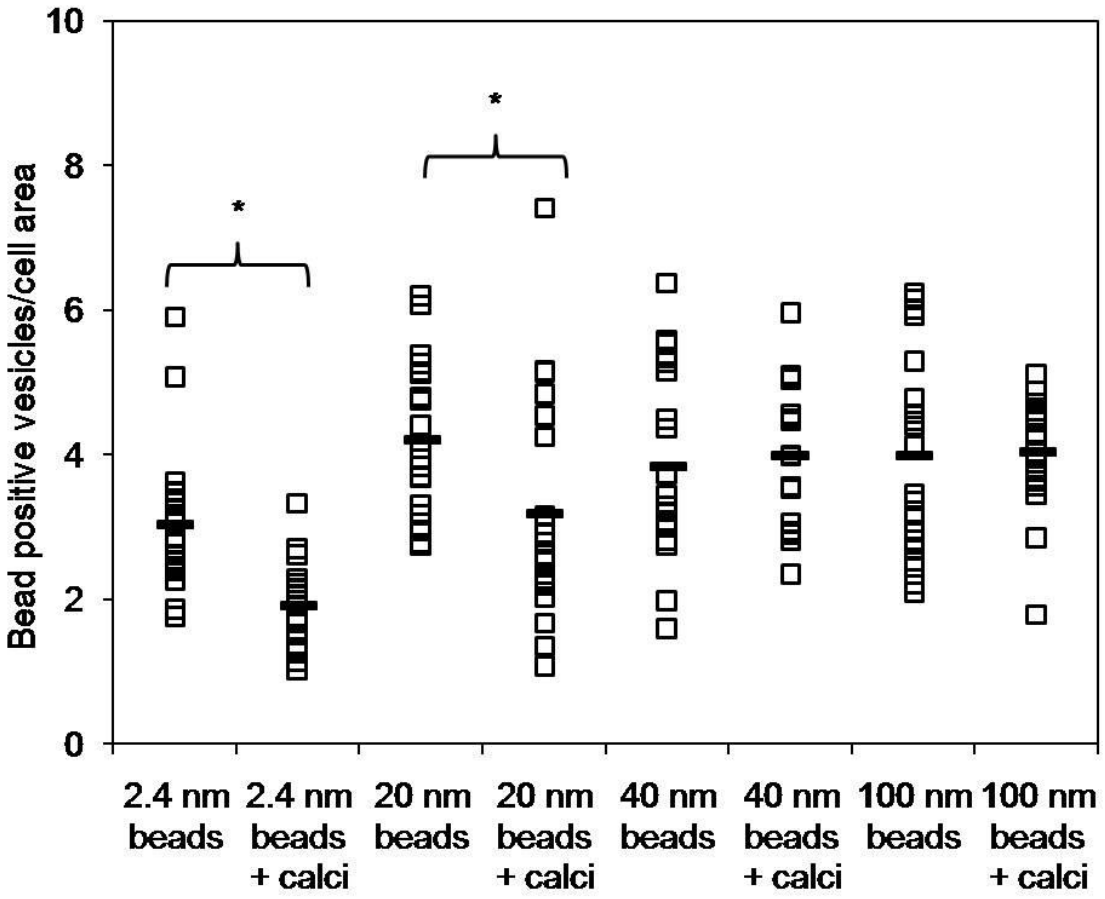

Figure 4.7: The release of fluorescent beads from calcimycin-treated unaffected skin fibroblasts. Unaffected cells were incubated with fluorescent beads (2.4, 20, 40 and 100 nm in diameter) to allow internalisation into the endosome-lysosome network. Cells were calcimycin-treated and the amount of bead exocytosis was measured and then compared to untreated controls. Results are presented as the number of bead-positive vesicles per cell area (i.e. indicates the relative number of beads that could not be released from the cell). Greater than 20 cells were evaluated per treatment group. Significance * $P < 0.05$.

4.2.5: Vesicular glycogen granules in Pompe and unaffected skin fibroblasts

An increase in the size of the vesicular glycogen granules in Pompe cells, compared to unaffected cells, may provide an explanation for the decrease in glycogen release from Pompe cells. To test this, glycogen granules were purified from Pompe and unaffected cells that were either glycogen-depleted (i.e. containing predominantly vesicular glycogen) or non-depleted (containing both cytosolic and vesicular glycogen). Visualisation of the glycogen granules by transmission electron microscopy allowed individual granules to be identified by their characteristic globular shape (**Figure 4.8**). To confirm that these were in fact granules of glycogen, duplicate samples were digested with amylase prior to visualisation, which resulted in the removal of these globular structures (data not shown). Glycogen granules isolated from non-depleted Pompe and unaffected cells were similar in size (**Table 4.4**). As shown in **Figure 4.9**, the diameter of the granules for each glycogen preparation ranged between 5 to 110 nm, but displayed a skewed distribution with a peak between 30 to 50 nm in diameter. Glycogen granules isolated from cytoplasmic glycogen-depleted Pompe cells were significantly larger than those isolated from depleted unaffected cells ($P < 0.05$). In the unaffected cells 47% of granules were smaller than 40 nm, while in the Pompe cells 33% were smaller than 40 nm (**Figure 4.10**). Transmission electron microscopy was also used to visualise glycogen granules (electron-dense material) within the vesicles of Pompe and unaffected cells, showing the presence of glycogen-filled vesicles in Pompe cells (**Figure 4.11**). These vesicles appeared to contain both intact granules and partially degraded material (**Figure 4.11C**).

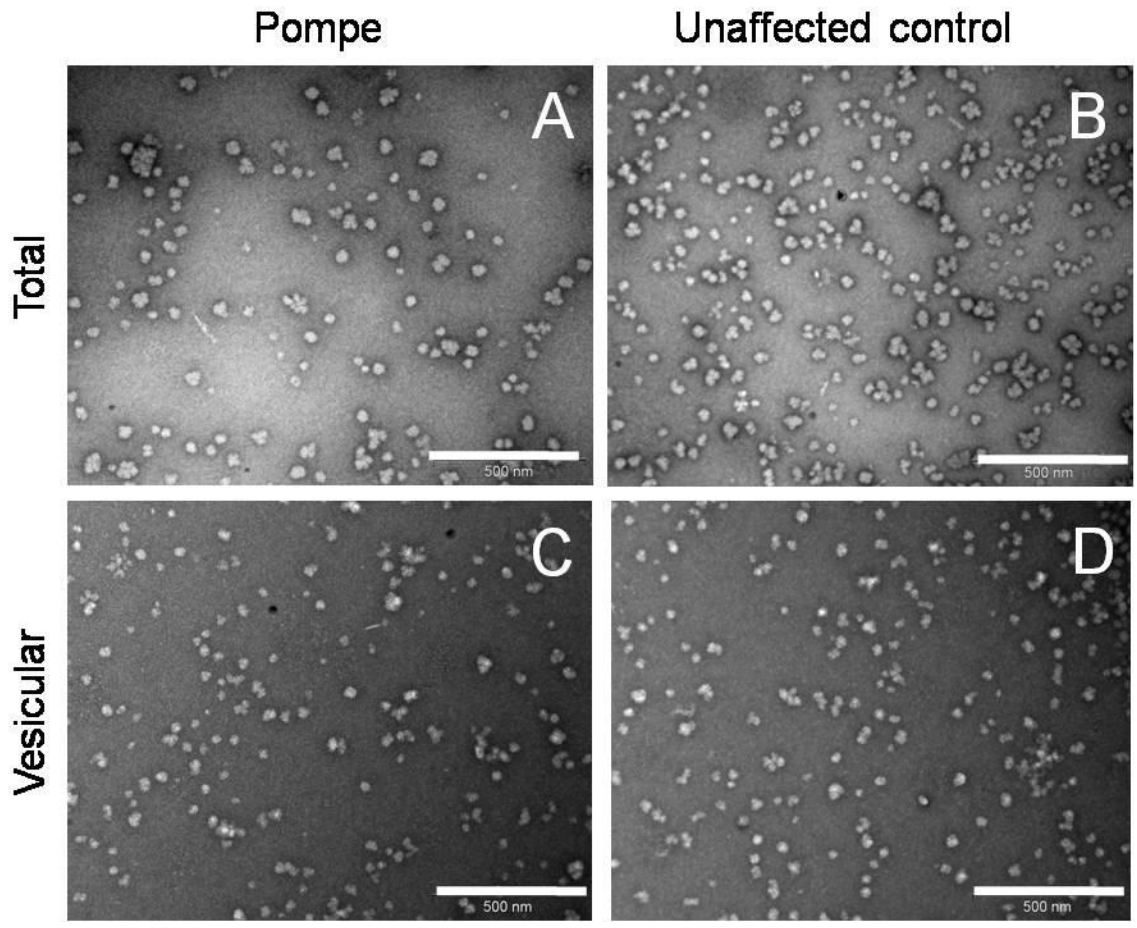

Figure 4.8: Electron microscopic visualisation of purified glycogen granules from skin fibroblasts. Transmission electron microscopy images were captured of glycogen purified from non-glycogen-depleted (containing vesicular and cytosolic glycogen) Pompe (A) and unaffected (B) cells. Glycogen granules purified from depleted (containing predominantly vesicular glycogen) Pompe and unaffected cells are shown in panels (C) and (D). All images are representative for each cell line or culture condition (>40 images were evaluated for each group). Size bar equals 500 nm.

Table 4.4: The mean diameter of glycogen extracted from skin fibroblasts

Glycogen source	n	Mean diameter (nm)	Standard deviation	95% confidence	P-value
Pompe	1328	46.5	16.9	43.1 – 50.9	P = 0.63[2]
Unaffected	1415	47.7	18.5	44.3 – 51.3	
Depleted Pompe[1]	1630	50.8	21.1	47.3 – 55.1	P < 0.05[3]
Depleted unaffected[1]	610	46.1	18.2	41.8 – 49.6	

[1]Cells depleted of cytosolic glycogen (contain predominantly vesicular glycogen).

[2]The statistical difference in glycogen size between Pompe and unaffected skin fibroblasts that were non-depleted of cytosolic glycogen (student's t-test).

[3]The statistical difference in glycogen size between Pompe and unaffected skin fibroblasts that were depleted of cytosolic glycogen (student's t-test).

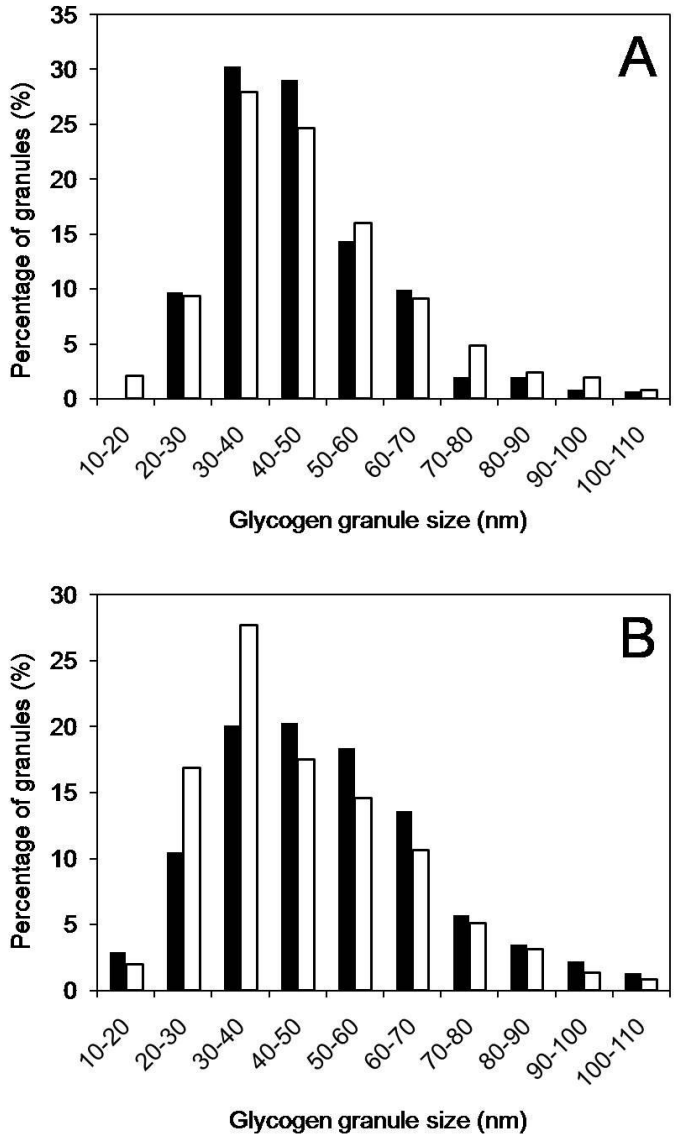

Figure 4.9: The size of glycogen granules isolated from skin fibroblasts. The diameter of glycogen granules purified from Pompe and unaffected fibroblasts was determined and presented as the percentage of glycogen granules within each size range (10 nm divisions). The diameter of glycogen granules purified from non-glycogen-depleted Pompe (filled bars) and non-depleted unaffected (open bars) fibroblasts are shown in panel (A). The diameter of glycogen granules purified from depleted Pompe (filled bars) and depleted unaffected (open bars) cells are shown in panel (B). The diameter of >800 glycogen granules was evaluated for each group.

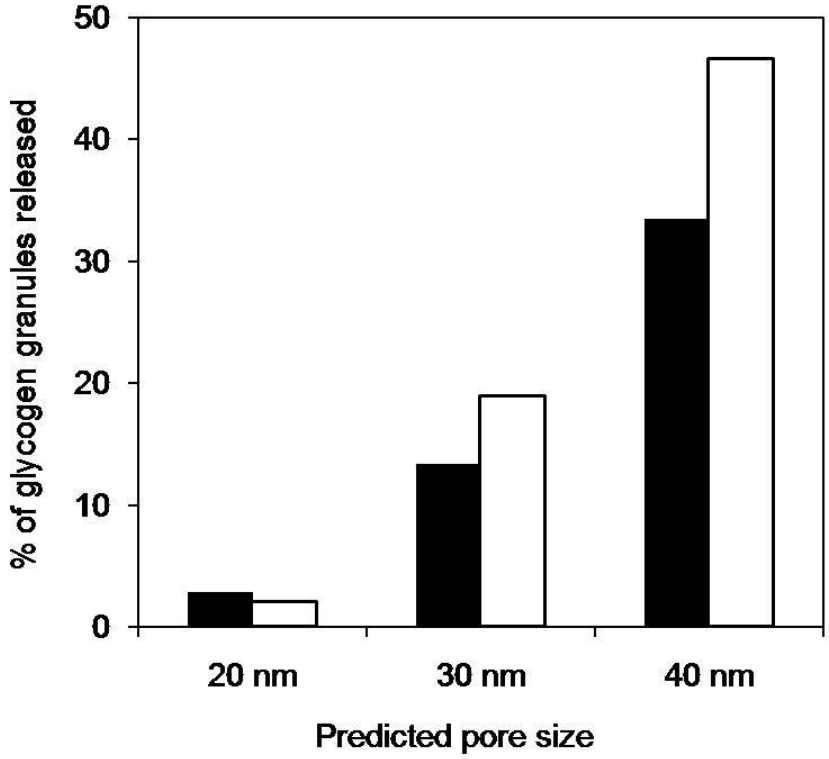

Figure 4.10: The predicted theoretical maximum number of glycogen granules to be exocytosed from calcimycin-treated skin fibroblasts. The percentage of glycogen granules small enough to pass through calcimycin-induced exocytic pores in Pompe (filled bars) and unaffected (open bars) cells. The pore sizes of 20, 30 and 40 nm were based on the exocytic release of dextran beads from skin fibroblasts (see **Figures 4.6 and 4.7**).

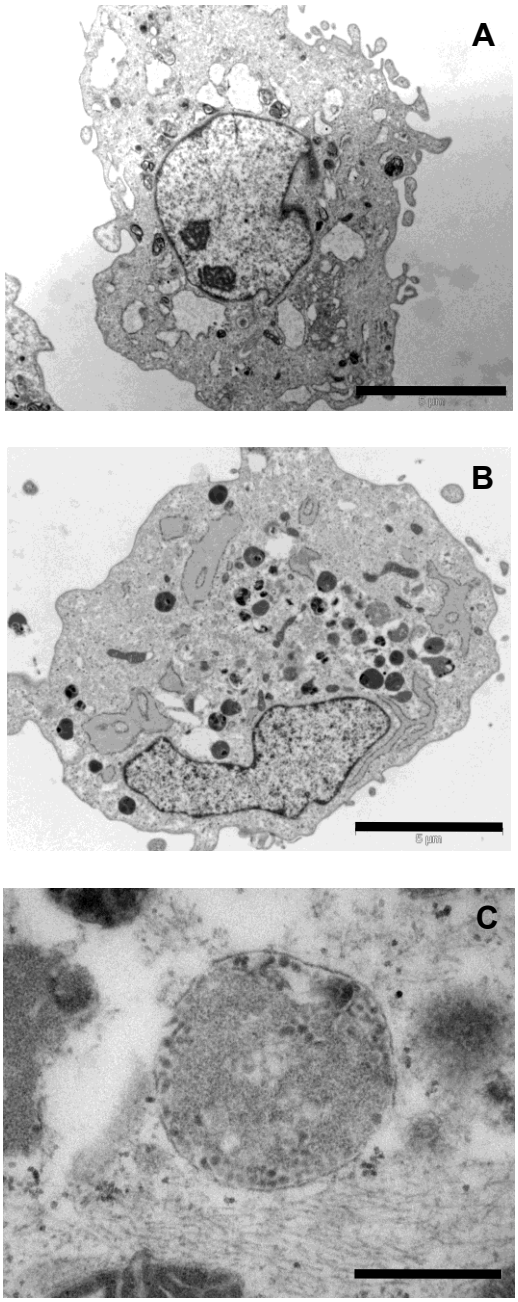

Figure 4.11: Glycogen accumulation in a Pompe skin fibroblast cell. Electron micrographs of a human unaffected control (A) and Pompe (B) skin fibroblast. Glycogen-filled vesicle inside a Pompe skin fibroblast cell (C). Glycogen can be visualised as electron-dense vacuoles in panels B and C. Size bar is equivalent to 5 µm for A and B and 30 nm for panel C.

4.3: Discussion

Calcimycin, an ionophore that triggers Ca^{2+} ion influx into the cytosol from the culture medium, resulted in increased exocytosis from Pompe, unaffected and MPS I skin fibroblasts, as measured by β-hexosaminidase release into the culture medium and cell surface LAMP-1 staining. The treatment of cultured basophilic cells with calcimycin has been reported to release approximately 22% of β-hexosaminidase into the culture medium (Santini and Beaven, 1993), whilst similarly treated mast cells released 15% (Baram *et al.*, 1999), >3-fold higher than observed here; though both of the latter are specialist secretory cells. The difference in the amount of exocytosis may therefore be explained by the basophilic and mast cells being more susceptible to fluctuations in the cytosolic Ca^{2+} concentration than fibroblasts (Jaiswal *et al*., 2002). The susceptibility of fibroblasts to cytosolic Ca^{2+} concentration has been previously reported in membrane resealing assays, with different rates of dye loss observed in sea urchin embryo and 3T3 fibroblasts after membrane puncture (Steinhardt *et al*., 1994). The amount of exocytosis in response to calcimycin treatment, as measured by the fraction of peripheral lysosomes that are trafficked to the cell surface, has been reported to vary depending on the cell type, ranging from 0% (HeLa cells) to 24% (murine embryonic fibroblasts; Jaiswal *et al.*, 2002).

It may be expected that glucagon, which also modulates Ca^{2+}-dependent exocytosis, would release the same or similar vesicular content as that observed for calcimycin-treated Pompe skin fibroblasts. However, Pompe cells treated with glucagon displayed increased β-hexosaminidase but not glycogen release compared to untreated

cells. A possible mechanism to explain why glycogen was not released is that specific vesicular pools may have a different susceptibility to the cytosolic concentration of Ca^{2+}. β-Hexosaminidase and glycogen are present in lysosomes (Mahuran, 1995), whilst glycogen is also expected to reside in autophagic compartments (Knecht and Hernández, 1978). The high cytosolic concentration of Ca^{2+} resulting from calcimycin treatment may induce the exocytosis of vesicles containing both β-hexosaminidase and glycogen. Conversely, the comparatively lower cytosolic concentration of Ca^{2+} associated with glucagon treatment may only exocytose a vesicular pool that contains β-hexosaminidase. Further studies are required to fully characterise this phenomenon.

LPC, arachidonic acid, EPA, and α-L-iduronidase induce Ca^{2+}-independent exocytosis, and treatment with both LPC- and α-L-iduronidase induced glycogen and β-hexosaminidase release from Pompe skin fibroblasts. A high concentration of LPC in vesicular membranes of chromaffin cells has been reported to give the vesicle a high curvature (inverted cone shape), which facilitates vesicle formation and exocytosis (Amatore *et al.,* 2006; **Figure 4.12**). Alteration in the curvature of the vesicular lipid bi-layer was not expected by the sequestration of PC, and no change in either glycogen or β-hexosaminidase release were observed here, when compared to untreated controls. Arachidonic acid treatment led to a reduction in β-hexosaminidase release, which has been previously reported in chromaffin cells. Arachidonic acid alters the curvature of the membrane in the opposite configuration to that observed for LPC, contributing to a decrease in membrane fusion and a reduction in the amount of exocytosis (Amatore *et al.,* 2006).

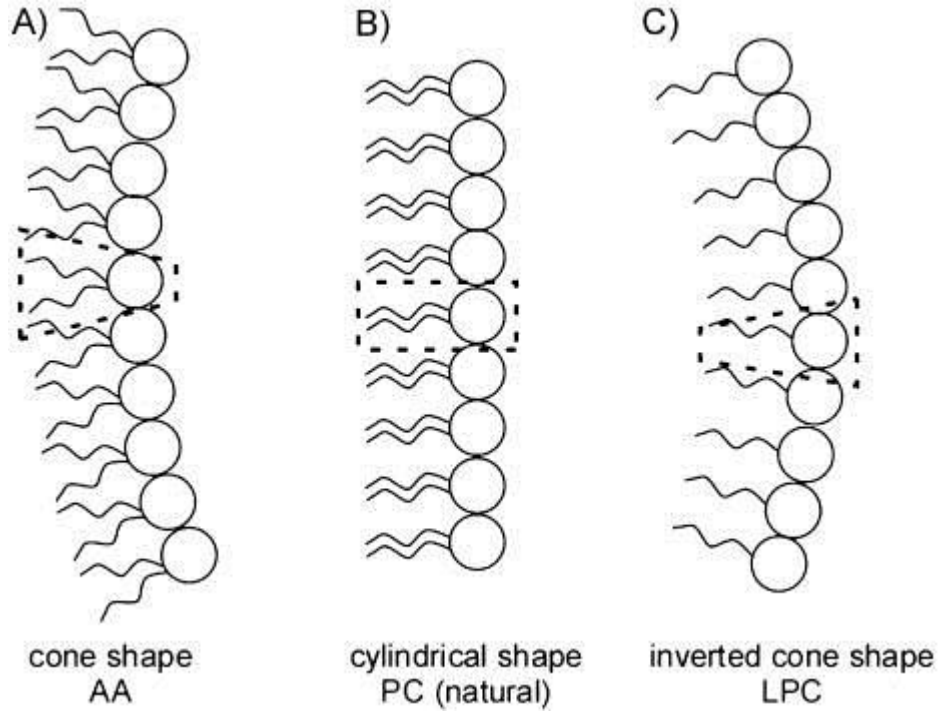

Figure 4.12: The effect of lipids and fatty acids on the curvature of vesicular membranes. The presence of arachidonic acid (AA) within membrane phospholipids (panel A), contributes to the formation of a cone shape orientation, which enhances membrane curvature; phosphatidylcholine (PC, panel B) contributes to a neutral orientation; and LPC (panel C) contributes to an inverted cone shape orientation leading to an opposite membrane curvature relative to AA. Image from Amatore *et al.*, 2006.

While calcimycin was shown to be the most effective compound for the induction of glycogen exocytosis in Pompe skin fibroblasts, the percentage of total glycogen released from calcimycin-treated Pompe cells (13% of total) was less than that released from calcimycin-treated MPS I (23% of total) and unaffected cells (27% of total). The lack of apparent change in both cell surface LAMP-1 staining and the release of β-hexosaminidase between these cell lines indicated that exocytosis per se was not

affected, rather the specific release of glycogen in the exocytic vesicles was impaired. Two possible explanations have been proposed to account for this phenomenon; (1) the calcimycin-induced exocytic pore size generated in Pompe cells may be smaller than in unaffected cells, and (2) vesicular glycogen granules in Pompe cells may be larger than those in unaffected cells.

The diameter of the exocytic pore that is opened by cavicapture controls the amount of vesicular material that is released from a cell (Thorn, 2009). Here, the capacity to release fluorescent beads of a known size from the phago-lysosomal compartment was defined in Pompe and unaffected skin fibroblasts, and was used to infer the size of the exocytic pore. Pompe and unaffected cells appeared to have a calcimycin-induced exocytic pore diameter that was >20 nm but <40 nm, similar to a previous report in fibroblasts (30 nm; Jaiswal *et al.,* 2004). Although additional experiments are required to more accurately assess the diameter of the pore sizes generated between 20 nm to 40 nm, the evidence here indicated that Pompe and unaffected cells generated similar pore sizes in response to calcimycin treatment. Differences in the exocytic pore size between Pompe and unaffected cells were therefore unlikely to be responsible for the impaired release of glycogen from Pompe cells.

Cytosolic glycogen granules in healthy cells range from 10 nm to 80 nm in diameter (Parker *et al*., 2007; Takeuchi *et al*., 1978), but the size of vesicular glycogen granules has not been reported. Here, vesicular glycogen granules from unaffected skin fibroblasts were shown to be similar in diameter to cytosolic glycogen observed in these other studies. The mean diameter of glycogen granules isolated from cytoplasmic glycogen-depleted Pompe cells was significantly greater than those from depleted

unaffected cells. In contrast, there was no difference in the mean diameter of the glycogen granule size between non-depleted Pompe (containing approximately 40% cytosolic glycogen) and unaffected cells (containing approximately 90% cytosolic glycogen). This demonstrated that the size of vesicular glycogen granules, but not cytosolic glycogen, was larger in Pompe than unaffected cells. The increased diameter of vesicular glycogen granules in Pompe cells may therefore reduce the overall amount of glycogen capable of passing through the calcimycin-induced exocytic pore, thereby providing a plausible explanation for reduced glycogen release from Pompe compared to unaffected cells.

In conclusion, glycogen release is induced in Pompe skin fibroblasts with modulators of both Ca^{2+}-dependent and Ca^{2+}-independent exocytosis. Calcimycin was the most effective compound for inducing glycogen release in Pompe cells, but >80% of the vesicular glycogen granules were too large to pass through calcimycin-induced exocytic pores. Despite this limitation, these modulators of exocytosis provide proof of concept for the strategy of reducing glycogen in Pompe cells.

Chapter 5:

Final Discussion

Pompe disease is caused by a deficiency of GAA, which is responsible for the catabolism of glycogen within phagolysosome compartments. GAA deficiency results in the progressive accumulation of glycogen in autophagosome-lysosome vesicles (Raben *et al*., 2005) and multivesicular bodies (Cardone *et al*., 2008). Skeletal and cardiac muscle are the primary sites of pathology, but undegraded vesicular glycogen can also accumulate in the diaphragm, brain and skin (Hirschhorn and Reuser, 2001). Muscle atrophy is the direct result of glycogen accumulation in muscle fibres, as this disrupts the contractile apparatus (Shea and Raben, 2009) and, if untreated, leads to premature death from respiratory failure. There is currently no effective cure for Pompe disease. ERT has been clinically approved for the treatment of infantile-onset Pompe disease and involves the intravenous administration of recombinant GAA, which is trafficked through the circulatory system to a range of tissues where it is internalised and targeted to the lysosomal compartment (Cardone *et al*., 2008). ERT has been shown to reduce the amount of glycogen in a number of affected tissues, including heart and skeletal muscle (Winkel *et al*., 2003), and there is evidence of prolonged patient survival (Van den Hout *et al*., 2004). However, it has been reported to be ineffective in some patients (Winkel *et al*., 2003), and appears to have limited access to the glycogen stored in some major sites of pathology, including type II skeletal muscle (Raben *et al*., 2005; Hawes *et al*., 2007). This impaired uptake of GAA into glycogen-filled autophagosomes-lysosomes (Shea and Raben, 2009) necessitates the development of novel or adjunct therapeutic options to more effectively treat the disorder.

Exocytosis is a process whereby intracellular vesicles are trafficked to the cell surface, allowing vesicle-plasma membrane fusion and the extracellular release of vesicle contents. Exocytosis has a role in regulatory and signaling functions, neurotransmission (Calì *et al*., 2009), melanosome transfer to endothelial cells (Stinchcombe *et al*., 2004), plasma membrane repair (Gerasimenko *et al*., 2001) and in maintaining cell surface area during cytokinesis (Boucrot and Kirchhausen, 2008). Exocytosis may also allow the cellular release of un-degraded waste products, amino acids, hydrolases, toxins, hormones, neurotransmitters and other organelle protein contents. Thus, it was proposed that vesicular glycogen may be exocytosed from Pompe cells. Studies in a variety of LSD cell types, including Pompe, multiple sulphatase deficiency, MPS IIIA and neuronal ceroid lipofuscinoses, indicate the potential exocytosis of storage material (Medina *et al*., 2011). Evidence for glycogen exocytosis also comes from the presence of elevated amounts of glucose tetrasaccharide (Glc_4, a breakdown product of glycogen) in the serum of Pompe patients, when compared to unaffected individuals (An *et al*., 2005).

A method has previously been developed to quantify the amount of intracellular glycogen in cultured skin fibroblasts derived from infantile-onset Pompe patients and unaffected individuals (Umapathysivam *et al*., 2005); and further developed at the initiation of this project to provide greater sensitivity (Fuller *et al*., 2012). Pompe cells were cultured in serum- and glucose-free culture medium to deplete cytoplasmic glycogen, and primarily retain undegraded vesicular glycogen. In confluent unaffected control cells approximately 10% of the total cellular glycogen was contained within these vesicles, which was similar to reports in rat liver (Geddes and Stratton, 1977;

Geddes and Taylor, 1985) and muscle (Calder and Geddes, 1989). However, cultured skin fibroblasts derived from infantile-onset Pompe patients contain 6-fold more vesicular glycogen than unaffected control cells. In this thesis, cultured Pompe skin fibroblasts that had been depleted of cytoplasmic glycogen provided a model system to evaluate the exocytosis of glycogen from vesicular storage compartments.

Vesicular glycogen was exocytosed from both cultured Pompe and unaffected control skin fibroblasts. Unaffected control cells contain a limited amount of vesicular glycogen, which is presumptively controlled by the balance between the amount of autophagosomal glycogen uptake from the cytosol and the catabolism of this glycogen by GAA in autolysosomes (Brown *et al*., 1978; Umapathysivam *et al*., 2005). From this study it is evident that glycogen exocytosis may contribute to the dynamic balance of this process. Whilst glycogen exocytosis occurred in Pompe cells, it was clearly unable to compensate for the GAA deficiency and progressive autolysosomal accumulation of undegraded glycogen still occurred. However, if exocytosis could be up-regulated it could be used to increase the amount of stored glycogen released from Pompe cells. Indeed, the ability to clear or prevent glycogen accumulation has recently been identified as an important target for Pompe treatment (Orlikowski *et al*., 2011; Fukuda *et al*., 2006a). Therefore, in a Pompe patient, increasing the amount of cellular exocytosis may expose glycogen to circulating amylases to increase its degradation and potentially reduce the rate of disease progression.

The culture conditions that govern the release of vesicular glycogen from cells were defined, prior to developing a strategy to increase the amount of exocytosis from Pompe fibroblasts. The amount of glycogen exocytosis in Pompe skin fibroblasts was

modulated by the concentration of Ca^{2+} and the degree of culture confluence. Notably, after only two hours in culture, greater than 75% of vesicular glycogen was released from sub-confluent Pompe skin fibroblasts (undergoing significant cell division/migration), indicating that under appropriate conditions most of the stored glycogen can be released from Pompe cells, without impacting on cell viability.

Pharmacological compounds that influence the process of exocytosis were investigated to identify a drug that can potentially facilitate efficient glycogen exocytosis from Pompe cells. In confluent Pompe skin fibroblasts, three pharmacological compounds were shown to induce glycogen exocytosis; calcimycin, LPC and α-L-iduronidase. These compounds triggered vesicular glycogen release through the modulation of either Ca^{2+}-dependent (calcimycin) or Ca^{2+}-independent (LPC and α-L-iduronidase) exocytosis. The amount of glycogen released from confluent Pompe fibroblasts by these pharmacological agents was less than that observed in untreated sub-confluent Pompe fibroblasts. While these drugs were not the most optimal for releasing vesicular glycogen from Pompe cells, this provided proof-of-concept that drug-induced exocytosis of vesicular glycogen could be developed as an alternative or adjunct therapy for Pompe patients.

The observation that exposure to α-L-iduronidase stimulates exocytosis begs the question; to what extent is enhanced exocytosis in response to exposure to large amounts of exogenous enzyme the basis for the decrease in storage inclusions observed in LSD patients receiving ERT? A future experiment to answer this question inolves determining if enhanced glycogen release is reversed in α-L-iduronidase-treated cells exposed to mannose-6-phophate, which blocks receptor-mediated uptake of the enzyme.

During the compilation of this thesis, Spampanato et al (2013) reported that exocytosis induction is a mechanism to reduce glycogen storage in Pompe cells. In that study, glycogen load was reduced in both cultured muscle cells and in a Pompe mouse model through the overexpression of TFEB, a protein that regulates lysosomal biogenesis and autophagy. Importantly, autophagic vesicles were shown to be exocytosed, confirming that a major glycogen storage compartment can be targeted for glycogen release, which is crucial in the development of exocytic induction as a therapeutic option for Pompe disease.

Calcimycin treatment induced more glycogen exocytosis from Pompe cells than the other compounds investigated. Calcimycin triggers a Ca^{2+}-dependent exocytic process that results in cavicapture (Jaiswal *et al.*, 2004), which involves only partial fusion between intracellular vesicles and the plasma membrane (Larina *et al*., 2007) and therefore only permits a limited release of vesicle content from treated cells. The calcimycin-induced exocytic pore size for cultured fibroblasts is approximately 30 nm in diameter (Jaiswal *et al*., 2004), which was similar to the diameter previously reported for glycogen granules isolated from healthy cells (10 nm to 80 nm; Parker *et al*., 2007; Takeuchi *et al*., 1978). In the present study, greater than 50% of the vesicular glycogen granules isolated from either Pompe or unaffected control cells were found to be larger than 30 nm, and Pompe cells had more vesicular glycogen than control cells. Therefore, a significant proportion of the vesicular glycogen in Pompe cells may not be exocytosed by calcimycin treatment. Drugs that aim to induce cavicapture exocytosis may therefore have limited effectiveness for glycogen release from Pompe cells, but may have some therapeutic benefit by removing some of the accumulated glycogen granules.

Expanding the diameter of the exocytic pore or reducing the size of vesicular glycogen in Pompe cells may increase the cavicapture exocytosis of glycogen. The Syt VII protein, a Ca^{2+}-dependent trigger for regulated exocytosis, has been reported to be a key regulator of the diameter of the exocytic pore (Martinez *et al*., 2000). In fibroblasts where latex beads were internalised into the vesicular network, the diameter of the ionophore-induced exocytic pore increased when Syt VII was inhibited, permitting the exocytosis of larger beads than from untreated cells (Jaiswal *et al*., 2004). ERT has been reported to decrease the amount of vesicular glycogen that accumulates in cultured Pompe fibroblasts (Yang *et al*., 1998) and other affected tissues (Van den Hout *et al*., 2004), which would presumably reduce the diameter of the accumulated glycogen granules. Combining ERT with calcimycin treatment may therefore be a strategy to improve glycogen release; ERT will decrease glycogen granule size, allowing more glycogen to pass through the exocytic pore; and calcimycin will decrease the amount of glycogen that needs to be catabolised by the infused GAA. However, significant toxicity issues have been associated with calcimycin so an alternative drug would need to be identified (Sobotka *et al*., 1987; Pruzansky and Patterson, 1979).

All-or-none exocytosis permits the complete fusion of vesicles with the plasma membrane, and this process may not limit the size or amount of vesicular glycogen release from the cell. All-or-none exocytosis involves a Ca^{2+}-independent event, and this may provide a more attractive target for therapeutic development. While α-L-iduronidase treatment was predicted to induce all-or-none exocytosis, it was not particularly effective at releasing the glycogen from Pompe cells. This may be due to the dose of α-L-iduronidase administered to the Pompe cells and the relative amount of

endocytic uptake and consequently the amount of compensatory exocytosis. Thus, the type of endocytosis may be important; as clathrin-mediated endocytosis, phagocytosis, macropinocytosis, and caveolin-dependent endocytosis each involve different amounts of plasma membrane internalisation (Zaki and Tirelli, 2010). Clathrin-mediated and caveolin-dependent endocytosis are associated with the uptake of protein and are expected to internalize relatively small amounts of plasma membrane. Conversely, macropinocytosis, which operates during cell migration, has been reported to internalise large quantities of plasma membrane into the vesicular network (Doherty and McMahon, 2009). This link between glycogen exocytosis in Pompe cells and the amount of cell surface membrane that is internalised by endocytosis may possibly explain the increased release of glycogen from sub-confluent (dividing/migrating) Pompe cells, when compared to confluent cells treated with protein. It appears that in order to maximise the amount of glycogen exocytosis from Pompe cells, there is a need to target a process that involves a large amount of cell surface plasma membrane internalisation, in order to induce sufficient compensatory exocytosis.

Further studies are required to devise a strategy to increase glycogen exocytosis in Pompe cells. This may be achieved by targeting the machinery involved in all-or-none exocytosis. F-Actin, clathrin and dynamin are each involved in vesicle fusion events (Jaiswal *et al*., 2009). The presence of F-actin at the cell membrane, clathrin on the vesicle, and dynamin on the neck of the fusing vesicle restrict both fusion pore expansion. It is therefore predicted that inhibiting F-actin, clathrin and dynamin may increase the exocytic release of glycogen from Pompe cells. In one study, reducing the association of vesicles with both clathrin and cortical F-actin increased the number of

total fusion events (Jaiswal *et al*., 2009). Glycogen exocytosis may also be enhanced by modulating cell membrane tension, as the rates of both endocytosis and exocytosis depend on cell surface plasma membrane tension (Keren, 2011). Changes in membrane tension can be induced by osmotic shock; thus, hypo-osmotic shock contributes to cell swelling and is accompanied by an increase in membrane tension, whereas hyper-osmotic conditions cause an outward water flux from the cell leading to a decrease in membrane tension. An increase in osmotic pressure may therefore provide a mechanism to induce changes in tension, possibly leading to the induction of exocytosis and increased glycogen release.

Pompe disease is a debilitating disorder that can contribute to premature death in patients. The induction of glycogen exocytosis has the potential to reduce glycogen accumulation, thereby delaying/reducing the impact of the disease and increasing the life span of patients. Studies to gain a more detailed understanding of the mechanisms and the molecular machinery involved in exocytosis as well as the regulation of these events are required, as these may identify other targets to modulate glycogen release. Compounds that demonstrate both clinical safety and efficacy may provide a therapeutic option for Pompe disease and improve the quality of life for patients.

References

1. Alberts GL, Pregenzer JF, Im WB (2000). Advantages of heterologous expression of human D2 long dopamine receptors in human neuroblastoma SH-SY5Y over human embryonic kidney 293 cells. *Br J Pharmacol*. 131(3):514-20.
2. Alés E, Tabares L, Poyato JM, Valero V, Lindau M, Alvarez de Toledo G (1999). High calcium concentrations shift the mode of exocytosis to the kiss-and-run mechanism. *Nat Cell Biol*. 1(1):40-4.
3. Alonso MD, Lomako J, Lomako WM, Whelan WJ (1995). A new look at the biogenesis of glycogen. *FASEB J*. 9(12):1126-37.
4. Amatore C, Arbault S, Bouret Y, Guille M, Lemaître F, Verchier Y (2006). Regulation of exocytosis in chromaffin cells by trans-insertion of LPC and arachidonic acid into the outer leaflet of the cell membrane. *Chembiochem.* 7(12):1998-2003.
5. An Y, Young SP, Kishnani PS, Millington DS, Amalfitano A, Corz D, Chen YT (2005). Glucose tetrasaccharide as a biomarker for monitoring the therapeutic response to enzyme replacement therapy for Pompe disease. *Mol Genet Metab*. 85(4):247-54.
6. Andersson U, Reinkensmeier G, Butters TD, Dwek RA, Platt FM (2004). Inhibition of glycogen breakdown by imino sugars in vitro and in vivo. *Biochem Pharmacol*. 67(4):697-705.
7. Arico S, Petiot A, Bauvy C, Dubbelhuis PF, Meijer AJ, Codogno P, Ogier-Denis E (2001). The tumor suppressor PTEN positively regulates macroautophagy by

inhibiting the phosphatidylinositol 3-kinase/protein kinase B pathway. *J Biol Chem*. 276(38):35243-6.

8. Ashford TP, Porter KR (1962). Cytoplasmic components in hepatic cell lysosomes. *J Cell Biol*. 12:198-202.

9. Ausems MG, Verbiest J, Hermans MP, Kroos MA, Beemer FA, Wokke JH, Sandkuijl LA, Reuser AJ, van der Ploeg AT (1999). Frequency of glycogen storage disease type II in The Netherlands: implications for diagnosis and genetic counselling. *Eur J Hum Genet*. 7(6):713-6.

10. Bainton DF (1981). The discovery of lysosomes. *J Cell Biol*. 91(3 Pt 2):66s-76s.

11. Baram D, Adachi R, Medalia O, Tuvim M, Dickey BF, Mekori YA, Sagi-Eisenberg R (1999). Synaptotagmin II negatively regulates Ca2+-triggered exocytosis of lysosomes in mast cells. *J Exp Med.* 189(10):1649-58.

12. Barg S and Macado JD (2008). Compensatory endocytosis in chromaffin cells. *Acta Physiol.* 192(2):195-201.

13. Beaumont V, Llobet A, Lagnado L (2005). Expansion of calcium microdomains regulates fast exocytosis at a ribbon synapse. *Proc Natl Acad Sci U S A*. 102(30):10700-5.

14. Beck M (2010). Therapy for lysosomal storage disorders. *IUBMB Life*. 62(1):33-40. Review.

15. Becker SM, Delamarre L, Mellman I, Andrews NW (2009). Differential role of the Ca(2+) sensor synaptotagmin VII in macrophages and dendritic cells. *Immunobiology*. 214(7):495-505.

16. Bellu AR, Kiel JA (2003). Selective degradation of peroxisomes in yeasts. *Microsc Res Tech*. 61(2):161-70. Review.

17. Berg, JM.; Tymoczko, JL, and Stryer, L (2002). *Biochemistry.* 5th ed. New York: W. H. Freeman and Co. Chapter 21.

18. Besterman JM, Airhart JA, Low RB, Rannels DE (1983). Pinocytosis and intracellular degradation of exogenous protein: modulation by amino acids. *J Cell Biol*. 96(6):1586-91.

19. Bodamer OA, Dajnoki A (2012). Diagnosing lysosomal storage disorders: pompe disease. *Curr Protoc Hum Genet*. Chapter 17:Unit17.11.

20. Boucrot E, Kirchhausen T (2007). Endosomal recycling controls plasma membrane area during mitosis. *Proc Natl Acad Sci U S A.* 104(19):7939-44.

21. Boucrot E, Kirchhausen T (2008). Mammalian cells change volume during mitosis. *PLoS ONE.* 3(1):1477.

22. Boya P (2012). Lysosomal function and dysfunction: mechanism and disease. *Antioxid Redox Signal*. 17(5):766-74. Review.

23. Braulke T, Bonifacino JS (2009). Sorting of lysosomal proteins. *Biochim Biophys Acta*.1793(4):605-14.

24. Brown DH, Waindle LM, Brown BI (1978). The apparent activity in vivo of the lysosomal pathway of glycogen catabolism in cultured human skin fibroblasts from patients with type III glycogen storage disease. *J Biol Chem.* 253(14):5005-11.

25. Bucurenciu I, Kulik A, Schwaller B, Frotscher M, Jonas P (2008). Nanodomain coupling between Ca2+ channels and Ca2+ sensors promotes fast and efficient transmitter release at a cortical GABAergic synapse. *Neuron*. 57(4):536-45.

26. Bursch W, Hochegger K, Torok L, Marian B, Ellinger A, Hermann RS (2000). Autophagic and apoptotic types of programmed cell death exhibit different fates of cytoskeletal filaments. *J Cell Sci*. 113 (Pt 7):1189-98.

27. Byrne BJ, Falk DJ, Pacak CA, Nayak S, Herzog RW, Elder ME, Collins SW, Conlon TJ, Clement N, Cleaver BD, Cloutier DA, Porvasnik SL, Islam S, Elmallah MK, Martin A, Smith BK, Fuller DD, Lawson LA, Mah CS (2011). Pompe disease gene therapy. *Hum Mol Genet*. 20(R1):R61-8. Review.

28. Calder PC, Geddes R (1989). Rat skeletal muscle lysosomes contain glycogen. *Int J Biochem.* 21(5):561-7.

29. Calì C, Marchaland J, Spagnuolo P, Gremion J, Bezzi P (2009). Regulated exocytosis from astrocytes physiological and pathological related aspects. *Int Rev Neurobiol*. 85:261-93.

30. Cardone M, Porto C, Tarallo A, Vicinanza M, Rossi B, Polishchuk E, Donaudy F, Andria G, De Matteis MA, Parenti G (2008). Abnormal mannose-6-phosphate receptor trafficking impairs recombinant alpha-glucosidase uptake in Pompe disease fibroblasts. *Pathogenetics*. 1(1):6.

31. Chen FW, Li C, Ioannou YA (2010). Cyclodextrin induces calcium-dependent lysosomal exocytosis. *PLoS One*. 5(11):e15054.

32. Chen WT (1981). Mechanism of retraction of the trailing edge during fibroblast movement. *J Cell Biol.* 90(1):187-200.

33. Chen Y, Klionsky DJ (2011). The regulation of autophagy - unanswered questions. *J Cell Sci*. 15;124(Pt 2):161-70. Review.

34. Chien YH, Chiang SC, Zhang XK, Keutzer J, Lee NC, Huang AC, Chen CA, Wu MH, Huang PH, Tsai FJ, Chen YT, Hwu WL (2008). Early detection of Pompe disease by newborn screening is feasible: results from the Taiwan screening program. *Pediatrics*. 122(1):e39-45.

35. Chieregatti E, Meldolesi J (2005). Regulated exocytosis: new organelles for non-secretory purposes. *Nat Rev Mol Cell Biol*. 6(2):181-7

36. Clark SL (1957). Cellular differentiation in the kidneys of newborn mice studies with the electron microscope. *J Biophys Biochem Cytol.* 25;3(3):349-62.

37. Clements PR, Muller V, Hopwood JJ (1985). Human alpha-L-iduronidase. 2. Catalytic properties. *Eur J Biochem*. 152(1):29-34.

38. Cocucci E, Racchetti G, Podini P, Meldolesi J (2007). Enlargeosome traffic: exocytosis triggered by various signals is followed by endocytosis, membrane shedding or both. *Traffic*. 8(6):742-57.

39. Codogno P, Meijer AJ. (2005). Autophagy and signaling: their role in cell survival and cell death. *Cell Death Differ*. 2:1509-18.

40. Cresawn KO, Fraites TJ, Wasserfall C, Atkinson M, Lewis M, Porvasnik S, Liu C, Mah C, Byrne BJ (2005). Impact of humoral immune response on distribution and efficacy of recombinant adeno-associated virus-derived acid alpha-glucosidase in a model of glycogen storage disease type II. *Hum Gene Ther*. 16(1):68-80.

41. Cryer PE, Davis SN, Shamoon H (2003). Hypoglycemia in diabetes. *Diabetes Care*. 26(6):1902-12.

42. Darios F, Connell E, Davletov B (2007). Phospholipases and fatty acid signalling in exocytosis. *J Physiol*. 585(Pt 3):699-704.

43. De Duve C, Wattiaux R (1966). Functions of lysosomes. *Annu Rev Physiol*. 28:435-92. Review.

44. De Duve C (1983). Lysosomes revisited. *Eur J Biochem*. 137(3):391-7. Review.

45. Deretic V, Singh S, Master S, Kyei G, Davis A, Naylor J, de Haro S, Harris J, Delgado M, Roberts E, Vergne I (2007). Phosphoinositides in phagolysosome and autophagosome biogenesis. *Biochem Soc Symp*. (74):141-8.

46. DeRuisseau LR, Fuller DD, Qiu K, DeRuisseau KC, Donnelly WH Jr, Mah C, Reier PJ, Byrne BJ (2009). Neural deficits contribute to respiratory insufficiency in Pompe disease. *Proc Natl Acad Sci U S A*. 106(23):9419-24.

47. de Saint Basile G, Ménasché G, Fischer A (2010). Molecular mechanisms of biogenesis and exocytosis of cytotoxic granules. *Nat Rev Immunol*. 10(8):568-79. Review.

48. Dice JF (2007). Chaperone-mediated autophagy. *Autophagy*. 3(4):295-9. Review.

49. Dyachok O, Gylfe E (2004). Ca(2+)-induced Ca(2+) release via inositol 1,4,5-trisphosphate receptors is amplified by protein kinase A and triggers exocytosis in pancreatic beta-cells. *J Biol Chem*. 279(44):45455-61.

50. Eggers CT, Schafer JC, Goldenring JR, Taylor SS (2009). D-AKAP2 interacts with Rab4 and Rab11 through its RGS domains and regulates transferrin receptor recycling. *J Biol Chem*. 284(47):32869-80.

51. Elsner P, Quistorff B, Hansen GH, Grunnet N (2002). Partly ordered synthesis and degradation of glycogen in cultured rat myotubes. *J Biol Chem.* 277(7):4831-8.

52. Eskelinen EL, Tanaka Y, Saftig P (2003). At the acidic edge: emerging functions for lysosomal membrane proteins. *Trends Cell Biol*. 13(3):137-45.

53. Eskelinen EL (2006). Roles of LAMP-1 and LAMP-2 in lysosome biogenesis and autophagy. *Mol Aspects Med*. 27(5-6):495-502. Review.

54. Eskelinen EL (2008). Fine structure of the autophagosome. *Methods Mol Biol*. 445:11-28.

55. Fernández-Chacón R, Alvarez de Toledo G (1995). Cytosolic calcium facilitates release of secretory products after exocytotic vesicle fusion. *FEBS Lett*. 363(3):221-5.

56. Ferraro F, Eipper BA, Mains RE (2005). Retrieval and reuse of pituitary secretory granule proteins. *J Biol Chem*. 280(27):25424-35.

57. Flanagan JJ, Rossi B, Tang K, Wu X, Mascioli K, Donaudy F, Tuzzi MR, Fontana F, Cubellis MV, Porto C, Benjamin E, Lockhart DJ, Valenzano KJ, Andria G, Parenti G, Do HV (2009). The pharmacological chaperone 1-deoxynojirimycin increases the activity and lysosomal trafficking of multiple mutant forms of acid alpha-glucosidase. *Hum Mutat.* 30(12):1683-92.

58. Fukuda T, Ahearn M, Roberts A, Mattaliano RJ, Zaal K, Ralston E, Plotz PH, Raben N (2006). Autophagy and mistargeting of therapeutic enzyme in skeletal muscle in Pompe disease. *Mol Ther*. 14(6):831-9.

59. Fukuda T, Ewan L, Bauer M, Mattaliano RJ, Zaal K, Ralston E, Plotz PH, Raben N (2006). Dysfunction of endocytic and autophagic pathways in a lysosomal storage disease. *Ann Neurol*. 59(4):700-8.

60. Fuller M, Duplock S, Turner C, Davey P, Brooks DA, Hopwood JJ, Meikle PJ (2012). Mass spectrometric quantification of glycogen to assess primary substrate accumulation in the Pompe mouse. *Anal Biochem*. 421(2):759-63.

61. Geppert M, Goda Y, Hammer RE, Li C, Rosahl TW, et al. (1994) Synaptotagmin I: A major Ca2þ sensor for transmitter release at a central synapse. *Cell* 79:717–727.

62. Gerasimenko JV, Gerasimenko OV, Petersen OH (2001). Membrane repair: Ca(2+)-elicited lysosomal exocytosis. *Curr Biol.* 11(23):R971-4.

63. Givan, A.L (2001). Flow cytometry: first principles 2nd ed. New York: Wiley, John & Sons, Inc.

64. Glauert, A.M., Lewis, P.R. (1998). Biological Specimen Preparation for Transmission Electron Microscopy. Practical Methods in Electron Microscopy: vol. 17.

65. Goldsmith E, Sprang S and Fletterick R (1982). Structure of maltoheptaose by difference Fourier methods and a model for glycogen. *J. Mol. Biol*. 156:411-427.

66. Goss JW, Toomre DK (2008). Both daughter cells traffic and exocytose membrane at the cleavage furrow during mammalian cytokinesis. *J Cell Biol*. 181(7):1047-54.

67. Grant BD, Donaldson JG (2009). Pathways and mechanisms of endocytic recycling. *Nat Rev Mol Cell Biol*. 10(9):597-608.

68. Grapengiesser E, Gylfe E, Hellman B (1991). Cyclic AMP as a determinant for glucose induction of fast Ca2+ oscillations in isolated pancreatic beta-cells. *J Biol Chem*. 266(19):12207-10.

69. Harmatz P, Yu ZF, Giugliani R, Schwartz IV, Guffon N, Teles EL, Miranda MC, Wraith JE, Beck M, Arash L, Scarpa M, Ketteridge D, Hopwood JJ, Plecko B, Steiner R, Whitley CB, Kaplan P, Swiedler SJ, Hardy K, Berger KI, Decker C (2010). Enzyme replacement therapy for mucopolysaccharidosis VI: evaluation of long-term pulmonary function in patients treated with recombinant human N-acetylgalactosamine 4-sulfatase. *J Inherit Metab Dis*. 33(1):51-60.

70. Hasilik A (1992). The early and late processing of lysosomal enzymes: proteolysis and compartmentation. *Experientia*. 48(2):130-51. Review.

71. Hawes ML, Kennedy W, O'Callaghan MW, Thurberg BL (2007). Differential muscular glycogen clearance after enzyme replacement therapy in a mouse model of Pompe disease. *Mol Genet Metab.* 91(4):343-51.

72. Hayashi-Nishino M, Fujita N, Noda T, Yamaguchi A, Yoshimori T, Yamamoto A (2009). A subdomain of the endoplasmic reticulum forms a cradle for autophagosome formation. *Nat Cell Biol*. 11(12):1433-7.

73. He C, Klionsky DJ (2009). Regulation mechanisms and signaling pathways of autophagy. *Annu Rev Genet*. 43:67-93. Review.

74. He B, Guo W (2009). The exocyst complex in polarized exocytosis. *Curr Opin Cell Biol*. 21(4):537-42.

75. Hermans MM, Kroos MA, de Graaff E, Oostra BA, Reuser AJ (1993). Two mutations affecting the transport and maturation of lysosomal alpha-glucosidase in an adult case of glycogen storage disease type II. *Hum Mutat.* 2(4):268-73.

76. Hermans MM, Kroos MA, Smeitink JA, van der Ploeg AT, Kleijer WJ, Reuser AJ (1998).

77. Hermans MM, van Leenen D, Kroos MA, Beesley CE, Van Der Ploeg AT, Sakuraba H, Wevers R, Kleijer W, Michelakakis H, Kirk EP, Fletcher J, Bosshard N, Basel-Vanagaite L, Besley G, Reuser AJ (2004). Twenty-two novel mutations in the lysosomal alpha-glucosidase gene (GAA) underscore the genotype-phenotype correlation in glycogen storage disease type II. *Hum Mutat.* 23(1):47-56.

78. Hers HG (1963). alpha-Glucosidase deficiency in generalized glycogen storage disease (Pompe's disease). *Biochem J.* 86:11-6.

79. Hesselink RP, Wagenmakers AJ, Drost MR, Van der Vusse GJ (2003). Lysosomal dysfunction in muscle with special reference to glycogen storage disease type II. *Biochim Biophys Acta.* 1637(2):164-70.

80. Hirschhorn, R., and Reuser, A.J.J, (2001). Glycogen storage disease type II; acid α-glucosidase (acid maltase) deficiency. In Scriver, C.R., Beaudet, A.L., Valle, D., Sly, W.S., (eds.). *The metabolic and molecular bases of inherited disease*. 8th ed. Vol. III. New York: McGraw-Hill, pp. 3389-3420.

81. Hoefsloot LH, Hoogeveen-Westerveld M, Kroos MA, van Beeumen J, Reuser AJ, Oostra BA (1988). Primary structure and processing of lysosomal alpha-

glucosidase; homology with the intestinal sucrase-isomaltase complex. *EMBO J.* 7(6):1697-704.

82. Holz GG, Kang G, Harbeck M, Roe MW, Chepurny OG (2006). Cell physiology of cAMP sensor Epac. *J Physiol*. 577(Pt 1):5-15.

83. Huie ML, Chen AS, Tsujino S, Shanske S, DiMauro S, Engel AG, Hirschhorn R (1994). Aberrant splicing in adult onset glycogen storage disease type II (GSDII): molecular identification of an IVS1 (-13T-->G) mutation in a majority of patients and a novel IVS10 (+1GT-->CT) mutation. *Hum Mol Genet*. 3(12):2231-6.

84. Huie ML, Tsujino S, Sklower Brooks S, Engel A, Elias E, Bonthron DT, Bessley C, Shanske S, DiMauro S, Goto YI, Hirschhorn R (1998). Glycogen storage disease type II: identification of four novel missense mutations (D645N, G648S, R672W, R672Q) and two insertions/deletions in the acid alpha-glucosidase locus of patients of differing phenotype. *Biochem Biophys Res Commun.* 244(3):921-7.

85. Huotari J, Helenius A (2011). Endosome maturation. *EMBO J*. 30(17):3481-500.

86. Hurley TD, Walls C, Bennett JR, Roach PJ, Wang M (2006). Direct detection of glycogenin reaction products during glycogen initiation. *Biochem Biophys Res Commun.* 22;348(2):374-8.

87. Ito N, Yokomizo T, Sasaki T, Kurosu H, Penninger J, Kanaho Y, Katada T, Hanaoka K, Shimizu T (2002). Requirement of phosphatidylinositol 3-kinase activation and calcium influx for leukotriene B4-induced enzyme release. *J Biol Chem*. 277(47):44898-904.

88. Jackson MB, Chapman ER (2008). The fusion pores of Ca(2+)-triggered exocytosis. *Nat Struct Mol Biol*. 15(n7):684-689.

89. Jaiswal JK, Andrews NW, Simon SM (2002). Membrane proximal lysosomes are the major vesicles responsible for calcium-dependent exocytosis in nonsecretory cells. *J Cell Biol.* 159(4):625-35.

90. Jaiswal JK, Chakrabarti S, Andrews NW, Simon SM (2004). Synaptotagmin VII restricts fusion pore expansion during lysosomal exocytosis. *PLoS Biol*. 2: 233.

91. Jaiswal JK, Fix M, Takano T, Nedergaard M, Simon SM (2007). Resolving vesicle fusion from lysis to monitor calcium-triggered lysosomal exocytosis in astrocytes. *Proc Natl Acad Sci U S A*104(35):14151-6.

92. Jaiswal JK, Rivera VM, Simon SM (2009). Exocytosis of post-Golgi vesicles is regulated by components of the endocytic machinery. *Cell*. 137(7):1308-19.

93. Jewell JL, Oh E, Ramalingam L, Kalwat MA, Tagliabracci VS, Tackett L, Elmendorf JS, Thurmond DC (2011). Munc18c phosphorylation by the insulin receptor links cell signaling directly to SNARE exocytosis. *J Cell Biol.* 193(1):185-99.

94. Jorgensen EM, Hartwieg E, Schuske K, Nonet ML, Jin Y, (1995). Defective recycling of synaptic vesicles in synaptotagmin mutants of Caenorhabditis elegans. *Nature*. 378: 196–199.

95. Jovic M, Sharma M, Rahajeng J, Caplan S (2010). The early endosome: a busy sorting station for proteins at the crossroads. *Histol Histopathol*. 25(1):99-112.

96. Juhaszova M, Church P, Blaustein MP, Stanley EF (2000). Location of calcium transporters at presynaptic terminals. *Eur J Neurosci*. 12(3):839-46.

97. Kasai K, Ohara-Imaizumi M, Takahashi N, Mizutani S, Zhao S, Kikuta T, Kasai H, Nagamatsu S, Gomi H, Izumi T (2005). Rab27a mediates the tight docking of insulin granules onto the plasma membrane during glucose stimulation. *J Clin Invest.* 115(2):388-96.

98. Kemper AR, Hwu WL, Lloyd-Puryear M, Kishnani PS (2007). Review. Newborn screening for Pompe disease: synthesis of the evidence and development of screening recommendations. *Pediatrics.* 120(5): 1327-34.

99. Khvotchev MV, Ren M, Takamori S, Jahn R, Südhof TC (2003). Divergent functions of neuronal Rab11b in Ca2+-regulated versus constitutive exocytosis. *J Neurosci*. 23(33):10531-9.

100. Kishnani PS, Steiner RD, Bali D, Berger K, Byrne BJ, Case LE, Crowley JF, Downs S, Howell RR, Kravitz RM, Mackey J, Marsden D, Martins AM, Millington DS, Nicolino M, O'Grady G, Patterson MC, Rapoport DM, Slonim A, Spencer CT, Tifft CJ, Watson MS (2006). Pompe disease diagnosis and management guideline. *Genet Med*. 8: 267–88.

101. Kishnani PS, Corzo D, Nicolino M, Byrne B, Mandel H, Hwu WL, Leslie N, Levine J, Spencer C, McDonald M, Li J, Dumontier J, Halberthal M, Chien YH, Hopkin R, Vijayaraghavan S, Gruskin D, Bartholomew D, van der Ploeg A, Clancy JP, Parini R, Morin G, Beck M, De la Gastine GS, Jokic M, Thurberg B, Richards S, Bali D, Davison M, Worden MA, Chen YT, Wraith JE (2007). Recombinant human acid [alpha]-glucosidase: major clinical benefits in infantile-onset Pompe disease. *Neurology*. 68(2):99-109.

102. Kishnani PS, Goldenberg PC, DeArmey SL, Heller J, Benjamin D, Young S, Bali D, Smith SA, Li JS, Mandel H, Koeberl D, Rosenberg A, Chen YT (2009). Cross-reactive immunologic material status affects treatment outcomes in Pompe disease infants. *Mol Genet Metab*. 99(1):26-33.

103. Klein D, Büssow H, Fewou SN, Gieselmann V (2005). Exocytosis of storage material in a lysosomal disorder. *Biochem Biophys Res Commun.* 327(3):663-7.

104. Klingauf J, Neher E (1997). Modeling buffered Ca2+ diffusion near the membrane: implications for secretion in neuroendocrine cells. *Biophys J*. 72(2 Pt 1):674-90.

105. Klionsky DJ (2005). Autophagy. *Curr Biol*. 15(8):R282-3.

106. Knecht E, Hernández J (1978). Ultastructural localization of polysaccharides in the vacuolar system of an established cell line. *Cell Tissue Res.* 193(3):473-89.

107. Kondomerkos DJ, Kalamidas SA, Kotoulas OB (2004). An electron microscopic and biochemical study of the effects of glucagon on glycogen autophagy in the liver and heart of newborn rats. *Microsc Res Tech*. 63(2):87-93.

108. Koster JF, Slee RG (1977). Some properties of human liver acid alpha-glucosidase. *Biochim Biophys Acta.* 482(1):89-97.

109. Kotoulas OB, Kalamidas SA, Kondomerkos DJ (2004). Glycogen autophagy. *Microsc Res Tech.* 64(1):10-20.

110. Kovács AL, Pálfia Z, Réz G, Vellai T, Kovács J (2007). Sequestration revisited: integrating traditional electron microscopy, de novo assembly and new results. *Autophagy*. 3(6):655-62.

111. Kroos M, Pomponio RJ, van Vliet L, Palmer RE, Phipps M, Van der Helm R, Halley D, Reuser A; GAA Database Consortium (2008). Update of the Pompe disease mutation database with 107 sequence variants and a format for severity rating. *Hum Mutat.* 29(6):13-26.

112. Kroos M, Hoogeveen-Westerveld M, Michelakakis H, Pomponio R, Van der Ploeg A, Halley D, Reuser A; GAA Database Consortium (2012). Update of the pompe disease mutation database with 60 novel GAA sequence variants and additional studies on the functional effect of 34 previously reported variants. *Hum Mutat*. 33(8):1161-5.

113. Kroos M, Hoogeveen-Westerveld M, van der Ploeg A, Reuser AJ (2012). The genotype-phenotype correlation in Pompe disease. *Am J Med Genet C Semin Med Genet*. 160(1):59-68.

114. Kumlien J, Andrén-Sandberg A, Zopf D, Lundblad A (1989). Determination of a glucose-containing tetrasaccharide in urine of patients with acute pancreatitis. *Int J Pancreatol.* 4(2):139-47.

115. Kuncl RW, Bilak MM, Craig SW, Adams R (2003). Exocytotic "constipation" is a mechanism of tubulin/lysosomal interaction in colchicine myopathy. *Exp Cell Res.* 285(2):196-207.

116. Kyosen SO, Iizuka S, Kobayashi H, Kimura T, Fukuda T, Shen J, Shimada Y, Ida H, Eto Y, Ohashi T (2010). Neonatal gene transfer using lentiviral vector for murine Pompe disease: long-term expression and glycogen reduction. *Gene Ther*. 17(4):521-30.

117. LaPlante JM, Sun M, Falardeau J, Dai D, Brown EM, Slaugenhaupt SA, Vassilev PM (2006). Lysosomal exocytosis is impaired in mucolipidosis type IV. *Mol Genet Metab.* 89(4):339-48.

118. Larina O, Bhat P, Pickett JA, Launikonis BS, Shah A, Kruger WA, Edwardson JM, Thorn P (2007). Dynamic regulation of the large exocytotic fusion pore in pancreatic acinar cells. *Mol Biol Cell.* 18(9):3502-11.

119. Launikonis BS, Murphy RM, Edwards JN (2010). Toward the roles of store-operated Ca2+ entry in skeletal muscle. *Pflugers Arch*. 460(5):813-23.

120. Lavrenova TP, Presnova VN (1994). Rat liver neutral alpha-glucosidase: isolation and characterization. *Biochem Mol Biol Int.* 32(4):671-9.

121. Leaback DH, Walker PG (1961). Studies on glucosaminidase. 4. The fluorimetric assay of N-acetyl-beta-glucosaminidase. Biochem J. 78:151-6.

122. Legrand C, Bour JM, Jacob C, Capiaumont J, Martial A, Marc A, Wudtke M, Kretzmer G, Demangel C, Duval D, *et al* (1992). Lactate dehydrogenase (LDH) activity of the cultured eukaryotic cells as marker of the number of dead cells in the medium [corrected]. *J Biotechnol*. 25(3):231-43.

123. Li D, Ropert N, Koulakoff A, Giaume C, Oheim M (2008). Lysosomes are the major vesicular compartment undergoing Ca2+-regulated exocytosis from cortical astrocytes. *J Neurosci.* 28(30):7648-58.

124. Lock JG, Stow JL (2005). Rab11 in recycling endosomes regulates the sorting and basolateral transport of E-cadherin. *MolBiol Cell*.16(4):1744-55.

125. Lord JM, Roberts LM, Stirling CJ (2005). Quality control: another player joins the ERAD cast. *Curr Biol*. 15(23):R963-4.

126. Low JT, Shukla A, Behrendorff N, Thorn P (2010). Exocytosis, dependent on Ca2+ release from Ca2+ stores, is regulated by Ca2+ microdomains. *J Cell Sci*. 123(Pt 18):3201-8.

127. Luzio JP, Rous BA, Bright NA, Pryor PR, Mullock BM, Piper RC (2000). Lysosome-endosome fusion and lysosome biogenesis. *J Cell Sci*. 113(Pt 9):1515-24. Review.

128. Luzio JP, Mullock BM, Pryor PR, Lindsay MR, James DE, Piper RC (2001). Relationship between endosomes and lysosomes. *Biochem Soc Trans*. 29(Pt 4):476-80.

129. Luzio JP, Pryor PR, Bright NA (2007). Lysosomes: fusion and function. *Nat Rev Mol Cell Biol*. 8(8):622-32. Review.

130. Luzio JP, Parkinson MD, Gray SR, Bright NA (2009). The delivery of endocytosed cargo to lysosomes. *Biochem Soc Trans* 37(Pt 5):1019-21. Review.

131. Luzio JP, Gray SR, Bright NA (2010). Endosome-lysosome fusion. *Biochem Soc Trans*. 2010 38(6):1413-6.

132. Lynch CM, Johnson J, Vaccaro C, Thurberg BL (2005). High-resolution light microscopy (HRLM) and digital analysis of Pompe disease pathology. *J Histochem Cytochem*. 53(1):63-73.

133. Ma X, Zhang Y, Gromada J, Sewing S, Berggren PO, Buschard K, Salehi A, Vikman J, Rorsman P, Eliasson L (2005). Glucagon stimulates exocytosis in mouse and rat pancreatic alpha-cells by binding to glucagon receptors. *Mol Endocrinol*. 19(1):198-212.

134. Mah C, Cresawn KO, Fraites TJ Jr, Pacak CA, Lewis MA, Zolotukhin I, Byrne BJ (2005). Sustained correction of glycogen storage disease type II using adeno-associated virus serotype 1 vectors. *Gene Ther*12(18):1405-9.

135. Mahuran DJ (1995). Beta-hexosaminidase: biosynthesis and processing of the normal enzyme, and identification of mutations causing Jewish Tay-Sachs disease. *Clin Biochem.* 28(2):101-6.

136. Majeski AE, Dice JF (2004). Mechanisms of chaperone-mediated autophagy. *Int J Biochem Cell Biol*. 36(12):2435-44.

137. Marchand I, Chorneyko K, Tarnopolsky M, Hamilton S, Shearer J, Potvin J, Graham TE (2002). Quantification of subcellular glycogen in resting human muscle: granule size, number, and location. *J Appl Physiol.* 93(5):1598-607.

138. Margolis ML, Howlett P, Goldberg R, Eftychiadis A, Levine S (1994). Obstructive sleep apnea syndrome in acid maltase deficiency. *Chest.* 105(3):947-9.

139. Martinet W, De Meyer GR, Herman AG, Kockx MM (2005). Amino acid deprivation induces both apoptosis and autophagy in murine C2C12 muscle cells. *Biotechnol Lett*. 27(16):1157-63.

140. Martinet W and De Meyer GR (2008). Autophagy in atherosclerosis. *Curr Atheroscler Rep*. 10(3):216-33.

141. Martinez I, Chakrabarti S, Hellevik T, Morehead J, Fowler K, Andrews NW (2000). Synaptotagmin VII regulates Ca(2+)-dependent exocytosis of lysosomes in fibroblasts. *J Cell Biol.* 148(6):1141-49.

142. Martiniuk F, Mehler M, Pellicer A, Tzall S, La Badie G, Hobart C, Ellenbogen A, Hirschhorn R (1986). Isolation of a cDNA for human acid alpha-glucosidase and detection of genetic heterogeneity for mRNA in three alpha-glucosidase-deficient patients. *Proc Natl Acad Sci U S A*. 83(24):9641-4.

143. Martiniuk F, Chen A, Mack A, Arvanitopoulos E, Chen Y, Rom WN, Codd WJ, Hanna B, Alcabes P, Raben N, Plotz P (1998). Carrier frequency for glycogen storage disease type II in New York and estimates of affected individuals born with the disease. *Am J Med Genet.* 79(1):69-72.

144. McNeil PL (2002). Review. Repairing a torn cell surface: make way, lysosomes to the rescue. *J Cell Sci.* 115(Pt 5):873-9.

145. Mechtler TP, Stary S, Metz TF, De Jesús VR, Greber-Platzer S, Pollak A, Herkner KR, Streubel B, Kasper DC (2012). Neonatal screening for lysosomal storage disorders: feasibility and incidence from a nationwide study in Austria. *Lancet*. 379(9813):335-41.

146. Medina DL, Fraldi A, Bouche V, Annunziata F, Mansueto G, Spampanato C, Puri C, Pignata A, Martina JA, Sardiello M, Palmieri M, Polishchuk R, Puertollano R, Ballabio A (2011). Transcriptional activation of lysosomal exocytosis promotes cellular clearance. *Dev Cell*. 21(3):421-30.

147. Meikle PJ, Hopwood JJ, Clague AE, Carey WF (1999). Prevalence of lysosomal storage disorders. *JAMA.* 281(3):249-54.

148. Meléndez R, Meléndez-Hevia E, Canela EI (1999). The fractal structure of glycogen: A clever solution to optimize cell metabolism. *Biophys J*. 77(3):1327-32.

149. Mellman I (1996). Endocytosis and molecular sorting. *Annu Rev Cell Dev Biol*. 12:575-625.

150. Meyer ZuHeringdorf D (2004) Lysophospholipid receptor-dependent and -independent calcium signaling. J Cell Biochem. 92(5):937-48. Review.

151. Montalvo AL, Bembi B, Donnarumma M, Filocamo M, Parenti G, Rossi M, Merlini L, Buratti E, De Filippi P, Dardis A, Stroppiano M, Ciana G, Pittis MG (2006). Mutation profile of the GAA gene in 40 Italian patients with late onset glycogen storage disease type II. *Hum Mutat*. 27: 999–1006.

152. Mullins C, Bonifacino JS (2001). The molecular machinery for lysosome biogenesis. *Bioessays*. 23(4):333-43. Review.

153. Munafó DB, Colombo MI (2001). A novel assay to study autophagy: regulation of autophagosome vacuole size by amino acid deprivation. *J Cell Sci*. 114(Pt 20):3619-29.

154. Navaroli DM, Bellvé KD, Standley C, Lifshitz LM, Cardia J, Lambright D, Leonard D, Fogarty KE, Corvera S (2012). Rabenosyn-5 defines the fate of the transferrin receptor following clathrin-mediated endocytosis. *Proc Natl Acad Sci U S A*. 109(8):E471-80.

155. Neher E (1993). Cell physiology. Secretion without full fusion. *Nature*. 363(6429):497-8.

156. Neufeld, E.F., and Muenzer, J. (2001). The mucopolysaccharidosis. In Scriver, C.R., Beaudet A.L., Valle, D., Sly, W.S. (eds). *The metabolic and molecular bases of inherited disease.* 8th ed. Vol. III. New York: McGraw-Hill, pp. 3421-3452.

157. Newsholme P, Lima MM, Procopio J, Pithon-Curi TC, Doi SQ, Bazotte RB, Curi R (2003). Glutamine and glutamate as vital metabolites. *Braz J Med Biol Res*. 36(2):153-63.

158. Ni X,Canuel M, Morales CR (2006). The sorting and trafficking of lysosomal proteins. *Histol Histopathol*. 21(8):899-913.

159. Novikoff AB (1959). The proximal tubule cell in experimental hydronephrosis. *J Biophys Biochem Cytol*. 6(1):136-8.

160. Obara K, Sekito T, Niimi K, Ohsumi Y (2008). The Atg18-Atg2 complex is recruited to autophagic membranes via phosphatidylinositol 3-phosphate and exerts an essential function. *J Biol Chem*. 283(35):23972-80.

161. Oheim M, Kirchhoff F, Stühmer W (2006). Calcium microdomains in regulated exocytosis.*Cell Calcium*. 40(5-6):423-39.

162. Okumiya T, Kroos MA, Vliet LV, Takeuchi H, Van der Ploeg AT, Reuser AJ (2007). Chemical chaperones improve transport and enhance stability of mutant alpha-glucosidases in glycogen storage disease type II. *Mol Genet Metab.* 90(1):49-57.

163. Ong WL, Jiang B, Tang N, Ling SF, Yeo JF, Wei S, Farooqui AA, Ong WY (2006). Differential effects of polyunsaturated fatty acids on membrane capacitance and exocytosis in rat pheochromocytoma-12 cells. *Neurochem Res.* 31(1):41-8.

164. Orci L, Vassalli JD, Perrelet A (1988). The insulin factory. *Sci Am*. 259(3):85-94.

165. Orlikowski D, Pellegrini N, Prigent H, Laforêt P, Carlier R, Carlier P, Eymard B, Lofaso F, Annane D (2011). Recombinant human acid alpha-glucosidase (rhGAA) in adult patients with severe respiratory failure due to Pompe disease. *Neuromuscul Disord*. 21(7):477-82.

166. Otomo T, Higaki K, Nanba E, Ozono K, Sakai N (2011). Lysosomal storage causes cellular dysfunction in mucolipidosis II skin fibroblasts. *J Biol Chem*. 286(40):35283-90.

167. Oude Elferink RP, Brouwer-Kelder EM, Surya I, Strijland A, Kroos M, Reuser AJ, Tager JM (1984). Isolation and characterization of a precursor form of lysosomal alpha-glucosidase from human urine. *Eur J Biochem*. 139(3):489-95.

168. Palmer TN (1971). The substrate specificity of acid -glucosidase from rabbit muscle. *Biochem J*. 124(4):701-11.

169. Pan CY, Lee H, Chen CL (2006). Lysophospholipids elevate [Ca2+]i and trigger exocytosis in bovine chromaffin cells. *Neuropharmacology*. 51(1):18-26.

170. Parenti G, Zuppaldi A, Gabriela Pittis M, Rosaria Tuzzi M, Annunziata I, Meroni G, Porto C, Donaudy F, Rossi B, Rossi M, Filocamo M, Donati A, Bembi B, Ballabio A, Andria G (2007). Pharmacological enhancement of mutated alpha-glucosidase activity in fibroblasts from patients with Pompe disease. *Mol Ther*. 15(3):508-14.

171. Parker GJ, Koay A, Gilbert-Wilson R, Waddington LJ, Stapleton D (2007). AMP-activated protein kinase does not associate with glycogen alpha-particles from rat liver. *Biochem Biophys Res Commun.* 362(4):811-5.

172. Pascual SI (2009). Phenotype variations in early onset Pompe disease: diagnosis and treatment results with Myozyme. *Adv Exp Med Biol.* 652:39-46.

173. Pillay CS, Elliott E, Dennison C (2002). Endolysosomal proteolysis and its regulation. *Biochem J*. 363(Pt 3):417-29.

174. Pisoni, R. L. and Thoene, J. G. (1991) The transport systems of mammalian lysosomes. *Biochim. Biophys. Acta* 1071, 351-373.

175. Pompe JC (1932). Over idiopatische hypertrophie van het hart. *Ned Tijdshr Geneeskd*. 76:304.

176. Ponce E, Witte DP, Hirschhorn R, Huie ML, Grabowski GA (1999). Murine acid alpha-glucosidase: cell-specific mRNA differential expression during development and maturation. *Am J Pathol*. 154(4):1089-96.

177. Porto C, Cardone M, Fontana F, Rossi B, Tuzzi MR, Tarallo A, Barone MV, Andria G, Parenti G (2009). The pharmacological chaperone N-butyldeoxynojirimycin enhances enzyme replacement therapy in Pompe disease fibroblasts. *Mol Ther*. 17(6):964-71.

178. Poteryaev D, Datta S, Ackema K, Zerial M, Spang A (2010). Identification of the switch in early-to-late endosome transition. *Cell*. 141(3):497-508.

179. Poupetová H, Ledvinová J, Berná L, Dvoráková L, Kozich V, Elleder M (2010). The birth prevalence of lysosomal storage disorders in the Czech Republic: comparison with data in different populations. *J Inherit Metab Dis*. 33(4):387-96.

180. Pressman BC (1976). Biological applications of ionophores. *Annu Rev Biochem*. 45:501-30. Review.

181. Pruzansky JJ, Patterson R (1979). Cytotoxicity of ionophore A23187 for basophils and other human blood cells. *J Allergy ClinImmunol*. 64(1):50-5.

182. Qureshi OS, Paramasivam A, Yu JC, Murrell-Lagnado RD (2007). Regulation of P2X4 receptors by lysosomal targeting, glycan protection and exocytosis. *J Cell Sci.* 120:3838-49.

183. Raben N, Plotz P, Byrne BJ (2002). Acid alpha-glucosidase deficiency (glycogenosis type II, Pompe disease). *Curr Mol Med.* 2(2):145-66.

184. Raben N, Danon M, Gilbert AL, Dwivedi S, Collins B, Thurberg BL, Mattaliano RJ, Nagaraju K, Plotz PH (2003). Enzyme replacement therapy in the mouse model of Pompe disease. *Mol Genet Metab*. 80(1-2):159-69.

185. Raben N, Fukuda T, Gilbert AL, de Jong D, Thurberg BL, Mattaliano RJ, Meikle P, Hopwood JJ, Nagashima K, Nagaraju K, Plotz PH (2005). Replacing acid alpha-glucosidase in Pompe disease: recombinant and transgenic enzymes are equipotent, but neither completely clears glycogen from type II muscle fibers. *Mol Ther.* Jan;11(1):48-56.

186. Raben N, Takikita S, Pittis MG, Bembi B, Marie SK, Roberts A, Page L, Kishnani PS, Schoser BG, Chien YH, Ralston E, Nagaraju K, Plotz PH (2007). Deconstructing Pompe disease by analyzing single muscle fibers: to see a world in a grain of sand... *Autophagy*. 3(6):546-52.

187. Raposo G, Cordonnier MN, Tenza D, Menichi B, Dürrbach A, Louvard D, Coudrier E (1999). Association of myosin I alpha with endosomes and lysosomes in mammalian cells. *Mol Biol Cell.* 10(5):1477-94.

188. Reggiori F, Tucker KA, Stromhaug PE, Klionsky DJ (2005). The Atg1-Atg13 complex regulates Atg9 and Atg23 retrieval transport from the pre-autophagosomal structure. *Dev Cell*. 6(1):79-90.

189. Riederer MA, Soldati T, Shapiro AD, Lin J, Pfeffer SR (1994). Lysosome biogenesis requires Rab9 function and receptor recycling from endosomes to the trans-Golgi network. J Cell Biol. 125(3):573-82.

190. Rizzuto R, Pozzan T (2006). Microdomains of intracellular Ca2+: molecular determinants and functional consequences. *Physiol Rev*. 86(1):369-408. Review.

191. Roach PJ, Depaoli-Roach AA, Hurley TD, Tagliabracci VS (2012). Glycogen and its metabolism: some new developments and old themes. *Biochem J*. 441(3):763-87.

192. Robinson LJ, Pang S, Harris DS, Heuser J, James DE (1992). Translocation of the glucose transporter (GLUT4) to the cell surface in permeabilized 3T3-L1 adipocytes: effects of ATP insulin, and GTP gamma S and localization of GLUT4 to clathrin lattices. *J Cell Biol.* 117(6):1181-96.

193. Rodríguez A, Webster P, Ortego J, Andrews NW (1997). Lysosomes behave as Ca2+-regulated exocytic vesicles in fibroblasts and epithelial cells. *J Cell Biol.* 137(1):93-104.

194. Rodríguez A, Martinez I, Chung A, Berlot CH, Andrews NW (1999). cAMP regulates Ca2+-dependent exocytosis of lysosomes and lysosome-mediated cell invasion by trypanosomes. *J Biol Chem.* 274(24):16754-9.

195. Roederer M, Mays RW, Murphy RF (1989). Effect of confluence on endocytosis by 3T3 fibroblasts: increased rate of pinocytosis and accumulation of residual bodies. *Eur J Cell Biol.* 48(1):37-44.

196. Rozaklis T, Ramsay SL, Whitfield PD, Ranieri E, Hopwood JJ, and Meikle PJ (2002). Determination of Oligosaccharides in Pompe Disease by Electrospray Ionization Tandem Mass Spectrometry. *Clin Chem*. 48(1):131-9.

197. Rutter GA, Varadi A, Tsuboi T, Parton L, Ravier M (2006). Insulin secretion in health and disease: genomics, proteomics and single vesicle dynamics. *Biochem Soc Trans.* 34(Pt 2):247-50.

198. Ryter SW, Choi AM (2013). Regulation of autophagy in oxygen-dependent cellular stress. *Curr Pharm Des*. 19(15):2747-56.

199. Ryu JH, Drain J, Kim JH, McGee S, Gray-Weale A, Waddington L, Parker GJ, Hargreaves M, Yoo SH, Stapleton D (2009). Comparative structural analyses of purified glycogen particles from rat liver, human skeletal muscle and commercial preparations. *Int J Biol Macromol*. 45(5):478-82.

200. Saftig P, Klumperman J (2009). Lysosome biogenesis and lysosomal membrane proteins: trafficking meets function. *Nat Rev Mol Cell Biol*. 10(9):623-35. Review.

201. Sagherian C, Thorner P, Mahuran D (1994). The pro-peptide of the pro beta-polypeptide chain of human beta-hexosaminidase is necessary for proper protein folding and exit from the endoplasmic reticulum. *Biochem Biophys Res Commun*. 204(1):135-41.

202. Sagi-Eisenberg E (2007). The mast cell: where endocytosis and regulated exocytosis meet. *Immunol Rev.* 217:292-303.

203. Santini F, Beaven MA (1993). Tyrosine phosphorylation of a mitogen-activated protein kinase-like protein occurs at a late step in exocytosis. Studies with tyrosine phosphatase inhibitors and various secretagogues in rat RBL-2H3 cells. *J Biol Chem.* 268(30):22716-22.

204. Sardiello M, Palmieri M, di Ronza A, Medina DL, Valenza M, Gennarino VA, Di Malta C, Donaudy F, Embrione V, Polishchuk RS, Banfi S, Parenti G, Cattaneo E, Ballabio A (2009). A gene network regulating lysosomal biogenesis and function. *Science*. 325(5939):473-7.

205. Sardiello M, Ballabio A (2009). Lysosomal enhancement: a CLEAR answer to cellular degradative needs. *Cell Cycle*. 8(24):4021-2.

206. Scepek S, Coorssen JR, Lindau M (1998). Fusion pore expansion in horse eosinophils is modulated by Ca2+ and protein kinase C via distinct mechanisms. *EMBO J.* 17(15):4340-5.

207. Schmoranzer J, Goulian M, Axelrod D, Simon SM (2000). Imaging constitutive exocytosis with total internal reflection fluorescence microscopy. *J Cell Biol.* 149(1):23-32.

208. Schröder BA, Wrocklage C, Hasilik A, Saftig P (2010). The proteome of lysosomes. *Proteomics*. 10(22):4053-76. Review.

209. Scott RB, Still WJ (1970). Properties of liver glycogen isolated in density gradients of sodium iothalamate. *Arch Biochem Biophys*. 139(1):87-92.

210. Scott CC, Gruenberg J (2011). Ion flux and the function of endosomes and lysosomes: pH is just the start: the flux of ions across endosomal membranes influences endosome function not only through regulation of the luminal pH. *Bioessays*. 33(2):103-10.

211. Seaman MN (2008). Endosome protein sorting: motifs and machinery. *Cell Mol Life Sci*. 65(18):2842-58. Review.

212. Seino S, Shibasaki T (2005). PKA-dependent and PKA-independent pathways for cAMP-regulated exocytosis. *Physiol Rev*. 85(4):1303-42.

213. Seino S, Takahashi H, Fujimoto W, Shibasaki T (2009). Roles of cAMP signalling in insulin granule exocytosis. *Diabetes Obes Metab*. 11 Suppl 4:180-8.

214. Sesaki H, Ogihara S (1997). Protrusion of cell surface coupled with single exocytotic events of secretion of the slime in Physarum plasmodia. *J Cell Sci.* 110 (Pt 7):809-18.

215. Shea L, Raben N (2009). Autophagy in skeletal muscle: implications for Pompe disease. *Int J Clin Pharmacol Ther*. 47 Suppl 1:S42-7.

216. Shearer J, Graham TE (2002). New perspectives on the storage and organization of muscle glycogen. *Can J Appl Physiol*. 27(2):179-203.

217. Smith PK, Krohn RI, Hermanson GT, Mallia AK, Gartner FH, Provenzano MD, Fujimoto EK, Goeke NM, Olson BJ, Klenk DC (1985). Measurement of protein using bicinchoninic acid. *Anal Biochem*. 150(1):76-85.

218. Sobotka TJ, Brodie RE, Quander Y, O'Donnell M, West GL (1987). Neurobehavioral effects of the calcium ionophore A23187. *NeurotoxicolTeratol*. 9(2):99-106.

219. Sokac AM, Co C, Taunton J, Bement W (2003). Cdc42-dependent actin polymerization during compensatory endocytosis in Xenopus eggs. *Nat Cell Biol*. 5(8):727-32.

220. Spampanato C, Feeney E, Li L, Cardone M, Lim JA, Annunziata F, Zare H, Polishchuk R, Puertollano R, Parenti G, Ballabio A, Raben N (2013). Transcription factor EB (TFEB) is a new therapeutic target for Pompe disease. *EMBO Mol Med*. 5(5):691-706.

221. Stanley EF (1993). Single calcium channels and acetylcholine release at a presynaptic nerve terminal. *Neuron*. 11(6):1007-11.

222. Steinhardt RA, Bi G, Alderton JM (1994). Cell membrane resealing by a vesicular mechanism similar to neurotransmitter release. *Science*. 263(5145):390-3.

223. Stinchcombe J, Bossi G, Griffiths GM (2004). Linking albinism and immunity: the secrets of secretory lysosomes. *Science*. 305(5680):55-9.

224. Sugo T, Tachimoto H, Chikatsu T, Murakami Y, Kikukawa Y, Sato S, Kikuchi K, Nagi T, Harada M, Ogi K, Ebisawa M, Mori M (2006). Identification of a lysophosphatidylserine receptor on mast cells. *Biochem Biophys Res Commun.* 341(4):1078-87.

225. Sun B, Zhang H, Franco LM, Young SP, Schneider A, Bird A, Amalfitano A, Chen YT, Koeberl DD (2005). Efficacy of an adeno-associated virus 8-pseudotyped vector in glycogen storage disease type II. *Mol Ther*. 11(1):57-65.

226. Sun B, Young SP, Li P, Di C, Brown T, Salva MZ, Li S, Bird A, Yan Z, Auten R, Hauschka SD, Koeberl DD (2008). Correction of multiple striated muscles in

murine Pompe disease through adeno-associated virus-mediated gene therapy. *Mol Ther*. 16(8):1366-71.

227. Sun B, Kulis MD, Young SP, Hobeika AC, Li S, Bird A, Zhang H, Li Y, Clay TM, Burks W, Kishnani PS, Koeberl DD (2010). Immunomodulatory Gene Therapy Prevents Antibody Formation and Lethal Hypersensitivity Reactions in Murine Pompe Disease. *Mol Ther.* 18(2):353-60.

228. Suzuki K, Kubota Y, Sekito T, Ohsumi Y (2007). Hierarchy of Atg proteins in pre-autophagosomal structure organization. *Genes Cells*. 12(2):209-18.

229. Taha TA, Argraves KM, Obeid LM (2004). Sphingosine-1-phosphate receptors: receptor specificity versus functional redundancy. Biochim Biophys Acta. 1682(1-3):48-55. Review.

230. Tager JM, Oude Elferink RP, Reuser A, Kroos M, Ginsel LA, Fransen JA, Klumperman J (1987). alpha-Glucosidase deficiency (Pompe's disease). *Enzyme*. 38(1-4):280-5.

231. Takahashi S, Kubo K, Waguri S, Yabashi A, Shin HW, Katoh Y, Nakayama K (2012). Rab11 regulates exocytosis of recycling vesicles at the plasma membrane. *J Cell Sci*. 125(Pt 17):4049-57.

232. Takeuchi T, Iwamasa T, Miyayama H (1978). Ultrafine structure of glycogen macromolecules in mammalian tissues. *J Electron Microsc (Tokyo).* 27(1):31-8.

233. Tanida I (2011). Autophagy basics. *Microbiol Immunol*. 55(1):1-11.

234. Taraska JW, Perrais D, Ohara-Imaizumi M, Nagamatsu S, Almers W (2003). Secretory granules are recaptured largely intact after stimulated exocytosis in cultured endocrine cells. *Proc Natl Acad Sci U S A*. 100(4):2070-5.

235. Tassa A, Roux MP, Attaix D, Bechet DM (2003). Class III phosphoinositide 3-kinase--Beclin1 complex mediates the amino acid-dependent regulation of autophagy in C2C12 myotubes. *Biochem J*. 376(Pt 3):577-86.

236. Tengholm A (2012). Cyclic AMP dynamics in the pancreatic β-cell. *Ups J Med Sci*. 117(4):355-69.

237. Thorn P (2009). New insights into the control of secretion. *Commun Integr Biol.* 2(4):315-7.

238. Thorn P (2012). Measuring calcium signals and exocytosis in tissues. *Biochim Biophys Acta*. 1820(8):1179-84. Review.

239. Tiwari N, Wang CC, Brochetta C, Ke G, Vita F, Qi Z, Rivera J, Soranzo MR, Zabucchi G, Hong W, Blank U (2008). VAMP-8 segregates mast cell-preformed mediator exocytosis from cytokine trafficking pathways. *Blood*. 111(7):3665-74.

240. Tsuboi T, McMahon HT, Rutter GA (2004). Mechanisms of dense core vesicle recapture following "kiss and run" ("cavicapture") exocytosis in insulin-secreting cells. *J Biol Chem.* 279(45):47115-24.

241. Ugorski M, Seder A, Lundblad A, Zopf D (1983). Studies on the metabolic origin of a glucose-containing tetrasaccharide in human urine. *J. Exp. Pathol*. 1(1):27-38.

242. Umapathysivam K, Hopwood JJ, Meikle PJ. Correlation of acid alpha-glucosidase and glycogen content in skin fibroblasts with age of onset in Pompe disease (2005). *Clin Chim Acta.* 361(1-2):191-8.

243. Unger EG, Durrant J, Anson DS, Hopwood JJ (1994). Recombinant alpha-L-iduronidase: characterization of the purified enzyme and correction of mucopolysaccharidosis type I fibroblasts. *Biochem J.* 304(1):43-9.

244. van Capelle CI, van der Beek NA, Hagemans ML, Arts WF, Hop WC, Lee P, Jaeken J, Frohn-Mulder IM, Merkus PJ, Corzo D, Puga AC, Reuser AJ, van der Ploeg AT (2010). Effect of enzyme therapy in juvenile patients with Pompe disease: a three-year open-label study. *Neuromuscul Disord*. 20(12):775-82.

245. Van der Kraan M, Kroos MA, Joosse M, Bijvoet AG, Verbeet MP, Kleijer WJ, Reuser AJ (1994). Deletion of exon 18 is a frequent mutation in glycogen storage disease type II. *Biochem Biophys Res Commun*. 203: 1535–41.

246. Van der Ploeg AT, Kroos MA, Willemsen R, Brons NH, Reuser AJ (1991). Intravenous administration of phosphorylated acid alpha-glucosidase leads to uptake of enzyme in heart and skeletal muscle of mice. J Clin Invest. 87(2):513-8.

247. Van den Hout JM, Kamphoven JH, Winkel LP, Arts WF, De Klerk JB, Loonen MC, Vulto AG, Cromme-Dijkhuis A, Weisglas-Kuperus N, Hop W, Van Hirtum H, Van Diggelen OP, Boer M, Kroos MA, Van Doorn PA, Van der Voort E, Sibbles B, Van Corven EJ, Brakenhoff JP, Van Hove J, Smeitink JA, de Jong G, Reuser AJ, Van der Ploeg AT (2004). Long-term intravenous treatment of Pompe disease with recombinant human alpha-glucosidase from milk. *Pediatrics.* 113(5):448-57.

248. van Schaftingen E, Gerin I (2002). The glucose-6-phosphatase system. *Biochem J*. 362(Pt 3):513-32.

249. van Til NP, Stok M, Aerts Kaya FS, de Waard MC, Farahbakhshian E, Visser TP, Kroos MA, Jacobs EH, Willart MA, van der Wegen P, Scholte BJ, Lambrecht BN, Duncker DJ, van der Ploeg AT, Reuser AJ, Verstegen MM, Wagemaker G (2010). Lentiviral gene therapy of murine hematopoietic stem cells ameliorates the Pompe disease phenotype. *Blood*. 115(26):5329-37.

250. Vellodi A (2005). Lysosomal storage disorders. *Br J Haematol*. 128(4):413-31.

251. Vergne I, Roberts E, Elmaoued RA, Tosch V, Delgado MA, Proikas-Cezanne T, Laporte J, Deretic V (2009). Control of autophagy initiation by phosphoinositide 3-phosphatase Jumpy. *EMBO J*. 28(15):2244-58.

252. von Figura K, Weber E (1978). An alternative hypothesis of cellular transport of lysosomal enzymes in fibroblasts. Effect of inhibitors of lysosomal enzyme endocytosis on intra- and extra-cellular lysosomal enzyme activities. *Biochem J*. 176:943-50.

253. von Figura K, Hasilik A (1986). Lysosomal enzymes and their receptors. *Annu Rev Biochem*. 55:167-93.

254. Wang CT, Grishanin R, Earles CA, Chang PY, Martin TF, et al (2001). Synaptotagmin modulation of fusion pore kinetics in regulated exocytosis of dense-core vesicles. *Science*. 294: 1111–1115.

255. Wang Z, Thurmond DC (2009). Mechanisms of biphasic insulin-granule exocytosis - roles of the cytoskeleton, small GTPases and SNARE proteins. *J Cell Sci*. 122(Pt 7):893-903.

256. Wang RY, Bodamer OA, Watson MS, Wilcox WR; ACMG Work Group on Diagnostic Confirmation of Lysosomal Storage Diseases (2011). Lysosomal

storage diseases: diagnostic confirmation and management of presymptomatic individuals. *Genet Med*. 13(5):457-84.

257. Watanabe Y, Makino Y, Omichi K (2008). Donor substrate specificity of 4-alpha-glucanotransferase of porcine liver glycogen debranching enzyme and complementary action to glycogen phosphorylase on debranching. *J Biochem.* Mar;143(3):435-40.

258. Whybra C, Miebach E, Mengel E, Gal A, Baron K, Beck M, Kampmann C (2009). A 4-year study of the efficacy and tolerability of enzyme replacement therapy with agalsidase alfa in 36 women with Fabry disease. *Genet Med*. 11(6):441-9.

259. Winkel LP, Kamphoven JH, van den Hout HJ, Severijnen LA, van Doorn PA, Reuser AJ, van der Ploeg AT (2003). Morphological changes in muscle tissue of patients with infantile Pompe's disease receiving enzyme replacement therapy. *Muscle Nerve.* 27(6):743-51.

260. Winkel LP, Hagemans ML, van Doorn PA, Loonen MC, Hop WJ, Reuser AJ, van der Ploeg AT (2005). The natural course of non-classic Pompe's disease; a review of 225 published cases. *J Neurol*. 252: 875–84.

261. Wisselaar HA, Kroos MA, Hermans MM, van Beeumen J, Reuser AJ (1993). Structural and functional changes of lysosomal acid alpha-glucosidase during intracellular transport and maturation. *J Biol Chem.* 268(3):2223-31.

262. Wong AS, Cheung ZH, Ip NY (2011). Molecular machinery of macroautophagy and its deregulation in diseases. *Biochim Biophys Acta*. 1812(11):1490-7.

263. Xie Z, Klionsky DJ (2007). Autophagosome formation: core machinery and adaptations. *Nat Cell Biol*. 9(10):1102-9.

264. Yang YP, Liang ZQ, Gu ZL, Qin ZH (2005). Molecular mechanism and regulation of autophagy. *ActaPharmacol Sin*. 26(12):1421-34. Review.

265. Yang Z, Klionsky DJ (2010). Mammalian autophagy: core molecular machinery and signaling regulation.*Curr Opin Cell Biol*. 22(2):124-31. Review.

266. Yang Z, Klionsky DJ (2010). Eaten alive: a history of macroautophagy. *Nat Cell Biol*. 12(9):814-22. Review.

267. Yen WL, Klionsky DJ (2008). How to live long and prosper: autophagy, mitochondria, and aging. *Physiology (Bethesda)*. 23:248-62.

268. Yogalingam G, Bonten EJ, van de Vlekkert D, Hu H, Moshiach S, Connell SA, d'Azzo A (2008). Neuraminidase 1 is a negative regulator of lysosomal exocytosis. *Dev Cell.* 15(1):74-86.

269. Yoshihara M, Littleton JT (2002) Synaptotagmin I functions as a calcium sensor to synchronize neurotransmitter release. *Neuron.* 36: 897–908.

270. Zaki NM, Tirelli N (2010). Gateways for the intracellular access of nanocarriers: a review of receptor-mediated endocytosis mechanisms and of strategies in receptor targeting. *Expert Opin Drug Deliv*. 7(8):895-913.

271. Zerial M, McBride H (2001). Rab proteins as membrane organizers. *Nat Rev Mol Cell Biol*. 2(2):107-17.

272. Zhao KW, Faull KF, Kakkis ED, Neufeld EF (1997). Carbohydrate structures of recombinant human alpha-L-iduronidase secreted by Chinese hamster ovary cells. *J Biol Chem*. 272(36):22758-65. Zhu Y, Li X, McVie-Wylie A, Jiang C,

Thurberg BL, Raben N, Mattaliano RJ, Cheng SH (2005). Carbohydrate-remodelled acid alpha-glucosidase with higher affinity for the cation-independent mannose 6-phosphate receptor demonstrates improved delivery to muscles of Pompe mice. *Biochem J.* 389(3):619-28.

273. Zhu Y, Jiang JL, Gumlaw NK, Zhang J, Bercury SD, Ziegler RJ, Lee K, Kudo M, Canfield WM, Edmunds T, Jiang C, Mattaliano RJ, Cheng SH (2009). Glycoengineered acid alpha-glucosidase with improved efficacy at correcting the metabolic aberrations and motor function deficits in a mouse model of Pompe disease. *Mol Ther*. 17(6):954-63.

Supplementary Data

Supplementary data A: Phagocytosis and exocytosis of fluorescent beads in skin fibroblasts

---

Introduction: The diameter of the exocytic pore was hypothesised to limit the size of vesicular cargo, including glycogen, small enough to be released from cultured Pompe skin fibroblasts. An exocytic pore size of 30 nm has been previously estimated in cultured fibroblasts, using the release of various-sized fluorophore-labelled dextran beads as a marker of pore size (Jaiswal *et al*., 2004). This technique was replicated in the current study to estimate the calcimycin-induced exocytic pore size in Pompe skin fibroblasts, which was then compared to unaffected control fibroblasts. The method required optimisation for Pompe and unaffected skin fibroblasts, including the determination of which sized beads were able to be phagocytosed into the endosome-lysosome network, and the effect of bead-exposure on cell viability.

Methods: Pompe and unaffected skin fibroblasts were incubated separately with 2.4, 20, 40, 100, 500, 1000 or 2000 nm diameter Texas-red conjugated beads, for 4 hours at 37°C. Cells were washed to remove non-internalised beads, and the cells then fixed to coverslips and images captured using a Leica SP5 spectral scanning confocal microscope at 100X magnification. Cell viability after both bead-treatment and the induction of exocytosis with calcimycin was determined using LDH release into the culture medium.

Results: **Supp. Figure A1** shows that 2.4, 20, 40 and 100 nm diameter beads were effectively phagocytosed into the cultured Pompe cells, as observed by distinct punctate staining; whilst the beads of $\geq$ 500 nm in diameter were too large to be

internalised. Similar results were obtained for unaffected skin fibroblasts (data not shown). Bead internalisation and calcimycin-treatment did not increase the amount of LDH released into the culture medium for either Pompe (**Supp. Table A1**) or unaffected cells (data not shown; <5 µg/mg LDH release).

Conclusion: The ability to exocytose vesicular cargo of a known size provides a useful estimate of the diameter of the exocytic pore. The accuracy of the pore size measurement could be improved by treating cells individually with a larger range of sized beads. However, different bead sizes to those used in this study were unavailable. This technique allowed an estimate of the calcimycin-induced exocytic pore in Pompe skin fibroblasts, which could be compared to calcimycin-treated unaffected cells (see section 4.2.4).

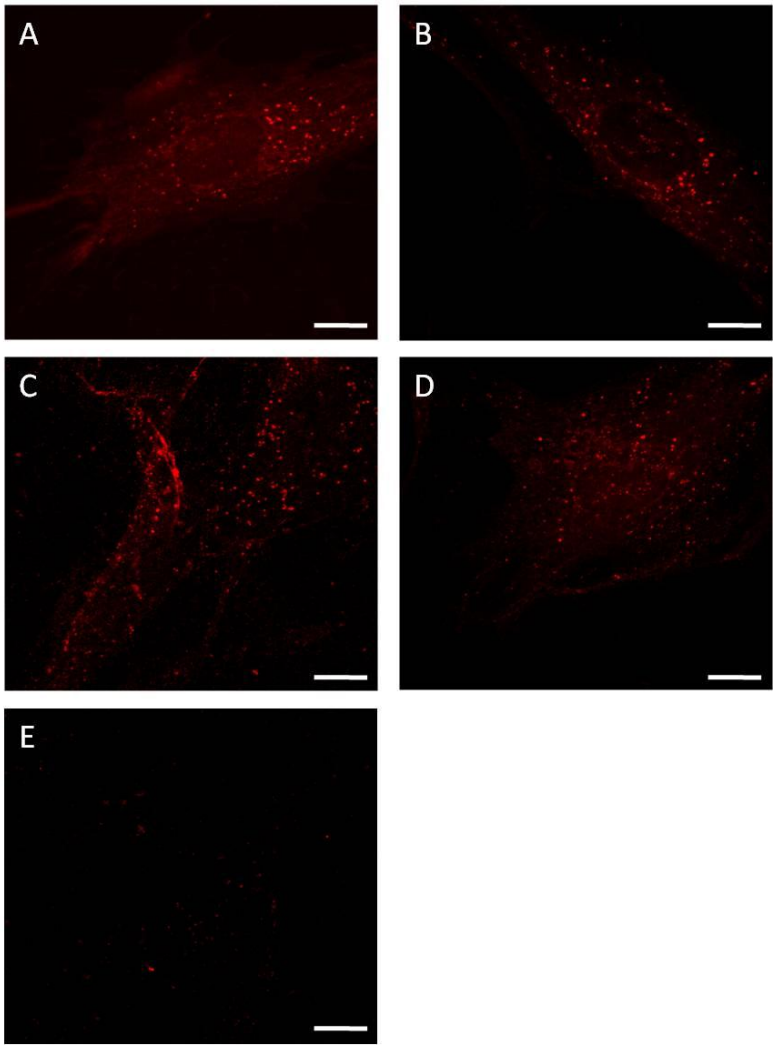

Supp. Figure A1: Dextran bead uptake into cultured skin fibroblasts. Cells were grown to 30% confluence prior to experimentation. Pompe skin fibroblasts were treated with Texas red-labelled dextran beads for 4 hrs at 37°C. Dextran beads were 2.4 (A), 20 (B), 40 (C), 100 (D) and 500 (E) nm in diameter. Each image is representative of greater than 20 images with each experiment performed in triplicate. Size bar equals 30 nm.

Supp. Table A1: The viability of Pompe skin fibroblasts treated with fluorescent-labelled dextran beads and calcimycin

Dextran bead diameter (nm)	Calcimycin treatment	LDH release (µg/mg)
2.4	-	2.9 +/- 0.5
2.4	+	2.8 +/- 0.6
20	-	3.9 +/- 0.5
20	+	2.9 +/- 0.2
40	-	2.4 +/- 0.9
40	+	3.7 +/- 0.7
100	-	2.8 +/- 0.8
100	+	3.4 +/- 0.6
500	-	2.6 +/- 1.3
500	+	3.2 +/- 0.6

Pompe skin fibroblasts were incubated with fluorescent-labelled dextran beads for 4 hrs at 37°C, rinsed with PBS to remove non-internalised beads and then treated with 1 µM calcimycin for 1 hr at 37°C.

Supplementary data B: The quantification of glycogen

Introduction: At the commencement of this study, a colorimetric assay was available for glycogen quantification, involving the enzymatic digestion of glycogen granules with amyloglucosidase to liberate glucose (Umapathysivam *et al*., 2005). Free glucose was then detected by a linked enzymatic reaction involving the phosphorylation of glucose with hexokinase, then the action of G6P dehydrogenase on the product. This assay contained a calibration curve, containing parallel samples of purified glycogen that were digested to liberate glucose, thereby allowing glycogen quantification. Using this method, both vesicular and total cell glycogen was quantified in Pompe and unaffected skin fibroblast extracts. However, this assay was not sensitive enough to detect glycogen released into the culture medium from cells. A more sensitive glycogen quantification assay was therefore required to enable the amount of glycogen exocytosis to be defined.

Mass spectrometry: ESI-MS/MS was introduced to improve the sensitivity of the glycogen assay. Glycogen containing samples were digested with amyloglucosidase as described above, and glucose was then PMP-derivitized for detection by ESI-MS/MS. This assay allowed the detection of glycogen in culture medium. Over the course of the project, the assay was adapted to include an in-line liquid chromatographic step (LC/ESI-MS/MS), which improved sample reproducibility and reduced the amount of labour required to prepare each sample. This assay was subsequently optimised and utilised to quantify glycogen in other biological samples as described below and formed the basis of a publication on glycogen quantification (Fuller *et al*., 2012).

Assay performance: The assay required optimisation, involving the development of a calibration curve and quality control samples, together with the measurement of assay precision, accuracy and internal standard recovery. **Supp. Figure B1** shows that the calibration curve for ESI-MS/MS was linear over the range 4-200 μg/mL glycogen ($y = 0.058x + 0.285$, $R^2 = 0.99$). The limit of detection of the assay was 140 ng. ESI-MS/MS performance was determined using quality control samples, containing low-, medium- and high-concentrations of purified glycogen in each sample run. Inter- and intra-assay measures of precision and accuracy were all ≤ 10% and internal standard recovery was ≥ 89% (**Supp. Table B1**). The calibration curve for LC/ESI-MS/MS was linear over the range 2-40 μg/mL glycogen (Fuller *et al*., 2012). The limit of detection of the assay was 10 ng of glycogen, 14-fold more sensitive than ESI-MS/MS. Inter- and intra-assay measures of precision and accuracy were all ≤ 12% and internal standard recovery was ≥ 93%.

Quantification of glycogen in biological samples: The glycogen assay was used to study glycogen exocytosis in Pompe, MPS I and unaffected skin fibroblasts, and glycogen was also measured in tissue extract from Pompe and control mice (Fuller *et al*., 2012). Each of these studies required the glycogen assay to be specifically optimised for each type of biological sample, including skin fibroblast extracts, culture medium (ESI-MS/MS and LC/ESI-MS/MS) and extracts from seven different mouse tissues (LC/ESI-MS/MS only). Spiking the quality control samples with cell/tissue extract (≤ 5 μg) or culture medium (≤ 250 μL) displayed no evidence of inhibitory effects (data not shown). The assays were compared by quantifying the amount of glycogen in skin fibroblast

extract and culture medium samples; detecting a similar concentration of glycogen and glucose in each sample (**Supp. Table B2**).

Contribution: My role in the development of the mass spectrometry assays was to quantify glycogen in skin fibroblast and culture medium; and included the culture and harvesting of cells, the enzymatic digestion and derivatisation of samples, preparation of quality controls and calibrators, determination of assay precision, accuracy and internal standard recovery. My role in the development of the LC/ESI-MS/MS assay for the quantification of glycogen in Pompe and control mouse tissues included animal handling, humane killing, tissue retrieval, enzymatic digestion, derivatisation of samples, preparation of quality controls and calibrators, determination of assay precision, accuracy and internal standard recovery. Assay development and sample analysis for the mouse studies was performed with Philippa Davey (equal contribution). The operation of the mass spectrometer was performed by Stephen Duplock, Tomas Rozek and Troy Stomski.

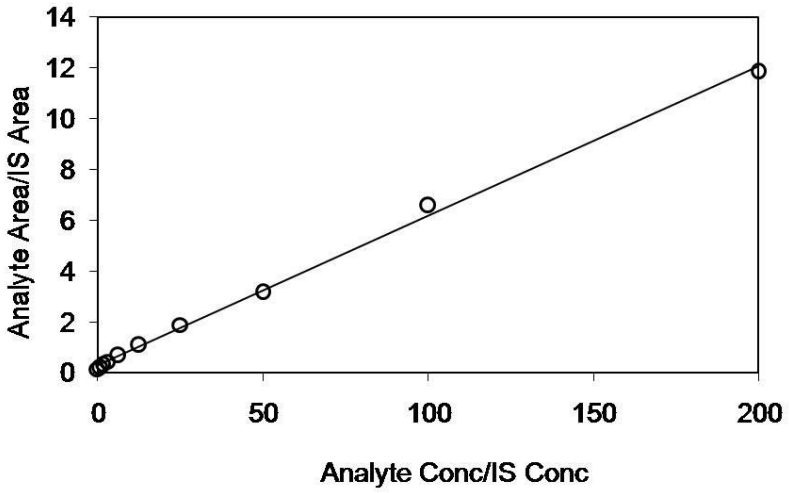

Supp. Figure B1: Calibration curve for glycogen ESI-MS/MS. Bovine liver glycogen type IX was digested with amyloglucosidase, and the liberated glucose derivatised and quantified by ESI-MS/MS. IS = internal standard.

Supp. Table B1: Performance of ESI-MS/MS for the quantification of glycogen

Quality control	Glycogen (ng)	Precision		Accuracy		Recovery of internal standard (%)
		Intra-assay (%CV)	Inter-assay (%CV)	Intra-assay (%)	Inter-assay (%)	
Low	150	6	5	7	10	89
Medium	600	10	6	9	7	97
High	3000	6	7	2	3	98
n		6	5	6	5	6

Quality control samples contained 5 µg of myoblast cell extract (containing negligible levels of glycogen). Precision was a measure of the closeness of multiple replicates, accuracy was a measure of the closeness to the true value and recovery was a measure of the percentage of peak area internal standard signal in each quality control sample compared to pure internal standard.

Supp. Table B2: Comparison of ESI-MS/MS and LC/ESI-MS/MS for the quantification of glycogen in Pompe skin fibroblast extract and culture medium

	Sample	Amount analysed	Glycogen (µg/mg)	Glucose (µg/mg)	Recovery of internal standard (%)
ESI-MS/MS	Skin fibroblast extract	5 µg	111 +/- 13	6.3 +/- 2	92
	Culture medium	250 µL	4.5 +/- 0.5	0.5 +/- 0.1	96
LC/ESI-MS/MS	Skin fibroblast extract	0.1 µg	120 +/- 7	11 +/- 5	95
	Culture medium	100 µL	4.3 +/- 0.3	0.3 +/- 0.1	99

Cell extract and culture medium was derived from cytoplasmic glycogen-depleted Pompe skin fibroblast, at confluence. Samples were processed then analysed by mass spectrometry in triplicate. Recovery was a measure of the percentage of peak area internal standard signal in each quality control sample compared to pure internal standard.

Supplementary data C: Purification of glycogen granules from cultured skin fibroblasts

---

Introduction: The size of vesicular glycogen granules has not been reported, but cytosolic glycogen in healthy cells can range from 10 to 80 nm (Parker *et al*., 2007; Takeuchi *et al*., 1978). The calcimycin-induced exocytic pore in Pompe and unaffected skin fibroblasts is approximately 30 nm in diameter (Jaiswal *et al*., 2004), suggesting that the amount of glycogen exocytosis may be restricted by the amount of glycogen small enough to pass through an exocytic pore. In this study, glycogen granules were isolated from cultured Pompe and unaffected skin fibroblasts, which were then visualised by transmission electron microscopy; allowing granule size to be determined. Cells were depleted of cytoplasmic glycogen to provide an intracellular pool of predominantly vesicular glycogen, as previously described (Umapathysivam *et al*., 2005). The method used for glycogen purification has been previously described, using rat liver extracts, which contained both α- and β- granules (Parker *et al*., 2007). In collaboration with Dr. David Stapleton (Department of Biochemistry and Molecular Biology, University of Melbourne), this method was optimised for the purification of vesicular glycogen from Pompe and unaffected skin fibroblasts.

Methods and Results: Glycogen was purified by centrifuging skin fibroblast extracts at high speed (300,000 *g*) on a sucrose gradient (25% and 50% (v/v) sucrose layers; Parker *et al*., 2007). The membrane-fraction was expected to migrate to the 25/50% sucrose interface, whilst glycogen pellets at the bottom of the tube. However, the presence of glycogen in the vesicular pool necessitated the introduction of a

membrane lysis step, involving the addition of NP-40, to ensure glycogen was not retained in the membrane fraction. Aliquots were decanted from the sucrose gradient and glycogen was quantified using LC/ESI-MS/MS, showing that glycogen was successfully released from vesicles, with all glycogen detected in the pellet. The high background level of glucose associated with the sucrose gradient did not interfere with the glycogen quantification assay (data not shown). In cytoplasmic glycogen-depleted cells, cultured to 3-weeks post-confluence, 147 µg of vesicular glycogen was isolated from Pompe fibroblasts, with 95 µg from unaffected cells. In the non-depleted cells, Pompe cells contained 446 µg and unaffected cells had 180 µg of total cell glycogen.

Conclusion: Layered sucrose gradients provide a useful tool for the isolation of glycogen from biological materials. This technique allowed cytosolic and vesicular pools of glycogen granules to be isolated from cultured Pompe skin fibroblasts, which could be compared to those purified from unaffected cells (see section 4.2.5).